Design of Cooperative Control Algorithm for Multi-vehicle System in Modern Intelligent Transportation

A thesis submitted to the University of Manchester for the degree of

Doctor of Philosophy

in the Faculty of Science & Engineering

2023

Songtao Xie

Department of Electrical and Electronic Engineering

School of Engineering

Contents

Word Count: 30633

List of figures

Terms and abbreviations

ACC Adaptive Cruise Control

ADAS Advanced Driving Assistance System

APF Artificial Potential Field

ATSS Asymptotically Time-domain String Stability

AV Autonomous Vehicles

CACC Cooperative Adaptive Cruise Control

CAV Connected and Autonomous Vehicle

MAS Multi-agent System

MPC Model Predictive Control

MVS Multi-vehicle System

MVCC Multi-vehicle Cooperative Control

IFT Information Flow Topology

SDEM Spring Damping Energy Model

TTC Time-to-Collision

V2V Vehicle-to-Vehicle Communication

Abstract

Global traffic transportation is facing several challenges that require innovative solutions to ensure sustainability, safety, and efficiency. One of the solutions is the integration of connected and autonomous vehicles that can communicate and coordinate with each other to optimise traffic flow, reduce emissions, and improve safety. A multi-vehicle cooperative control system requires sophisticated algorithms and protocols that enable vehicles to share information about their state and intended trajectory and collaborate on route planning and traffic management. This research aims to design cooperative control and motion planning algorithms for multi-vehicle systems, thus advancing the application of multi-vehicle cooperative technology and promoting the development of intelligent transportation.

Firstly, this thesis reviews three basic and important aspects of multi-vehicle cooperative control systems: system structure and function strategy, control methods, and applications. The review concludes by proposing future research directions for the development of multi-vehicle cooperative control, based on the analysis of the current research status and the growth of the automotive industry. Secondly, a solution to the distributed motion planning problem in a complex multi-lane platoon is proposed, which may comprise both connected and autonomous vehicles and human-operated vehicles. The algorithm effectively deals with sudden changes in the acceleration of the lead vehicle and ensures speed synchronisation of unmanned follower vehicles with the leader's variable acceleration, while avoiding obstacles and maintaining the desired formation objectives. Furthermore, a distributed cooperative adaptive cruise control protocol is developed based on the spring damping energy model, which defines the vehicle-to-vehicle relationship using a nonlinear spring and linear damping. Mathematical proofs demonstrate the stability of the connected vehicle platoon under this control protocol, enabling distance and speed stabilisation of the platoon. The proposed algorithm ensures stable control and system stability, even if platoon communication is lost and the cooperative adaptive cruise control system degrades.

Declaration of originality

I hereby confirm that no portion of the work referred to in the thesis has been submitted in support of an application for another degree or qualification of this or any other university or other institutes of learning.

Copyright statement

List of publications

S. Xie, J. Hu, P. Bhowmick, Z. Ding and F. Arvin, ”Distributed Motion Planning for Safe Autonomous Vehicle Overtaking via Artificial Potential Field,” **IEEE Transactions on Intelligent Transportation Systems**, vol. 23, no. 11, pp. 21531-21547, 2022.

S. Xie, J. Hu, Z. Ding and F. Arvin, ”Cooperative Adaptive Cruise Control for Connected Autonomous Vehicles using Spring Damping Energy Model,” **IEEE Transactions on Vehicular Technology**, 2022.

S. Xie, J. Hu, Z. Ding and F. Arvin, ”Collaborative Overtaking of Multi-Vehicle Systems in Dynamic Environments: A Distributed Artificial Potential Field Approach,” **20th International Conference on Advanced Robotics (ICAR)**, 2021, pp. 873-878.

S. Xie, J. Hu, Z. Ding and F. Arvin, ”Distributed Cooperative Autonomous Driving of Intelligent Vehicles Based on Spring-Damper Energy System,” **IEEE International Conference on Mechatronics (ICM)**, 2023.

Acknowledgements

After enduring many hardships and experiences, I can finally begin to write this acknowledgements section. Looking back on my nearly twenty years of schooling, countless emotions flood my heart.

My journey has not been easy. I spent my primary school years in a remote mountain village in Sichuan Province, China. Muddy mountain roads, run-down classrooms, endless mountains, and heavy farm work are still vivid memories. Fortunately, my parents always believed that knowledge can change one's destiny. When I was preparing to attend middle school, my parents overcame all difficulties and sent me to Guangdong for better educational opportunities. From a backward mountain village to a modern city, everything I experienced was a challenge, but also an opportunity. With ups and downs, I completed my secondary education and successfully entered Sichuan University. Thanks to God's grace, my master's and doctoral careers went relatively smoothly. As my doctoral career is coming to an end, I want to express my sincere gratitude to everyone who helped and took care of me.

Firstly, I want to thank my parents who overcame all difficulties and brought me out of the mountains. Despite our hardships in Guangdong during the first few years, they still spared no effort to support my education. They taught me how to face difficulties calmly and how to resist fate.

Next, I sincerely thank my supervisors, Prof. Zhengtao Ding, and Dr. Farshad Arvin. I am grateful for their full respect for my research ideas, their tremendous assistance to my research, and their concern for my life and job careers. I also thank Dr. Hu for his guidance and help with my academic research publication.

Furthermore, I want to thank the friends I met during my studies in the UK. They accompanied me through the difficult three years of COVID-19. There were classmates who did sports together, travel companions, DOTA2 buddies, and friends who cooked together. They made my dull doctoral career more enjoyable.

In addition, I would like to thank my bonne amie Yayue Li. Thank her for coming into my life as my doctoral career is coming to an end, and for opening up the next chapter of my life. The road ahead is still long, and I am grateful to have her by my side in the future.

Finally, I want to thank myself for never giving up. I also want to thank those strangers who have passed through my life with a casual greeting or smile. I want to thank this era and this world for its infinite possibilities and great tenderness.

Chapter 1

Introduction

1.1 Background and motivation

Transportation is an essential aspect of modern society, and it plays a vital role in the economy and the daily lives of people worldwide. However, the current transportation is facing several challenges that require innovative solutions to ensure sustainability, safety, and efficiency. The problems include congestion, air pollution, accidents, and inefficiencies. One of the solutions to these challenges is the integration of connected and autonomous vehicles (CAVs) that can communicate and cooperate with each other to optimise traffic flow, reduce emissions, and improve safety. Multi-vehicle cooperative control (MVCC) requires sophisticated algorithms and protocols that enable vehicles to share information about their position, speed, and intended trajectory, and collaborate on route planning and traffic management. As a result, there has been a growing interest in the development of MVCC systems and their control algorithms in recent years.

In the past few decades, with the acceleration of urbanization, traffic congestion and frequent traffic accidents have become serious problems facing many large cities. With the development of vehicle-to-vehicle (V2V) communication and advanced driver assistance systems (ADAS), the MVCC system has become feasible and has garnered widespread attention. In an MVCC system, vehicles optimize their driving routes, avoid collisions and congestion, and enhance traffic efficiency and safety through communication and cooperation. For instance, vehicles can utilise wireless communication devices to exchange information such as position, speed, and driving direction, enabling better coordination of their driving routes. The most common approach in the MVCC system is the utilization of network-connected distributed control methods. This distributed control methodology is based on the cooperation among multiple agents, where agents can be different vehicles, traffic lights, or other control devices.

In a network-connected distributed control system, each agent only needs to comprehend the state information of its adjacent agents to make local decisions and ultimately achieve the global control objective. Network-connected distributed control technology can improve the efficiency and robustness of traffic control, thereby enhancing the reliability of the MVCC system.

As early as the early 20th century, various automobile manufacturers began researching MVCC systems. Starting in 1986, the University of California, Berkeley launched the California Partners for Advanced Transportation Technology (PATH) project, which focused on intelligent transportation systems and advanced transportation technology. In the early stages of the project, PATH developed and evaluated a strongly coupled platoon system, which shows the feasibility of the MVCC system and gives a good start for the development of the MVCC system [1]. In 1989, Ford provided PATH with four vehicles as an experimental platform for close-range automatic longitudinal control. PATH equipped these vehicles with throttle and brake actuators, forward-ranging radar, wireless local area network communication systems, control computers and software to achieve close-range cooperative vehicle tracking [2]. Subsequently, PATH added V2V communication to the adaptive cruise control (ACC) system, creating a cooperative adaptive cruise control (CACC) system. The idea behind the CACC system was not only to enable the cruise control system of a vehicle to maintain an appropriate following distance behind other vehicles by slowing down if it gets too close but also to allow the vehicles to cooperate by communicating with each other while in ACC mode. As a result, the vehicles could follow each other more closely, accurately, and safely with braking and acceleration being cooperative and synchronized. PATH conducted experiments on the CACC system using four Nissan vehicles and the results showed significant improvements in the vehicle following stability compared to the same four vehicles using their production ACC controllers without cooperation [3]. Subsequently, from 2014 to 2017, PATH equipped CACC systems on four Infiniti M56 vehicles, using V2V communication to share real-time information about their motion. The results showed that the CACC system made all vehicles follow the same speed curve as the leader, with no significant amplification or delay, indicating that V2V communication is capable of providing the necessary preview information to achieve stable vehicle-following control, thereby forming a high-performance traffic flow [4]. Since 2015, PATH has been working with the Volvo Group to develop CACC systems for heavy trucks, as part of an exploratory advanced research project sponsored by the Federal Highway Administration and the California Department of Transportation (Caltrans). PATH's research shows that CACC systems can improve the following performance of trucks, significantly reducing the following distance and making the vehicle-following dynamics more stable. The prototype systems are typically able to react automatically to cut-in vehicles, increasing gaps to accommodate them safely, while significantly reducing fuel consumption of heavy trucks [5].

Similar projects have also been carried out in Europe. The first truck platooning research started in Europe in 1996 as the CHAUFFEUR project funded by the European Commission, which presented the initial idea of electronically coupling heavy trucks [6], [7]. Additionally, the Safe Road Trains for the Environment (SARTRE) project [8] is a research project supported by the European Commission. The project aims to develop and test an environmentally friendly road platoon composed of mixed vehicle types, such as trucks and cars, that can operate on public roads without any changes to infrastructure and fully interact with other road users. The project intends to encourage a gradual shift towards the use of individual transport by developing these road platoons. The developed systems will help adopt road trains safely on unmodified public roads and fully interact with non-platooned vehicles. The results of the SARTRE project can be summarized into three different categories of potential benefits: fuel consumption, commercial viability, and infrastructure and environment. Firstly, in terms of fuel consumption, the project demonstrates that vehicles can save 7%-15% of fuel if there is a space of 8 metres between them [9]. Secondly, in terms of commercial viability, the project shows that platooning is economically feasible for transporters [9]. Finally, in terms of infrastructure and environment, the project demonstrated that platooning can reduce congestion and emissions [9].

Early MVCC systems were mainly developed based on the car-following model, with the mainstream model being the Constant Time Headway Strategy (CTHS) CACC model proposed by the Berkeley PATH laboratory in California [10]. Xiao et al. [11], [12] conducted a more in-depth study of the CTHS of CACC systems and proposed four control modes for CACC systems: speed control mode, gap control mode, gap-closing control mode, and collision avoidance control mode. The CACC system in the Simulation of Urban Mobility (SUMO) was developed based on Wang's CACC model. With the increasing requirements for performance and stability of MVCC systems, control theory-based MVCC systems have been widely studied, and linear controllers have been widely applied in MVCC systems [13], [14], especially in commercially available MVCC systems. It is well known that a single Proportional-Derivative (PD) or Proportional-Integral-Derivative (PID) method in the MVCC system focuses on a very limited control objective, namely the consensus of speed and following distance. However, more advanced MVCC systems require higher requirements for vehicle fuel consumption and comfort in addition to speed and following distance, so optimization control methods have attracted great attention. Following distance, fuel consumption, and comfort can all be modelled as optimized objectives, hence, a feasible control input can be obtained by solving an optimisation problem [15], [16]. The rapid development of Vehicle-to-Vehicle (V2V) communication has made the MVCC system gradually expand from cooperation between two vehicles to cooperation between a group of vehicles, so the information that the vehicle cooperative controller needs to process has increased sharply. The increasing communication load poses a huge challenge to the communication capacity and chip computing power of vehicles. At this time, network-connected distributed control methods provide potential solutions [17], [18]. The cooperative controller can achieve the common control objectives of the entire multi-vehicle system without the need to obtain global information. The common distributed control methods used in MVCC systems mainly include distributed Model Predictive Control (MPC) [19], [20] and distributed consensus control [21]. In recent years, data-driven and learning-based control methods have achieved great success, and researchers have begun to attempt to use reinforcement learning to achieve control of MVCC systems [22], [23]. However, these studies are still largely in the experimental and simulation stages, and there is still a long way to go before commercialisation.

Currently, research on MVCC still faces many challenges. One of the obvious challenges is that most existing MVCC algorithms have very strict communication topology requirements and driving scenario limitations. For example, the CACC system proposed in [24], [25] requires vehicles to use predecessor following (PF) information flow topology (IFT). In practical applications, the dynamic switching of IFT is very common, and even V2V communication can be temporarily lost. In this case, it is necessary to develop MVCC algorithms that can cope with dynamic IFT and system degradation caused by communication loss. With the gradual promotion of MVCC systems for practical applications, especially with the commercialisation of platooning technology approaching, it is increasingly important to study the driving environment of platooning technology. However, most of the research on platooning technology has strict limitations on its driving environment. Firstly, high homogenisation requirements for multi-vehicle systems impose stringent conditions on realistic industrial applications. Therefore, in recent years, more and more algorithms for heterogeneous vehicle platooning have been proposed [26]. As CAVs and human-driven vehicles will coexist for a long time, how to improve the driving performance of multi-vehicle systems in mixed traffic flow should be a focus of attention [27]. Additionally, driving scenarios for multi-vehicle systems are singular; for example, how to cooperate with other multi-vehicle systems for overtaking and merging has not been extensively studied.

Accelerated global urbanisation puts urgent demands on the efficiency and safety of road traffic. The development of coordination and control algorithms for the MVCC systems in this thesis is motivated by the need to address the aforementioned shortcomings in the development of MVCC systems and create a more efficient and sustainable transportation system. To solve the aforementioned technical problems of the MVCC system, this research work starts from the perspective of the MVCC algorithm, aiming to provide a feasible control algorithm and motion planning algorithm for the upcoming industrialised MVCC system, namely vehicle platooning nowadays. Existing research works on vehicle platooning have rarely considered the presence of human-driven vehicles and complex driving scenarios (such as overtaking, merging, etc.). Additionally, the unreliability of communication poses a challenge to the stability and safety of vehicle platooning technology. To overcome these challenges and contend with the current technical challenges, we have conducted research on motion planning algorithms for overtaking in vehicle platooning and on multi-vehicle CACC algorithms for vehicles.

1.2 Achievements and contributions

In this section, the contributions of the thesis and the related publications are listed. A distributed motion planning algorithm to ensure the safe overtaking of autonomous vehicles in a dynamic environment using the Artificial Potential Field method is proposed. Unlike conventional overtaking techniques, autonomous driving strategies can be used to implement safe overtaking via formation control of unmanned vehicles in a complex vehicle platoon in the presence of human-operated vehicles. Firstly, we formulate the overtaking problem of a group of autonomous vehicles into a multi-target tracking problem, where the targets are dynamic. To model a multi-vehicle system (MVS) consisting of both autonomous and human-operated vehicles, we introduce the notion of velocity difference potential field and acceleration difference potential field. We then analyze the stability of the multi-lane vehicle platoon and propose an optimization-based algorithm for solving the overtaking problem by incorporating a dynamic target into the traditional artificial potential field. A simulation case study has been performed to verify the feasibility and effectiveness of the proposed distributed motion control strategy for safe overtaking in a multi-lane vehicle platoon.

- S. Xie, J. Hu, Z. Ding and F. Arvin, ”Collaborative Overtaking of Multi-Vehicle Systems in Dynamic Environments: A Distributed Artificial Potential Field Approach,” 20th International Conference on Advanced Robotics (ICAR), 2021, pp. 873-878.
- S. Xie, J. Hu, P. Bhowmick, Z. Ding and F. Arvin, ”Distributed Motion Planning for Safe Autonomous Vehicle Overtaking via Artificial Potential Field,” IEEE Transactions on Intelligent Transportation Systems, 2022.

Moreover, to overcome the shortcomings of the traditional CACC system which is prone to degradation, this thesis innovatively applies a spring damping energy model (SDEM) to construct a robust autonomous vehicle platoon system. The proposed design of the energy model ensures that the stability and safety of the platoon system are maintained in the event of such sudden degradation. Based on this technique, a distributed control protocol that only utilises local information from neighbours is then proposed. Furthermore, some practical constraints such as the connectivity of the vehicle platoon system and the bound of the control inputs are guaranteed. Finally, the effectiveness of the proposed CACC system strategy is validated by multiple simulation experiments in Unreal Engine.

- S. Xie, J. Hu, Z. Ding and F. Arvin, ”Distributed Cooperative Autonomous Driving of Intelligent Vehicles Based on Spring-Damper Energy System,” IEEE International Conference on Mechatronics (ICM), 2023.
- S. Xie, J. Hu, Z. Ding and F. Arvin, ”Cooperative Adaptive Cruise Control for Connected

Autonomous Vehicles using Spring Damping Energy Model," IEEE Transactions on Vehicular Technology, 2022.

1.3 Thesis organisation

The remaining sections of this thesis are organized as follows: Chapter 2 provides fundamental knowledge about the multi-agent system, graph theory, ADAS, string stability, and V2V communication. Chapter 3 reviews three fundamental and critical aspects of the MVCC system, including the system structure and functional strategy, control methods, and applications. Chapter 4 presents a distributed motion planning algorithm for safe autonomous vehicle overtaking using an artificial potential field. Chapter 5 introduces a cooperative adaptive cruise control algorithm for connected autonomous vehicles, incorporating a spring damping energy model. Chapter 6 concludes the thesis by summarizing the main findings and providing an outlook on future research directions.

Chapter 2

Preliminaries

This chapter introduces some preparatory basics for better understanding the content in the following chapters. This preparatory knowledge includes concepts of distributed cooperative control, basic algebraic graph theory, advanced driver assistance systems and autonomous driving levels, the concept of string stability, and V2V communication.

2.1 Distributed cooperative control of multi-agent system

In general, an agent refers to a physical or abstract entity that perceives its environment and applies knowledge and rules to generate appropriate responses. A multi-agent system (MAS) is a complex system consisting of multiple such agents, along with their organizational rules and information exchange protocols, aimed at addressing specific coordination problems. Within this intricate system, each agent communicates with its neighbouring agents to achieve a common goal of interest. The communication topology determines the connectivity among agents, while the information exchange protocol facilitates the determination and updating of agent states. MASs find practical applications in various domains such as drone formations [28], [29], smart grids [30], autonomous driving fleets [31], and sensor networks [32].

In the control design of MASs, the prevalent approach is distributed control, where each agent relies only on local neighbouring information. As illustrated in Fig. 2.1, an agent shares information with neighbouring agents within its communication range. Distributed cooperative control in MASs can be broadly categorized into three main types: consensus control, formation control, and containment control [33]. One of the earliest models of distributed cooperative control is Boids [34], which describes the coordinated behaviour of birds or schools of fish. Reynolds' rules [34] represent a simple distributed cooperative control approach that effectively captures the collective motion of animal groups. These rules can also be applied as control schemes for human-made systems such as drone formations, vehicle platoons, and underwater robot formations. The Couzin model [35] demonstrates that efficient information transfer and decision-making can occur within animal groups even without explicit signals or complex mechanisms for information exchange. This model allows for the achievement of global motion objectives and obstacle avoidance in MASs with limited information. Potential functions [36], [37] are widely used in studying MAS aggregation and flocking behaviour. They provide a framework for agents to navigate their movements based on attractive and repulsive forces, leading to coordinated motion patterns. Consensus control is considered one of the most widely used control methods in artificial MASs. Some classic synchronization models include the Vicsek model [38], the Kuramoto model [39], and other control protocols proposed in [40], [41].

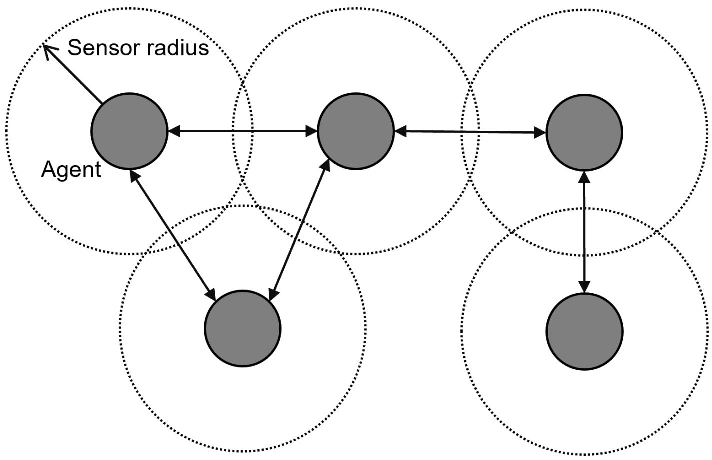

Figure 2.1. Distributed control and communication connection network

Within the framework of distributed control, more advanced control methods are employed in the cooperative control of artificial MASs. Model-based approaches are commonly used, as discussed in [42], [43]. These methods rely on accurate kinematic and dynamic models of the controlled system. However, constructing precise models for complex systems can be challenging. Distributed cooperative control methods based on optimization have also seen significant development in recent decades [44]–[46]. These approaches formulate the control problem as an optimization task, seeking to optimize certain objectives or criteria to achieve desired cooperative behaviour. Data-driven control methods are gaining popularity as well [47]. These approaches leverage data and past control experiences to develop control strategies. Iterative learning control, for instance, is an intelligent data-driven control method widely used in cooperative control problems such as formation control [48], consensus problems [49], and containment control problems [50]. It utilizes historical control data to improve control performance over iterations. Adaptive dynamic programming [51]–[53], based on reinforcement learning and adaptive control, is another effective data-driven control method for coordinating MASs. It combines the principles of dynamic programming and adaptive control to learn and optimize control policies in a distributed manner. These advanced control methods enhance the capabilities of distributed cooperative control in MASs, enabling more effective coordination and achieving desired system behaviour.

2.2 Graph theory

Assuming that MAS interact with each other through a communication network and perception network, it is natural to think of using a directed graph or an undirected graph to establish an interaction model between agents.

A graph is a pair $\mathcal{G} = (\mathcal{V}, \mathcal{E})$ with $\mathcal{V} = \{\mathcal{V}_1, ..., \mathcal{V}_N\}$ being finite non-empty set of N nodes or vertices and $\mathcal{E}$ is a set of edges or arcs. Elements of $\mathcal{E}$ are represented as $\left(\mathcal{V}_i, \mathcal{V}_j\right)$ which are termed an edge from $\mathcal{V}_i$ to $\mathcal{V}_j$, and are represented as an arrow with tail at $\mathcal{V}_i$ and head at $\mathcal{V}_j$. An edge $\left(\mathcal{V}_i, \mathcal{V}_j\right)$ is said to be outgoing with respect to node $\mathcal{V}_i$ and incoming with respect to node $\mathcal{V}_j$. The in-degree of $\mathcal{V}_i$ is the number of edges having $\mathcal{V}_i$ as a head. The set of neighbours of a node $\mathcal{V}_i$ is $\mathcal{N}_i = \left\{\mathcal{V}_j : \left(\mathcal{V}_j, \mathcal{V}_i\right) \in \mathcal{E}\right\}$, i.e, the set of nodes with edges incoming to $\mathcal{V}_i$. A graph can be represented by an adjacency matrix $A = \left[a_{ij}\right]$ with weights $a_{ij} > 0$ if $\left(\mathcal{V}_j, \mathcal{V}_i\right) \in \mathcal{E}$ and $a = 0$ otherwise, especially, $a_{ii} = 0$. Define the weighted in-degree of node $\mathcal{V}_i$ as the i^{th} row sum of A

$$d_i = \sum_{j=1}^{N} a_{ij}. \tag{2.1}$$

The diagonal in-degree matrix $D = \text{diag}\left\{d_i\right\}$ and the graph Laplacian matrix $L = D - A$. A (directed) tree is a connected digraph where every node except one has an in-degree equal to one. A spanning tree of a digraph is a directed tree formed by graph edges that connects all the nodes of the graph. If a subset of the edges forms a directed tree, this graph is said to have a spanning tree.

2.3 Advanced driver assistance systems and autonomous driving

ADAS stands for Advanced Driver Assistance Systems and refers to a range of technologies and features designed to assist drivers in controlling their vehicles and improving safety on the road. ADAS typically includes sensors, cameras, and computer algorithms that can monitor the environment around the vehicle, detect potential hazards, and provide alerts or assistance to the driver. Examples of ADAS features include ACC, lane departure warning, blind spot detection, automatic emergency braking, and parking assistance. ADAS technology is designed to reduce the risk of accidents, improve driver awareness and decision-making, and ultimately make driving safer and more convenient. However, it is important to note that ADAS is not a substitute for responsible driving and drivers must remain attentive and engaged at all times.

Autonomous driving technology has the potential to revolutionise transportation, making travel safer, more efficient, and more convenient. To help define the capabilities and limitations of autonomous driving systems, the Society of Automotive Engineers (SAE) has established a classification system for autonomous vehicles based on six levels of autonomy.

The first two levels are considered driver assistance levels, where the human driver is still in control of the vehicle. At Level 0, the human provides the ”dynamic driving task” although there may be systems in place to help the driver. Level 1 refers to a vehicle with basic driver assistance features, such as ACC or lane departure warning. Level 2 vehicles have more advanced driver assistance features, such as automatic braking and lane centring, but the human driver is still responsible for monitoring the road and being ready to take control at any time.

Levels 3 to 5 are considered higher levels of autonomy, where the vehicle can perform more complex driving tasks without human intervention. At Level 3, a vehicle can take over all aspects of driving under certain conditions, such as on highways, but the human driver must be ready to take control if needed. At Level 4, a vehicle is fully autonomous in certain driving conditions or environments, such as a specific geographic area or weather conditions. Finally, at Level 5, the vehicle is fully autonomous in all driving conditions and environments, and there is no need for a human driver to be present.

The SAE levels of autonomous driving provide a useful framework for understanding the capabilities of autonomous vehicles, and they are widely used by automakers, researchers, and regulators around the world. As technology continues to advance, it is expected that more vehicles will reach higher levels of automation, leading to a future where driving is safer, more convenient, and more comfortable.

2.4 String stability

The tight formation control of platoons has a particular challenge known as "string instability", i.e., disturbances of system states are amplified along the string of vehicles. The string instability of tight formation platoons can cause convoy congestion and increase the risk of collision, which seriously compromises the benefits of platoon control. To overcome this problem, string stability theory was proposed [54]. String stability theory is a mathematical framework used to study the stability of traffic flow in a queue, where vehicles are arranged linearly and are subject to delays and perturbations. This theory is of great importance in the design and analysis of traffic control systems, as it provides a systematic way to understand and predict the behaviour of queues.

Intuitively, a vehicle platoon is considered to be string stable if the disturbances are not amplified when propagating backwards along the vehicle platoon. In the mainstream, several mathematical descriptions are applied to define string stability, which are presented in the following sections.

2.4.1 Frequency-domain string stability

For a vector $x \in \mathbb{R}^n$, its ∞-norm is given as

$$\|x\|_\infty = \max_i |x_i| . \tag{2.2}$$

Define the Laplace transforms of signals $u_i(t)$, $x_i(t)$, and $e_i(t)$ as $\mathcal{L}(u_i(t)) = U_i(s)$, $\mathcal{L}(x_i(t)) = X_i(s)$, $\mathcal{L}(e_i(t)) = E_i(s)$, and $\Lambda \in \{U, X, E\}$. The $x_i(t)$, $u_i(t)$, and $e_i(t)$, respectively, represent the input, output, and error signals. Considering a distributed controller design for heterogeneous traffic, i.e., vehicles with possibly different characteristics and dynamics, conservative string-stability transfer functions $G_{\Lambda,i}(s)$ are defined as follows [24], [55]:

$$G_{\Lambda,i}(s) = \frac{\Lambda_i(s)}{\Lambda_{i-1}(s)}, \quad \text{for } i > 1 \ . \tag{2.3}$$

Then, a conservative sufficient condition for string stability is obtained, i.e.,

$$\left\| G_{\Lambda,i}(j\omega) \right\|_{\infty} \leq 1, \quad \text{for } i > 1 \ . \tag{2.4}$$

Targeting a broader communication topology, we define string stability transfer functions $G'_{\Lambda,i'}(s)$ between vehicle i and vehicle i'. We can also obtain a necessary condition for string stability:

$$\left\| G'_{\Lambda,i'}(j\omega) \right\|_{\infty} \leq 1, \quad \text{for } i' > 1 \ , \tag{2.5}$$

where i' denotes the last vehicle in the vehicle platoon. This condition strictly limits the amplification of oscillations upstream among the platoon. This kind of stability is defined as strong frequency-domain string stability (SFSS) [24]. It can be intuitively seen the SFSS emphasises that the disturbance between any two neighbouring vehicles is not amplified. A weaker version of SFSS is frequency-domain string stability (FSS), which only emphasises that the perturbations between the vehicle and the leader are not amplified. Similarly, in the Frequency-domain, eventual string stability (ESS) [54], and head-to-tail stability (HTS) [56] were proposed. Essentially, ESS is a special case of FSS. Especially, the HTS was originally designed for mixed traffic, where the human-operated vehicle was regarded as the front vehicle. However, it is important to note that these Frequency-domain methods share the fundamental assumption that the platoon system is identified as linear.

2.4.2 Time-domain string stability

To generalise the concept of string stability to a class of interconnected vehicle platoon systems as

$$\dot{x}_i = f_i\left(x_i, x_{i-1}, \cdots, x_{i-r}\right) \ , \tag{2.6}$$

where $f(0, \cdots, 0) = 0$, and there is no assumption of linearity in this system. The time-domain string stability is defined as follows:

$$\sup_i |x_i(0)| < \delta \Rightarrow \sup_i \|x_i(t)\|_\infty < \epsilon \tag{2.7}$$

For any given $\epsilon > 0$, there exists a $\delta > 0$ making (2.7) true. Especially, if the $\sup_i \|x_i(t)\|_\infty \to 0$ asymptotically, the equilibrium point of the system is asymptotically time-domain string stability (ATSS). Of course, the other string stability that corresponds to this is time-domain string stability (TSS) [57]. In addition, there are more definitions of string stability being widely utilised, such as Lyapunov string stability (LSS), Input-to-output string stability (IOSS), and Input-to-state string stability (ISSS) [58].

2.5 V2V communication

V2V communication enables vehicles to wirelessly exchange information about their speed, location, and heading. The technology behind V2V communication allows vehicles to broadcast and receive omnidirectional messages (up to 10 times per second), creating a 360-degree perception of other vehicles in proximity [59]. V2V communication is an inter-vehicle communication paradigm that does not rely on third-party networks like cellular networks to communicate, and its ad hoc communication spans up to 1000 m with 360-degree horizons of nearby vehicles [60].

The goal of V2V communication is to prevent accidents by allowing vehicles in transit to send position and speed data to one another over an ad hoc mesh network. V2V communication can also be used for traffic management systems, such as signal phase and timing (SPaT) broadcasts [61], which can help drivers avoid red lights and reduce congestion.

The development of V2V communication technology has been ongoing for many years. In 1999, the Federal Communications Commission (FCC) allocated 75 MHz of spectrum in the 5.9 GHz band for Dedicated Short Range Communications (DSRC) systems. In recent years, there has been a shift towards using cellular networks for V2V communication [62], however, DSRC remains a viable option for V2V communication.

Chapter 3

A Review of Multi-vehicle Cooperative Control System

3.1 Introduction

The ever-increasing number of cars is challenging the safety, efficiency and sustainability of urban transport. While autonomous driving is seen as promising to overcome these challenges, autonomous driving technology at L4 and above is still far from being commercially viable. Multi-vehicle cooperative control (MVCC) has emerged as a compromise but a reliable solution. MVCC refers to multiple vehicles communicating and cooperating to achieve global goals, such as improving traffic flow, reducing congestion, or increasing safety.

In the last decade, the intelligence and automation of vehicles have made remarkable developments. Most mainstream original equipment manufacturers (OEMs) and self-driving technology companies are already conducting extensive research in the field of ADAS and autonomous driving. Tesla, Mercedes Benz, Audi, and other mainstream OEMs have successfully launched their own L3 autonomous driving systems. With the development of sensor technology and wireless communication technology, vehicle-to-vehicle interaction is becoming more accessible and more common. The connections between automobiles and automobiles through sensors and wireless communication form a holistic system that interacts with each other. Fig. 3.1 shows some typical traffic scenarios in which a multi-vehicle system (MVS) can exhibit superior group performance through the MVCC system. The group performance of the MVCC system is characterized by improved traffic efficiency [63], increased road capacity [64], improved road safety [65], and reduced fossil fuel consumption [66]. In addition, with the development of intelligent transportation infrastructure, vehicle and road collaboration will further enhance the excellent performance of the MVCC system [67].

One of the most promising applications of the MVCC system is vehicle platooning [68]. Vehicle platooning involves a group of vehicles that travel close together, connected through wireless communication and controlled by a lead vehicle. The lead vehicle is responsible for controlling the speed and direction of the platoon, and the other vehicles follow closely behind. This technology has the potential to reduce fuel consumption and emissions, increase safety, and improve traffic flow. Another important application of the MVCC system is cooperative lane-changing [69]. In this application, vehicles in adjacent lanes communicate with each other to coordinate their lane-changing manoeuvres. Cooperative lane-changing can improve safety and reduce congestion, as vehicles can move more smoothly and efficiently through traffic. Cooperative merging [70]is a related application that involves coordinating the movement of vehicles entering or exiting a highway or other roadway. By coordinating the merging and diverging of multiple vehicles, cooperative merging can reduce congestion and improve safety. MVCC system can also be used to improve parking efficiency [71]. In cooperative parking, vehicles communicate with each other to find available parking spaces and coordinate their movements to enter and exit the parking lot or garage. Cooperative parking can reduce the time required to find a parking space, as well as improve traffic flow in and around parking areas. Finally, MVCC can also be used to enhance safety and efficiency at intersections [72]. By coordinating the movements of multiple vehicles, this technology can reduce the likelihood of collisions and improve traffic flow through busy intersections.

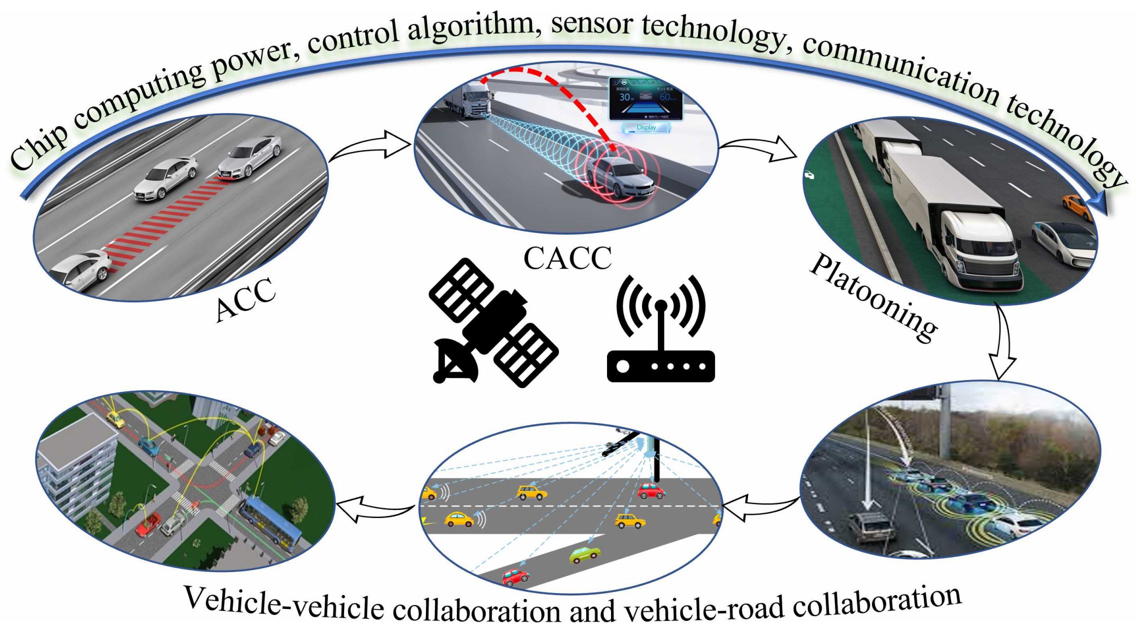

Figure 3.1. The development process of multi-vehicle collaboration and vehicle-road collaboration.

The development of multi-vehicle cooperative and vehicle-road collaboration is always accompanied by the development of chip computing power, control algorithms, sensors and communication technologies. As shown in Fig. 3.1, the ACC system relies on sensor technology and control algorithms. With the development and application of V2V communication, the CACC system, and platooning technology were born. The development of road communication facilities also brings the possibility of vehicle-road cooperation. With the increase of environmental state information, powerful computing chips have also become one of the key factors to drive multi-vehicle cooperative and vehicle-road collaboration. In addition, the development of the MVCC system and vehicle-road collaboration relies on powerful control algorithms designed for complex multi-agent systems with a mix of heterogeneous vehicles and complex environmental communication agents. MVCC is a rapidly evolving field with significant potential to transform how we move people and goods. With ongoing research and development, we can expect to evidence more and more application examples of MVCC systems in the coming years, and significant benefits in terms of safety, efficiency, and sustainability.

3.2 System structure and strategy

The existing MVCC system is an extension of the already commercialised ACC system. Through V2V communication connection and interaction, the existing MVCC system, namely the CACC system, has gradually formed [3]. On the basis of the CACC system, more diversified MVCC systems can be obtained by optimising the information flow topology (IFT) and control strategy [73].

3.2.1 System structure

Mainstream OEMs use the system architecture shown in Fig. 3.2 for their ACC and CACC system designs. UC Berkeley PATH's previous research has indicated that current CACC implementations in production vehicles are primarily developed as an extension of commercially available ACC systems [3]. More research es and experiments on the CACC system completed by Ploeg et al. [74] have also adopted similar system architectures. This CACC system architecture mainly consists of perception, planning, and actuation. During the sensing phase, the CAV acquires information from onboard sensors, such as LIDAR, odometer, and flag signals, and incorporates them into the data structure of the controller area network (CAN) bus. In addition, the CAV will also receive information from the wireless communication module. The information in the wireless communication module includes the following two parts: 1) data transmitted by other CAVs in the CACC system via V2V communication, such as speed, acceleration, inter-vehicle distance, current time interval, etc.; 2) data collected by GPS with differential correction of the wide-area augmentation system, including the detection and assignment of vehicle position sequences in the CACC system. The planning phase contains mainly the upper controller layer, where researchers and engineers propose and implement the vehicle longitudinal control algorithms. In this layer, the vehicle completes the motion planning for a limited time series range and outputs the motion reference parameters for the next control step. In practical engineering development, both ACC and CACC systems are present and available, and the driver implements switching between the two functions as required. The reference motion commands output from the planning phase will be controlled and executed by the execution layer.

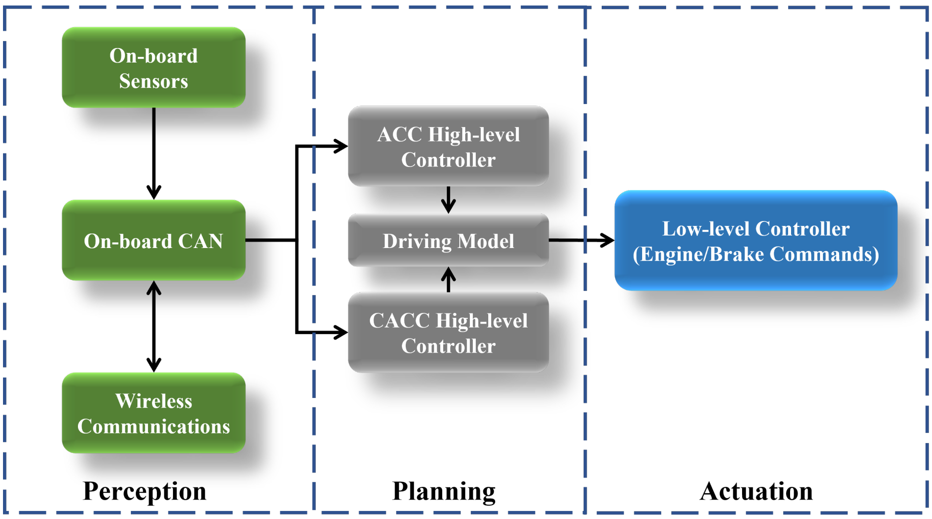

Figure 3.2. System architecture block diagram of CACC

In the context of the MVCC system, information flow topology (IFT) refers to the network structure that governs the exchange of information between different vehicles and between vehicles and their control system. The information flow topology is a critical aspect of the control system, as it determines how information is distributed, processed, and utilised by the various components of the system. In an MVCC system, information is typically exchanged using wireless communication links. The information flow topology defines the structure of these links, including which vehicles are connected to which other vehicles, and how information is transmitted and received across the network. The information flow topology can be

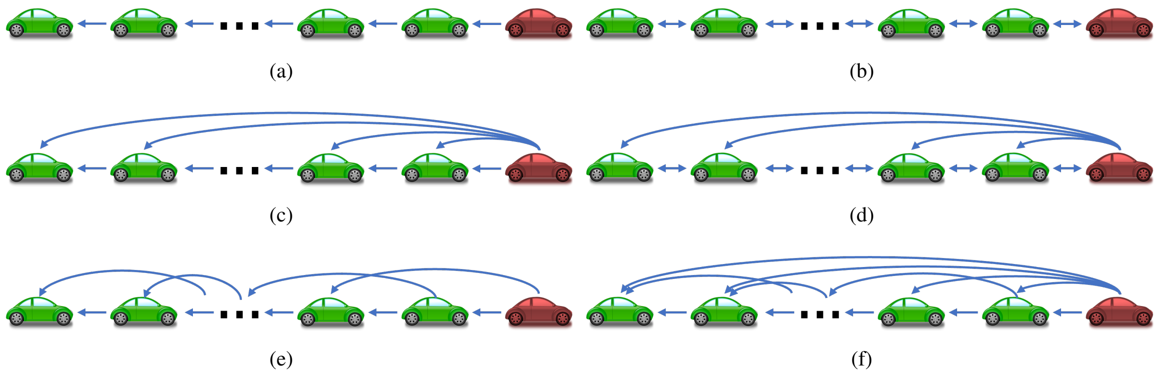

Figure 3.3. Common information flow topologies, where red cars represent the leader and green cars represent the following vehicles. (a) predecessor following [75]; (b) bidirectional [76]; (c) predecessor leader following [77]; (d) bidirectional-leader [78]; (e) two-predecessor following [77]; (f) two-predecessor-leader following [79].

represented as a graph, where the vehicles are represented as nodes and the communication links are represented as edges.

The control algorithm of the CACC system is mainly to plan the longitudinal motion of the vehicle. This longitudinal motion planning requires wireless communication data as the input of the CACC system control algorithm. Therefore, defining an IFT is very important for designing control algorithms for the CACC system. It not only affects the convergence speed and stability of the CACC system consistency but also affects the design of the control algorithm of the CACC system. By carefully selecting the connectivity and communication protocols between vehicles, the system can ensure that information is shared in a timely and efficient manner, enabling coordinated actions among the vehicles. In addition, a well-designed information flow topology can also enhance the robustness and fault-tolerance of the system, by enabling redundant communication paths and alternative routes for information exchange. Some typical IFTs include predecessor following (PF) [75], bidirectional (BD) [76], predecessor leader following (PLF) [77], bidirectional-leader (BDL) [78], two-predecessor following (TPF) [77], two-predecessor-leader following (TPLF) [79], which are illustrated in Fig. 3.3. In existing practical applications, PF and BD have been more widely used due to the more mature and reliable onboard sensors. However, with the development of wireless communication technology, PLF, BDL, TPF, and TPLF are also gradually studied and developed. In the network-connected distributed control framework, more information flow topology will be researched and applied.

3.2.2 System strategies

Adaptive cruise control

ACC system is a driver assistance technology that uses sensors to automatically adjust the speed and following distance of a vehicle based on the distance and speed of other vehicles on the road. The system typically uses radar or lidar sensors, along with cameras and computer algorithms, to monitor the vehicle's surroundings and respond accordingly. The basic idea of the ACC system is to maintain a safe distance from the vehicle ahead, while also reducing the workload of the driver in terms of accelerating and decelerating. This is accomplished by automatically adjusting the speed of the vehicle and controlling the throttle and brakes, based on real-time traffic conditions.

ACC system is a typical application [80] and has gradually become a standard ADAS of automobiles. Typically, deployed ACC systems operate in a limited velocity range of 40 km/h to 160 km/h with a maximum braking deceleration of approximately 0.5 g [81]. Without a preceding vehicle, a vehicle equipped with an ACC system travels at a user-set velocity, which is similar to the traditional cruise control system. When a preceding vehicle is detected, the ACC system calculates and determines if the vehicle is still travelling safely at the user-set velocity. If the preceding vehicle is too close to the host vehicle or if the preceding vehicle is travelling too slowly, the ACC system will automatically accelerate or decelerate, shifting from user-set velocity control to user-set safety distance control [82]. This is implemented by using a laser or radar to measure the relative distance between the host vehicle and the vehicle in front of it [83]. This kind of safety distance is influenced by the spacing strategies [84]. In the mainstream ACC system design, OEMs use two spacing strategies, namely the constant spacing strategy [85] and the variable spacing strategy [86]. Through the ACC system strategies of major vehicle OEMs, it is clear that the variable spacing strategy is preferred in more complex and changing traffic environments [87]–[89]. The ACC system does play a substantial role in relieving driver fatigue and reducing traffic congestion in highway scenarios and has also been recognized by the market [90]. But in complex road conditions at low speeds, the conventional ACC system no longer has applicability. This is because in complex road conditions and low-speed driving, the vehicle's acceleration and deceleration actions are more frequent, and the conventional ACC system may not be able to respond to these changes in a timely manner, resulting in an insufficiently safe distance from the vehicle ahead. The Stop and go control system is an extension of the ACC system, designed to reduce driver workload in urban areas where the ACC system is virtually ineffective [91].

However, the ACC system still has many shortcomings. For example, the current ACC system cannot accurately determine the sudden lane-changing of vehicles in the adjacent lane through the existing distance sensors alone, which can make the ACC system unable to complete the deceleration in a short time, thus causing tailgating [92]. On roads with large curves, the onboard distance sensor may lose the view of the vehicle in front of it, causing the ACC system to make a false determination that there is no vehicle ahead. This misjudgment can cause the vehicle to travel at the user-set velocity in the ACC system and increase the risk of a collision [93]. Additionally, the ACC system is actually susceptible to over-aggressive deceleration due to the deceleration behaviour of the vehicle ahead, i.e., successive vehicles equipped with the ACC system can substantially amplify the initial disturbance, even beyond the intelligent driver model (IDM) [10]. This amplification of the initial disturbance can create a significant crash risk for vehicle fleets equipped with ACC systems. The development of connected automobile technology offers the possibility to solve these challenges mentioned above [94]. Communication connection technology can obtain information not only about lane-changing of adjacent vehicles but also about the status of vehicles beyond the field of view of the onboard sensors. Obtaining this enhanced information can effectively reduce the number of failure scenarios for the ACC system.

Cooperative adaptive cruise control

Remarkable advances in CAVs have been achieved over the last two decades, with V2V communication, in particular, gaining widespread adoption [77]. Connectivity and automation are both integrated into the intelligent vehicles, enabling them to not only drive by themselves through onboard sensing but also to communicate with each other through V2V communication [95]. The CACC system is one of the most prospective technologies for CAVs, which extends the ACC system with cooperative control of CAVs.

The constant time spacing strategy is widely used in the CACC system. In general, the following equation is used to describe the CACC system model,

$$
\begin{aligned}
d_i(t) &= L + h_d \dot{x}_i(t) \ , \\
e_i(t) &= x_{i-1}(t) - x_i(t) - d_i(t) \ ,
\end{aligned}
\tag{3.1}
$$

where L represents the constant standstill distance between the two vehicles and also the minimum safe distance between two vehicles. $\dot{x}_i(t)$ denotes the velocity of the following vehicle. $x_i(t)$ and $x_{i-1}(t)$ represent, respectively, the position of the following and preceding vehicle. h_d is the desired time headway, $e_i(t)$ is the spacing error of i^{th} vehicle. CACC system model (3.1) describes such a realistic application scenario: when the velocity of the preceding vehicle drops to zero in a very short time, the time required for the following vehicle to travel at the current speed to the minimum safe distance is h_d. The following vehicle needs to decelerate effectively within the time h_d to avoid a collision with the preceding vehicle. Obviously, the following distance should be increased when the velocity of the following vehicle is larger.

In practical engineering applications, the CACC system usually has four modes, namely, speed control mode, gap control mode, gap-closing control mode, and collision avoidance control mode [12]. Taking the CACC system mode in Simulation of Urban Mobility (SUMO) as an example, the different models are defined as follows [96].

- Speed control mode: the CACC system switches to speed control mode when the headway is greater than 2 s [11] or when no preceding vehicle is within detection or communication range of the vehicle, i.e. the vehicle travels at the driver's desired driving speed.
- Gap control mode: when the distance between the front and rear is less than 0.2 m [11] or the speed difference is less than 0.1 m/s [11], this mode is activated to keep a fixed headway time distance with the front vehicle for driving.
- Gap-closing control mode: this mode is activated when the time distance between the front and rear ends is less than 1.5 s[11]. This mode ensures a smooth transition between the speed control and Gap control modes.
- Collision avoidance control mode: this mode is activated when the headway time distance is less than 1.5 s or the spacing deviation is negative. The main purpose of this

mode is to avoid rear-end collisions between vehicles [96].

3.3 Control

Generally speaking, the control objectives of an MVCC system mainly include appropriate inter-vehicle distance, consistent driving velocity, and safety avoidance between vehicles. These are the three most basic and obvious objectives of the MVCC algorithm. In addition, the energy consumption [16] of the vehicle, and the string stability of the MVS is also often one of the objectives of the MVCC system.

3.3.1 PD/PID control

Proportional-derivative (PD) and proportional-integral-derivative (PID) are the main control methods in the existing commercial MVCC system. In general, the front and rear spacing errors will be the feedback signal of the controller. Most OEMs use this traditional automatic control method to achieve the CACC system because PID has the characteristics of a simple algorithm principle, is easy to be implemented, and has simple parameters. Both Wang [13] and Gong [14] used an adaptive PD controller to design the CACC system under TPL information flow topology. Each specific IFT may be urgently exchanged for other forms of IFTs in actual operation. The adaptive PD controller is not highly dependent on the form of IFT, and it can be applied to most IFTs. the following behaviour of the vehicle is continuously determined during the operation of the adaptive PD controller vehicle, based on the degradation of the IFT. Also, the confirmation of dynamic parameters ensures the string stability of the MVS. Gong et al. [97] developed a parameter self-tuning fuzzy PID algorithm to design an ACC strategy. The parameters of the PID controller are adjusted online by fuzzy rules according to the traffic conditions. The results show that the parameter self-tuning fuzzy PID controller combines the advantages of PID controller and fuzzy controller. The control algorithm improves the driving safety of ACC and exhibits higher system response speed and driving comfort. Similarly, a learning control method combining a deep deterministic policy gradient and a PID controller was proposed by Yang et al.[98]. In line with the idea of fuzzy control, the method is also desired to dynamically adjust the parameters of the PID online. In this work, the authors automate the weight adjustment process of the PID parameters by deep reinforcement learning. The results show that by using the proposed method, the time for the vehicle platooning system to enter the steady state is reduced. The performance of the maximum distance error is also effectively improved.

3.3.2 Consensus control

The communication range of CAVs is limited and it is impossible to communicate with vehicles outside the communication range, so the network-connected distributed control framework is clearly the better solution for the MVCC system. This network-connected distributed control framework provides the possibility for the application of consensus control. The consensus control algorithm has proven to be an effective and efficient application in the control of vehicle CACC systems. Instead of relying on a centralized scheme that assumes the availability of global team knowledge to all network agents, a consensus-based approach can serve as a distributed scheme that operates through local interactions and evolves in parallel [18]. Additionally, the consensus control algorithm allows for more reliable coordination between vehicles, resulting in smoother and smoother flow, which results in improved safety and more efficient travel for all participants [99]. Ultimately, the application of consensus control algorithms has allowed for reliable and effective control of CACC systems, resulting in improved safety and efficiency for all drivers. The most basic consensus control algorithm can be expressed as:

$$\dot{x}_i(t) = -\sum_{j=1}^{n} a_{ij}(t)\left(x_i(t) - x_j(t)\right), i = 1, \ldots, n \tag{3.2}$$

where $a_{ij}(t)$ is the (i,j) entry of the adjacency matrix of the associated communication graph of the system at time t, $x_i(t)$ is the position information of the i^{th} vehicle. Obviously, this consensus algorithm will make the state of the agent tend to the state of the neighbourhood. In the MVCC system, we construct vehicles into a multi-agent network, with each vehicle corresponding to one agent. The state of each vehicle and the state of the front and rear vehicles always tend to reach the same agreement, which is the control objective of the MVCC system. Therefore, it is feasible to realise the MVCC system by the consensus control algorithm.

For consensus algorithms, a typical linear control algorithm, communication latency, nonlinearity, and heterogeneous MVSs all pose challenges to the feasibility of consensus control algorithms. Essentially, the control objectives of the MVCC system can be considered as a problem of achieving consensus in a network of dynamic systems affected by time-varying heterogeneous delays due to inter-vehicle wireless communication [17]. Typically, consensus control is used as a high-level control method to model the vehicle as a linear dynamics model. Consensus control focuses more on the interaction between vehicles and the dynamic changes of the vehicle information flow topology. In [100], the vehicle is modelled as a linear, second-order mass point dynamics model. A four-layer linear control framework in a connected vehicle environment is proposed to simultaneously achieve vehicle consensus in both the longitudinal and lateral directions. However, a single linear consensus controller can no longer meet realistic needs. Hu et al.[101] design a CACC system for a heterogeneous MVS using adaptive control combined with consensus control. To address the limitations of the consensus control algorithm in linear systems, they use a feedback linearisation tool to linearize the nonlinear vehicle model so that the consensus algorithm is feasible. Li et al. [102] design a control algorithm for connecting platoons of CAVs based on distributed nonlinear consensus with delay dependence. Specifically, a nonlinear function was designed to describe the inter-vehicle following interactions among CAVs, taking into account the fact that the behaviour of following vehicles depends on the distance to the preceding vehicle. The algorithm incorporates both the inter-vehicle following interactions and heterogeneous time delays. The convergence conditions of the proposed algorithm, which depend on the time delay, were analyzed using the Lyapunov-Krasovskii methods, and the algorithm's delay constraints were estimated. The proposed algorithm ensures both the consensus of CAVs and the consistency of vehicle behaviour with traffic flow theory. More consensus controllers have been designed for the cooperative control of nonlinear MVSs [21], [103], [104].

In [105], Wang et al. proposed a novel CACC system based on a distributed consensus algorithm that takes into account time-varying communication delays, as well as the length of different vehicles, the location of GPS antennas, and braking capabilities. In addition, they developed a distributed consensus protocol that enables the CACC system to handle the algorithm for formation platooning, merging, and splitting. Li et al. [106] presents a control strategy for interconnecting platoons of CAVs based on nonlinear consensus under different communication topologies. Specifically, the protocol uses pinning control to incorporate interaction between vehicles under both fixed and switching communication topologies. The proposed protocol's finite-time stability and consensus are analyzed rigorously using LaSalle's invariance principle and Lyapunov techniques. The theoretical analysis investigates how the communication topology affects the convergence and stability of the CAV platoon. The simulation results demonstrate the protocol's effectiveness in achieving stable convergence with respect to position and velocity profiles, reducing the convergence time. In order to resist the negative effects of both dynamic topology and time-varying communication delays, Yu [107] and their team conducted research on a distributed consensus protocol for a connected vehicle platoon with heterogeneous time-varying delays and switching topologies. To describe the longitudinal dynamic characteristics of the vehicles in the platoon, they proposed a third-order dynamic model that included a powertrain system inertia lag. In order to stabilise the heterogeneous vehicle platoon under external disturbances, they designed a novel distributed adaptive consensus protocol that took into account the time-varying delays and randomly switching communication topologies among the vehicles. Additionally, a method that depends on the delay range was adopted to handle the system's heterogeneous time-varying delays, which were characteristic of the platoon. Overall, the instability of communication remains a major challenge to be addressed for multi-vehicle consensus control. This instability includes transient loss of communication, time-varying delays, packet loss of transmission data, and network attacks. A lot of research is still needed to solve this challenge from the perspective of control methods, state estimation, and cybersecurity.

3.3.3 Optimisation-based control

Many research works consider optimal control as an effective method to implement MVCC systems. In general, the optimal controller design of an MVCC system can be equivalently formulated as a structured convex optimisation problem with the objective of minimising energy consumption or travel time. This allows the MVCC system implemented by optimal control to gain advantages in terms of energy consumption, the convergence time of the system, and other parameters. Also, optimal control methods usually consider nonlinearities and constraints, such as vehicle dynamics and vehicle aerodynamics. These advantages are not available for most consensus control methods.

Based on the properties of optimal control, it is easy to transform solving the control input of an MVCC system into solving an optimisation problem that results in the lowest energy consumption of the MVCC system. Minimising the overall fuel consumption Q_f, driving along the road, from a time 0 to time T, would require an operating strategy minimising

$$Q_f = \int_0^T q_f(\dot{x}_i(t), \ddot{x}_i(t))\mathrm{d}t \tag{3.3}$$

where q_f is the current fuel consumption depending on the vehicle's time-varying velocity $\dot{x}_i(t)$ and acceleration $\ddot{x}_i(t)$. The CACC system designed and developed according to this idea is called the Eco-CACC system. In [15], the authors construct energy consumption as a nonlinear function of acceleration and velocity. The optimal vehicle acceleration and velocity are obtained by solving a convex optimisation problem so that the energy consumption of the CACC system can be minimized. Also from the perspective of environmental protection, Wang et al. [105] propose a platoon-wide Eco-CACC system that aims to minimize the overall energy consumption and pollutant emissions of the platoon during CACC operation. Using optimal control for CACC system development, the final objective function to be optimised is similar, despite the different modelling approaches. Among the existing applications on optimal control in CACC, achieving energy consumption minimisation is the dominant control objective. More similar studies can be found in the literature [108]–[110].

In existing research, MPC is widely used. Essentially, MPC is a truncated version of optimal control. Unlike optimal control, MPC does not emphasise the optimality of the entire control process (time-domain) but retreats to consider only a finite number of future control cycles. Thomas et al. [16] develop a linear MPC method for CACC system that directly minimises fuel consumption rather than vehicle acceleration. In research [111], the authors use the MPC method to design a CACC system for the Volvo S60. Safety and string stability was enhanced by imposing additional constraints on the optimisation problem. In the design of the controller, the acceleration of the front vehicle is used as a measured disturbance, which leads to faster responses and shorter inter-vehicle distances. Bu et al. [112] developed a new CACC system based on the factory ACC system of the Infiniti FX-45 vehicle by adding a wireless communication system and an indirect adaptive MPC-based spacing adjustment controller. Unlike the previous controller design, in the MPC design here, the optimisation problem solves to minimising of the time gap error and smoother control inputs. Compared to the stock ACC system, the upgraded CACC system reduces the following distance while ensuring no collisions. In addition, the comfort of the vehicle has been improved.

Actually, traditional MPC implemented in a centralized manner assumes that all states are known. However, obtaining the state information of all agents and computing large-scale optimisation problems are very difficult, which makes centralized MPC not suitable for MVCC systems with large-scale quantities. Therefore, distributed MPC (DMPC) schemes have been proposed to solve this problem. Essentially, there is no obvious difference between distributed DMPC and traditional MPC except for the difference in the scope of information acquisition. Tapli et al. [19] designed a vehicle CACC system under bidirectional communication using DMPC. In the distributed controller design, the authors model the input and output errors as penalty functions and also introduce the idea of consensus control to keep the state of the vehicle close to the state of neighbouring vehicles. Similarly, Nie et al. [20] proposes a DMPC algorithm to solve the cruise control problem for a heterogeneous MVS. The vehicles in the MVS are dynamically decoupled with different dynamic parameters, which means that this DMPC controller can cope with unintended switching of the IFT. The cost function of the locally optimal control algorithm for each vehicle is designed with traceability as the control objective, and its asymptotic stability is ensured by using a terminal constraint approach.

In general, optimisation-based control methods are more capable of diversifying control objectives than consensus control and PD/PID control. Different control objectives can be achieved by designing different objective functions and constraints. Nowadays, the design of CACC systems is not only limited to the following distance and vehicle state consistency, but more and more OEMs are focusing on the environmental protection of the vehicle, passenger comfort, etc., which makes the optimisation-based control methods more and more popular in the design of existing CACC systems.

3.3.4 Reinforcement learning

Reinforcement learning (RL) has been applied to MVCC systems such as the CACC system and vehicle platoon. As a data-driven control-based approach, reinforcement learning does not rely highly on an accurate dynamics model. Therefore, reinforcement learning is advantageous in dealing with cooperative control tasks of heterogeneous multi-vehicle systems. Contending for a heterogeneous CACC system, Farag et al. [22] used the Deep Deterministic Policy Gradient (DDPG) algorithm and MPC control method for vehicle platooning, respectively. By comparing the performance of the two methods it was concluded that the DDPG-based RL controller outperformed MPC in terms of computation time and control effort, especially in more realistic and complex situations, while maintaining similar root mean square error of distance between vehicles. However, DDPG has the problem of low efficiency in exploring continuous action space, and single or homogenised vehicle data will reduce the robustness of the model. Although GGPG has an excellent performance in the MVCC system, there are still many challenges. Therefore, Lu et al. [23] proposes a platoon sharing deep deterministic policy gradient algorithm (PSDDPG) for multi-vehicle networks to improve the exploration efficiency of this controller in continuous action space. In addition, additional queuing noise is added to the noise-based DDPG algorithm to improve the diversity of training samples during the exploration process, thereby achieving the goal of improving model robustness. In [113], a deep reinforcement learning-based CACC system has been developed that allows platooning vehicles to learn a robust communication protocol alongside their coordination policies. Long short term memory (LSTM) model is used to implement the ACC system for each vehicle and trained using policy gradients. To coordinate driving, the LSTM of each vehicle adaptively exchanges relevant information with other vehicles to form the CACC system. This reduces the control difficulty caused by dynamic information flow topology in the CACC system. Shi et al. [114] propose a cooperative strategy of CAVs longitudinal control for a mixed connected and automated traffic environment based on a deep reinforcement learning algorithm, which enhances the string stability of mixed traffic, car following efficiency, and energy efficiency. The difference between the results of these two studies is that the approach proposed by Shi et al. is to obtain an effective control policy through reinforcement learning. While the method in [113] is more concerned with obtaining an optimised communication protocol. Unfortunately, these MVCC systems using RL methods are still in the theoretical research stage. There are still many challenges in real-vehicle validation as well as commercialisation.

3.3.5 Impact of wireless communication

MVCC system is highly dependent on wireless communication between vehicles. V2V communication provides enhanced information that enables vehicles to follow the vehicle in front with greater accuracy, faster response time, and shorter gaps. As a result, the stability of traffic flow and the safety of the vehicle are both improved [115]. It is due to the high dependence of the MVCC systems on V2V communication that the quality and stability of V2V communication will have an immediate impact on the performance of the MVCC system. Specifically, the communication delay will increase the risk of collision between CACC fleets, and secondly, in the case of communication loss, the CACC system will degrade to ACC, thus causing the fleet stability to decrease and the risk of collision to increase. Xing et al. [116] propose the use of a Smith predictor to compensate for the communication delay in homogeneous CACC systems in order to take more advantage of the CACC system from a road throughput perspective. In Zhang's study, a novel CACC controller based on optimal control in the space domain is proposed, where all variables are a function of longitudinal position rather than time. By developing the CACC in the space domain instead of the time-domain, its robustness to communication delay is greatly improved, thus reducing the minimum safety interval buffer and leading to better manoeuvrability [117]. More approaches for optimising the CACC systems in communication delay scenarios can be found in [118]–[120]. Compared to communication delays, communication loss poses a more serious hazard to the CACC system [121]. Acciani et al. [122] model communication losses as independent stochastic events and design a cooperative controller to mitigate their effects. This distributed cooperative controller is to make the variance of the trajectory minimised when this stochastic event occurs. From another perspective, when communication loss occurs, the CACC controller is missing feedback input. State estimation methods can obtain a suitable state estimate value in place of the feedback input. Wu et al. [123] use an adaptive Kalman filter for state estimation, which greatly eliminates the negative effects of transient loss of communication. In addition, there are more research results on solving system degradation of CACC due to unreliable V2V Communication in [124]–[126].

3.4 Applications

As shown in Fig. 3.4, the MVCC system can be applied in vehicle platooning, multi-vehicle cooperative lane-changing and merging, and cooperative driving at complex intersections. In the following sections, the multi-vehicle cooperative solutions are reviewed based

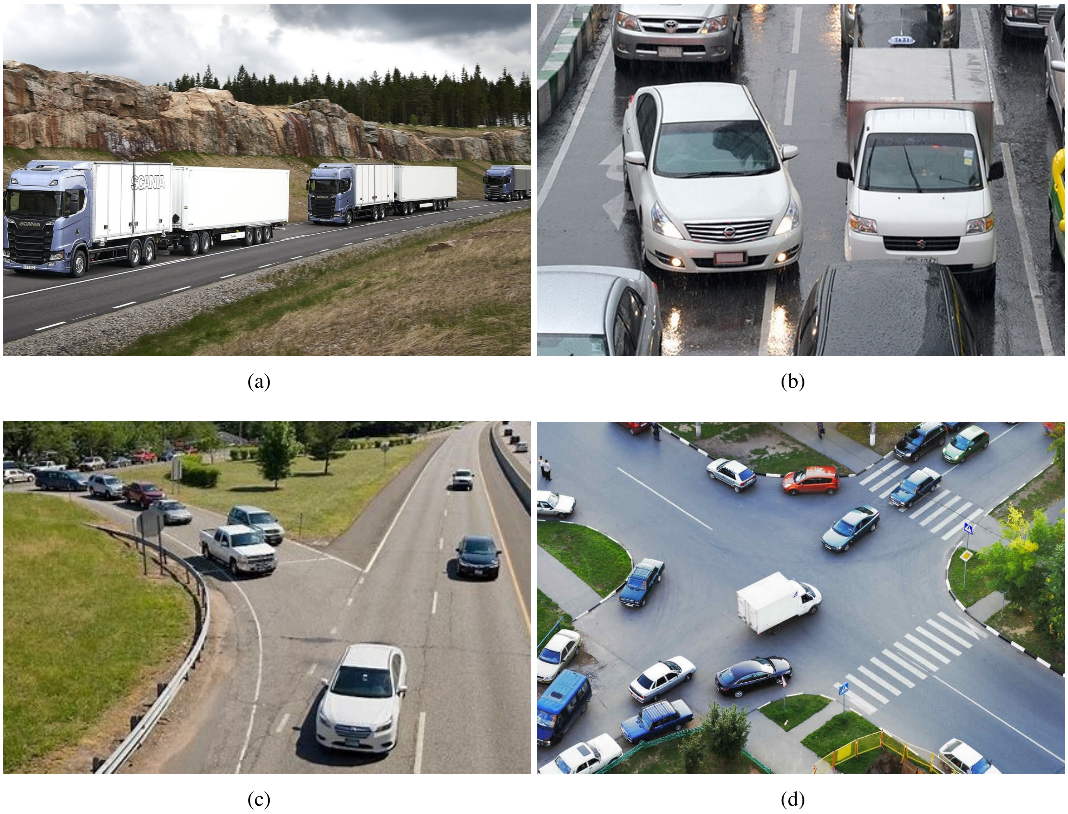

Figure 3.4. Potential application scenarios for multi-vehicle collaboration: (a). cooperative adaptive cruise of vehicles (adopted from: www.autotrader.co.uk), (b). cooperative lane-changing or merging of vehicles (adopted from: www.roadsafetyuae.com), (c). merging of vehicles on ramps (adopted from: www.myrecordjournal.com), (d). cooperative driving at complex intersections (adopted from: https://xsj.699pic.com).

on application scenarios.

3.4.1 Multi-vehicle platooning technology

Platooning technology is a special application scenario of the MVCC system. When multiple vehicles are connected through the CACC system to form a stable MVS, all vehicles except the lead vehicle are in automatic follow mode, which is platooning. In the past decade, autonomous driving technology has received great attention, and companies such as Waymo and Tesla have made outstanding achievements in the field of autonomous driving. However, from the perspective of the capital market and the development of the autonomous driving industry in recent years, the commercialisation of L4 and above autonomous driving technology has not been satisfactory, and the industry has frequently experienced bankruptcies, layoffs, and decreased valuations. Car manufacturers and autonomous driving technology companies are investing more effort in achieving mass production of L2 and L3 autonomous driving technology. With the commercialisation of L4 autonomous driving technology still a distant prospect, it is expected that platooning technology will become a backup option.

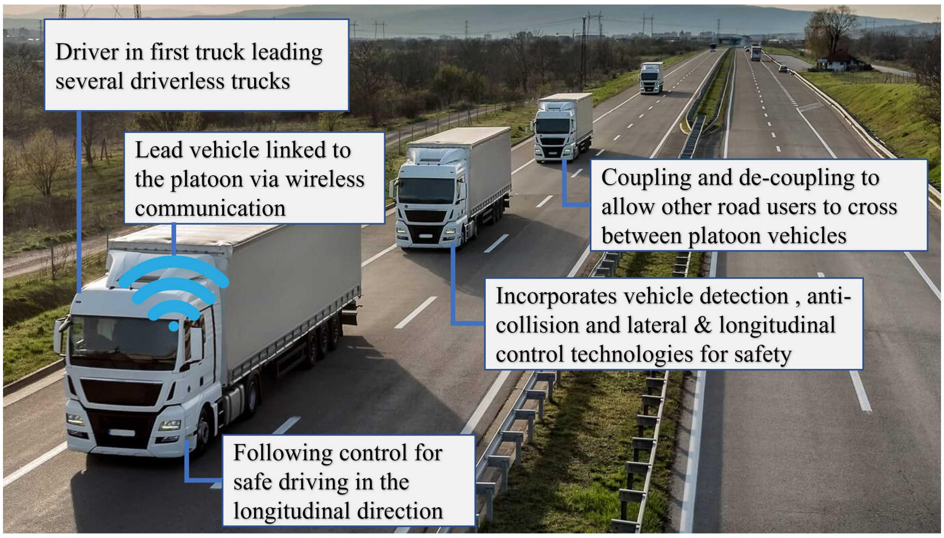

Figure 3.5. A commercially promising truck platooning transportation solution

In certain scenarios, such as large factories, mines, ports, logistics parks, and long-distance transportation, a multi-vehicle management system based on a platooning model seems to be a more promising solution for implementing autonomous driving technology. As shown in Fig. 3.5, in this mode, a fleet of several vehicles is led by a human driver in the first vehicle, while the following vehicles automatically follow. The following vehicles will drive in the same way as the preceding vehicle, including accelerating, changing direction, braking, and maintaining a certain formation. This configuration makes it possible for a single driver to manage multiple vehicles, saving on labour costs. In the event of special circumstances or technical malfunctions, the driver of the leading vehicle can still address the issues of the following vehicles, making the entire platoon of vehicles controllable. Platooning management is not truly autonomous driving technology but rather uses automated control to expand the driver's management range and handle unforeseeable situations that autonomous driving technology may encounter. This is undoubtedly a compromise, and it is also a relatively easy route to implement autonomous driving technology today.

The application of vehicle platooning technology, especially truck platooning, has been studied for a long time. California PATH Program [68], KONVOI project of RWTH Aachen University [127], Energy ITS project of Japan [128] delve into the impact of truck platooning technology in terms of energy savings and highway capacity, and CO_2 emissions. In general, the technical solution for implementing platooning are still largely convergent. The main functions implemented include lateral sensing and control, and longitudinal sensing and control. The lateral sensing relies on LIDAR, millimetre wave radar, ultrasonic radar, and vision sensors. The lateral control algorithm is based on the lateral deviation from the lane markers as a reference and the yaw angle relative to the lane markers [129]. For longitudinal sensing, it relies on V2V communication in addition to distance and vision sensors. The control inputs for longitudinal control are expressed as speed and clearance differences between the vehicle in front and the vehicle behind [130]. The CACC system is one of the most typical longitudinal control systems in platooning technology and is also the most widely used system. Some mainstream heavy truck manufacturers and research institutes have already implemented platooning technology to try in trucking. Daimler Trucks implemented a truck platoon with 3 identical Mercedes-Benz Actros trucks. Daimler Trucks successfully participated in the European Truck Platooning Challenge in April 2016 in Rotterdam and demonstrated to the community that truck platoons can be ready for public roads [131]. Nowakowski et al. [132] implemented PATH's third-generation CACC system for heavy trucks by adding dedicated short-range communications to the existing ACC system of Volvo heavy trucks. The upgraded system provides enhanced string stability, faster responses, and shorter gap settings than the production ACC system. Researchers for the "Partial Automation for Truck Platooning" (PATP) project and the "Driver-Assistive Truck Platooning" (DATP) project from the Federal Highway Administration, United States [133] developed CACC systems for commercial trucks that used DSRC for V2V communication, which allowed the trucks to safely maintain a constant time gap in the PATP project and a constant following distance in the DATP project. When engaged, a following truck's acceleration and braking were controlled by the CACC system. In addition, more platooning technology companies such as Peloton, Locomotion, Scania, etc. are gradually trying to commercialise this technology.

Although the development and commercialisation of platooning technology are relatively optimistic, there are still challenges to fully commercialising the technology on a large scale. One of the major challenges is to solve the dynamic decoupling and coupling problem in large-scale platooning fleets, which is critical for ensuring the safety and stability of the fleet under the intervention of external road users. In addition, cyber-attacks, loss of communication, etc. pose significant threats to platooning vehicle fleets, emphasising the need to refine and enhance cyber security in vehicle platooning technology.

3.4.2 Multi-vehicle cooperative lane-changing

Crash data from 2010 to 2017 [134] shows that the sudden lane-changing caused about 17.0% of total severe crashes, followed by speeding (12.8%) and tailgating (11.2%). This crash data also indicates that the severity of lane-change-related crashes is relatively high compared to other crash causes [134]. MVCC system offers the potential to reduce lane-changing collisions. The development of information interconnection technology has made it easy for vehicles to share lane-changing information within a localised range. This distributed information sharing provides the possibility for multi-vehicle cooperative lane-changing. Vehicles are able to plan their own lane-changing timing and change trajectory based on the lane-changing signals, position, speed, and acceleration signals of neighbouring vehicles in the local range.

Cooperative lane-changing stratery

Wang et al. [69] proposed a cooperative lane-changing strategy based on MPC to mitigate the adverse impact of lane-changing on traffic flow. The proposed strategy achieved active cooperation among the main vehicle performing lane-changing on the target lane and the leading and following vehicles on the target lane during the lane-changing process. In this MPC controller, safety, comfort, and traffic efficiency were modelled as optimisation objectives. Numerical simulation results of the cooperative lane-changing strategy demonstrated a reduction in the deceleration of following vehicles compared to traditional lane-changing, and the propagation of shockwaves in traffic flow can be alleviated to some extent. The research team from Chang'an University [135] has proposed a centralized, two-stage optimisation-based cooperative lane-changing method for CAVs on two-lane highways. The proposed method aims to minimise negative impacts on the traffic flow of both lanes by facilitating effective coordination between the changing vehicle and subsequent vehicles on both the target and original lanes. By solving a constrained optimisation demonstrated a reduction in the deceleration of following vehicles compared to traditional lane-changing, the ideal longitudinal control acceleration for each cooperative vehicle is generated. The results demonstrate that the proposed method can achieve safe and smooth cooperative lane-changing in a given driving scenario and reduce lane-changing vibrations on both the original and target lanes.

Ni et al. [136] propose a novel multi-vehicle cooperative lane-changing strategy for an interconnected vehicle environment. Unlike other lane-changing strategies, this approach determines the feasibility of cooperative lane-changing operations by establishing a gain function based on an incentive model. Specifically, the feasibility of cooperation is determined by comparing the gains from lane-changing and lane-keeping under current conditions. Once the lane-changing decision is obtained, a multi-objective optimal control function for cooperative lane-changing is established based on MPC to achieve distributed control. For the execution of lane-changing, the authors propose a novel two-stage cooperative lane-changing framework that divides the lane-changing process into a lane-changing stage and a longitudinal lane-adjustment stage. This two-stage lane-changing framework is important for solving complex numerical problems caused by collision constraints and the nonlinear dynamics of vehicles. However, most of the above-mentioned multi-vehicle lane-changing methods are passive and opportunistic, as they are only implemented when the environment allows for them. The new approach proposed by Kim et al. [137] relies on the role of facilitators assigned to CAVs. The facilitators interact with and modify the environment to enable other CAVs to change lanes. A distributed MPC path planner and a distributed coordination algorithm are used to control the facilitators and other CAVs in a proactive and cooperative manner.

Trajectory generation for cooperative lane-changing

In a multi-vehicle dynamic environment, it is extremely important to generate safe, comfortable lane-changing trajectories for vehicles that have already obtained lane-changing decisions. Li et al. [138] conducted research on collaborative lane-changing trajectory planning for vehicles in mandatory lane-changing scenarios. They propose an innovative model that considers traffic scenarios with multiple mandatory lane-changing requirements and accomplishes vehicle trajectory planning by considering safety and efficiency. The limitation of the model is that it does not take into account the free lane-changing scenario. Using similar ideas, Luo et al. [139] transform cooperative lane-changing into an optimisation solution problem, considering both same-direction and intersectant-direction lane-changing scenarios, ultimately maximising safety, comfort, and lane-changing efficiency. Among the many studies on collaborative lane-changing, multi-objective optimisation has received great attention and is widely used in the generation of lane-changing trajectories [136], [140].

Decision-making for cooperative lane-changing

From a fundamental perspective, trajectory generation for lane-changing in a multi-vehicle collaboration scenario is similar to trajectory generation in other scenarios. Research in this area focuses mainly on the decision-making process for lane-changing. In existing research, most multi-vehicle lane-changing strategies are based on specific rules. These rule-based strategies typically involve the establishment of a rule system. However, when traffic scenarios become more complex, the limitations of this system become evident, as new rules must be continuously added to the system. The addition of a large number of rules reduces the system's interpretability. In recent years, the development of computer computational capabilities and the increase in data has provided a foundation for the application of machine learning in multi-vehicle cooperative lane-changing decision-making. Machine learning provides new opportunities for autonomous driving by allowing strategies to be learned through data and experience. In particular, reinforcement learning [135] makes it feasible for vehicles to learn strategies through interaction with the environment. Reinforcement learning can address large-scale systems with potentially infinite states and action spaces in a model-free manner. However, such cooperative lane-changing strategies based on reinforcement learning are currently only in the simulation stage, and their reliability and safety in actual traffic scenarios have not been widely verified.

3.4.3 Multi-vehicle cooperative merging

With the increasing number of vehicles on the road, managing traffic congestion during peak hours has become a major challenge for urban transportation systems. In this context, multi-vehicle cooperative merging has emerged as an important task for traffic management. This technique involves using V2V communication to coordinate the movement of multiple vehicles simultaneously merging onto a highway or a main road, with the aim of reducing traffic congestion. In the process of merging, the combination of wireless communication and vehicular sensors forms a MAS for intelligent vehicles. The resulting MVS, composed of these interconnected vehicles, is susceptible to unstable cascading effects due to external interferences. When a vehicle or queue merges with another, a new interconnected MVS is formed, and this merging behaviour must ensure the stability of the new system; otherwise, traffic flow disruptions may occur.

Cooperative on-ramp merging

Cooperative on-ramp merging is a very common scenario. How to choose the merging timing and speed, and how to ensure the stability of traffic flow after merging have been investigated in [70], [73]. A typical technological approach consists of a two-tiered merging control framework, which is comprised of centralised sorting and distributed control. Roadside proxies installed in the merging area determine the merging order of approaching vehicles based on estimated arrival times at the merging point. Once the order is determined, the distributed controller guides the vehicles through the merging process. To achieve stable queueing of the resulting new traffic flow, optimisation of the distributed control protocol is required [141]. A similar strategy appears in [73], the key difference in the algorithms for determining merging sequences lies in the increased level of coordination between the mainline platoon and the merging ramp vehicles. The mainline platoon actively creates large gaps to facilitate the smooth merging of ramp vehicles. However, a limitation of these studies is that they only consider a specific case where the merging agent is a single vehicle rather than a platoon of vehicles. Another limitation is that these studies only consider the scenario where all vehicles are connected and automated. Chen et al. [142] conducted new explorations to address these limitations. They established a multi-vehicle cooperative merging control model for the merging area of a highway with dedicated lanes for CAVs and human-driven vehicles in a mixed-traffic environment. This was done to improve the overall efficiency of the merging area on the highway in a mixed-traffic environment.

Cooperative merging on main roads

In addition to ramp merging, another common scenario is vehicles travelling on a main road making a merging. Wang et al. [143] use an MPC approach with a look-ahead design to design the lateral controller for performing the merging manoeuvre, which successfully implements the merging of a platoon with the platoon. On the basis of MPC, Hang et al.[144] proposed a cooperative decision-making framework for multi-lane merging by combining game theory methods, which adapts to different driving characteristics for CAVs at the multi-lane merging zone. This decision-making framework ensures the safety and efficiency of CAVs in complex and dynamic traffic conditions while taking into account the objectives of individual vehicles. But more than that, we should note that the merging of mixed-vehicle platoons should be studied more often. In the next two decades, CAVs and human-driven vehicles will co-exist for a long time. How to achieve a high degree of collaboration between CAVs and human-driven vehicles is a key part of achieving road traffic intelligence.

3.4.4 Multi-vehicle cooperative driving at intersections

Multi-vehicle cooperative driving refers to the coordinated control of multiple vehicles on the road, with the aim of achieving improved traffic flow, safety, and energy efficiency. At intersections, multi-vehicle cooperative driving systems can be used to facilitate efficient and safe manoeuvring of vehicles through the intersection by enabling communication and collaboration between the vehicles. Specifically, these systems use V2V and vehicle-to-infrastructure (V2I) communication to share information about vehicle positions, speeds, and intended movements. This information is then used to optimise the coordination and sequencing of vehicle movements, thereby reducing congestion and increasing safety at the intersection. Additionally, multi-vehicle cooperative driving systems may employ advanced sensing and control technologies, such as lidar, radar, and camera systems, to enhance the accuracy and reliability of the system. Overall, multi-vehicle cooperative driving has the potential to significantly improve the efficiency and safety of traffic operations at intersections.

In urban road conditions, intersections are often more prone to traffic jams and collisions. Multi-vehicle collaboration and vehicle-road collaboration can greatly alleviate traffic congestion in intersection scenarios on urban roads. A systematic review of theories and experiments on multi-vehicle collaboration at intersections is presented by Zhang et al. [145]. The authors propose that it is important to strengthen the understanding and knowledge of the coming new hybrid traffic flow, to improve the control capability of the new hybrid traffic flow, and to promote the development of cooperative control technic of intelligent and connected vehicles in the new hybrid traffic flow oriented to traffic efficiency. Complex intersections are divided into two main categories, namely intersections with and without traffic signals. The proposed co-driving solutions for different intersection types also differ significantly. For intersections with traffic control signals, the main solution is to rely on vehicle-road cooperation and vehicle-vehicle cooperation. The traffic signal agent obtains real-time vehicle status information to dynamically adjust the traffic control signal, thus improving the traffic efficiency of the intersection, while vehicle-vehicle cooperation can ensure traffic safety [72]. In contrast, at intersections lacking traffic control signals, connected vehicles rely mainly on vehicle-to-vehicle collaboration and movement prediction of environmental vehicles and pedestrians to make reasonable and safe decisions.

Unsignalised intersections with regular right-of-way

Typically, common right-of-way rules make it less difficult for vehicles to make driving decisions at unsignalised intersections. In order to reduce the rate of intersection collisions, Deng et al. [146] proposed a method for resolving multi-vehicle collision conflicts that guarantees traffic safety and efficiency. This method consists of a Speed-based Intersection Coordination Model (SICM) and a Geometry-based Intersection Coordination Algorithm (TICA). The SICM model takes the designed speed as the decision variable to reduce the difficulty of controlling the overall vehicle speed and determines the constraints in the case of multi-vehicle collisions. The TICA algorithm assigns spatial and temporal resources of the intersection by transforming time blocks into combinatorial optimisation, to pursue higher computing efficiency and shorter computation time. However, a major drawback of this speed- and geometry-based method is that it requires extremely high wireless communication quality, including extremely low latency and extremely low data packet loss. When time-varying communication delays occur, cooperative control degrades, thus affecting the safety and efficiency of traffic flow through the intersection. In [147], a networked predictive control method has been proposed based on an improved model-free adaptive predictive control approach and a distributed collaborative control scheme for multi-intersection scenarios. The approach achieves collaborative control for multiple vehicles in signal-free multi-intersection systems under time-varying communication delays. It consists of a multi-intersection edge cloud networked predictive control layer and a multi-vehicle car-following control layer. By using an edge computing controller, a moving horizon predictive control approach based on a compact form of dynamic linearisation technique can be employed to compute the control targets. Then, the signal-free multi-intersection system is decoupled into multiple interconnected control intersection subsystems, and an expected speed is assigned for each target vehicle entering the intersection subsystem. Li et al. [148] proposed a game theory framework for simulating the interactive behaviours of vehicles in uncontrolled intersection scenarios with multiple cars. The method takes into account the common traffic rules and designates a leader-follower relationship between each pair of interacting vehicles. A model based on paired leader-follower relationships is used to express the decision-making process of vehicles' interactions. The interactive decision model is combined with a parameterized intersection model, enabling the modelling and simulation of interactive traffic situations in various uncontrolled intersections.

Unsignalized intersections without regular right-of-way

The collaboration of CAVs at signal-free intersections has the potential to eliminate time losses associated with traffic signal green light times and improve traffic efficiency. Existing research on signal-free intersection collaboration mostly considers fixed lane directions, which only allow specific turning behaviours for vehicles on each lane. However, fixed lane directions may result in inefficiencies at intersections due to changes in traffic volumes and the proportion of vehicles with different turning expectations over time. Cai et al. [149] propose a method for signal-free intersection collaboration with flexible lane directions for multi-lane roads. This approach calculates the two-dimensional distribution of vehicles and arranges non-conflicting vehicles to pass through the intersection simultaneously. A formation reconstruction method is employed to achieve non-colliding longitudinal and lateral position adjustments of vehicles. Simulations were conducted with different input traffic volumes and turning ratios of passing vehicles, and the results demonstrate that this method outperforms both fixed lane direction signal-free intersection collaboration and signal-controlled intersection methods. In consideration of the absence of clear right-of-way priorities, Cheng et al. [150] integrate game theory into decision-making to provide the system with evolving cooperative and non-cooperative strategies. When the system chooses to cooperate in driving, it takes into account the conflicting relationships with adjacent vehicles and plans joint actions to optimise the overall benefits of multiple vehicles based on cooperative game theory. When the system is unable to engage in cooperative driving or respond within the time limit, the vehicle unit will adopt a non-cooperative driving approach, optimizing its trajectory only for personal gain. The proposed model can provide stability and robustness to our system, effectively addressing conflict resolution issues in intersections with unclear right-of-way priorities. Similarly, for such non-fixed-lane intersections, Ge et al. [151] indicate that collisions can be avoided by allowing neighbouring vehicles to exchange their intentions. Based on this premise, the addition of a real-time distributed MPC controller allows heterogeneous traffic to efficiently and safely traverse unsignalized intersections without assuming a fixed path of vehicles or assigning any priority among them.

3.4.5 Multi-vehicle cooperative parking

In modern cities, especially in cities with high car densities, parking has become a laborious and tedious task. In areas with more vehicles and complex environments, parking becomes a challenge. Inefficient parking tends to cause vehicle congestion in the area and reduces the operational efficiency of the parking lot. Although automatic parking technology is becoming more and more mature [152], this function only considers its own parking task and does not bring significant improvement to the operational efficiency of the whole area. The development of V2V communication and vehicle-to-infrastructure (V2I) communication brings the possibility to optimise the efficiency of parking in a specific area. The collaboration between vehicles and vehicles, and between vehicles and infrastructure, equipped with an intelligent scheduling system, can greatly improve the speed and efficiency of parking within a parking area.

System framework for multi-vehicle cooperative parking

The development of automated valet parking (AVP) has progressed for several years, aimed at reducing accidents and improving parking lot efficiency. The Japan Automobile Research Institute JARI has been commissioned to develop AVP systems and has been promoting them since 2016. In order to put AVP into practical use, DENSO TEN Limited believes that the early practical use of AVP can be verified by coordinating the following three elements: AVP-equipped vehicles, control centres, and parking lot infrastructure, in order to ensure safety [153]. Based on similar ideas and strategies, Kneissl et al. [71] proposed a distributed multi-vehicle control architecture for automatic valet parking by distributing the trajectory generation between vehicles and infrastructure. Thanks to V2V communication and V2I communication, potential collision areas can be known and these potential collision areas are then taken into account in the coordination procedure. The above strategy framework is mainly developed for CAVs and has not shown its usability for multi-vehicle cooperative parking problems in mixed scenarios. The planning and coordination strategy introduced by Kessler et al. [154] is suitable for resolving conflicts that occur in parking scenarios involving autonomous and non-cooperative human-driven vehicles in mixed traffic. By quantifying the estimated intentions of non-communicating vehicles and considering these results in the optimisation program, a good conflict-free solution can be found, and an optimised trajectory plan can be calculated. It balances the intentions of oneself and other participants, avoiding collisions. The algorithm is symmetric among vehicles, and it does not favour any particular vehicle. Fair, selfish, or altruistic behaviours are modelled in the optimisation objective function through appropriate weights. This method resolves conflicts that occur in multi-vehicle parking situations and has been demonstrated in simulated scenarios.

Motion planning for multi-vehicle cooperative parking

In [155], the autonomous parking trajectory planning problem is transformed into an optimal control problem. The shortest parking time is set as the optimal cost function, and the optimal control problem is discretized using the Gaussian pseudospectral method. The results show that this method can effectively solve the trajectory planning problem of multi-vehicle cooperative autonomous parking. Cooperative parking motion planning for MVSs involves computing feasible trajectories for multiple vehicles, essentially solving an optimisation problem. There are two main approaches to solving this motion planning problem: centralized and decentralized. Centralized computation involves computing trajectories for all vehicles at once, producing high-quality solutions but with low computational efficiency. On the other hand, decentralized computation involves partitioning the original problem into smaller subproblems and then combining them, which leads to higher computational efficiency. Li et al. [156] propose a progressive constraint dynamic optimisation (PCDO) framework to alleviate the burden of centralized computation. Specifically, PCDO discards redundant constraints during the solution process to reduce problem size and facilitate problem-solving. The results show that this computational framework is effective in solving the cooperative parking motion planning problem for MVSs and outperforms traditional centralized approaches. Additionally, more research on trajectory planning and coordination strategies for MVSs was carried out in [154], [157], [158].

3.5 Summary and remaining research directions

3.5.1 Summary

In this chapter, we provide a review of the basic system structure, control methods, and application of MVCC in modern intelligent transportation. Among them, the basic MVCC system structure and function strategy are introduced in detail. In addition, we present and analyse the application and development of PID control, linear consensus control, optimal control and reinforcement learning in MVCC systems. Moreover, we also comprehensively review the applications of MVCC, including multi-vehicle platooning, cooperative lane-changing, cooperative merging, intersection passing, and cooperative parking. Numerous research results on MVCC indicate that MVCC technology has great potential to improve traffic efficiency, reduce congestion, and enhance driving safety.

However, several challenges still need to be addressed before the technology can be widely applied. The reliability and security of wireless communication need to be improved, as the unreliability of V2X communication can directly affect the performance of MVCC. For example, it can cause degradation of the CACC system and increase the risk of vehicle collisions. It can cause time lag or lane-changing failure of vehicle cooperative lane-changing, which increases the risk of traffic accidents. Insecure V2X communication is susceptible to hacking and can cause serious safety incidents. Moreover, the development of algorithms that can handle complex and uncertain traffic scenarios is another critical research area. Since human-driven vehicles without V2V communication, vehicles with ADAS, and vehicles with fully autonomous driving capabilities will co-exist for a long time, it is necessary to develop MVCC systems that accommodate mixed traffic. Integration of the MVCC system with existing traffic infrastructure and establishing standardised communication protocols to ensure interoperability between different vehicles and systems are significant challenges that need to be addressed.

3.5.2 Remaining research directions

Despite these challenges, the future of MVCC is promising, and several potential research directions can help overcome these challenges and further advance this technology.

Cybersecurity for MVCC system: With the increasing use of wireless communication and V2V communication systems, cybersecurity becomes a critical research area. The deployment of MVCC systems introduces new cybersecurity and privacy challenges, including the protection of data transmission and the prevention of cyber-attacks [159]. Future research can focus on developing secure and privacy-preserving communication protocols and intrusion detection systems to ensure the safe and reliable operation of MVCC systems.

Integration of MVCC with intelligent transportation systems: The integration of MVCC with intelligent transportation systems (ITS) can enhance overall traffic management and control. Future research can focus on developing an integrated framework that can utilise real-time data from ITS to improve the performance of MVCC systems [160]–[162].

Multi-Agent reinforcement learning: In the future, the availability of driving scenario data and the construction of driving scenarios will become easier, which provides the conditions for the training of reinforcement learning. Therefore, it will make sense to use reinforcement learning methods for cooperative driving of vehicles. The application of reinforcement learning (RL) to MVCC is a promising research direction. RL has demonstrated significant potential for handling complex and uncertain traffic scenarios. However, the traditional RL approach is limited to single-agent environments. Therefore, multi-agent reinforcement learning (MARL) should be explored to develop cooperative control strategies for multiple vehicles [113].

Cooperative control strategies for heterogeneous MVSs: Human-driven vehicles and connected smart vehicles will co-exist in the long term. It is essential to develop cooperative control strategies and algorithms that can adapt to such complex hybrid heterogeneous MVSs. The core elements of this include the prediction of the behaviour of human-driven vehicles and the study of the stability of heterogeneous MVSs [114].

Safety of the intended functionality (SOTIF) in the multi-vehicle cooperative area: Today, the practical application of MVCC relies heavily on platooning technology and the CACC system. Especially the CACC system is gradually becoming a standard feature of smart cars. However, due to the limitations of system design, algorithms, sensors, and communication devices, scenarios of multi-vehicle cooperative function failure are bound to occur. Therefore, it is necessary to strengthen the research and exploration of SOTIF in the field of multi-vehicle collaboration. This involves how to generate a sufficient number of functional failure scenarios and how to quickly and comprehensively complete the test verification of multi-vehicle cooperative functions [163], [164].

In conclusion, the MVCC system has significant potential for improving traffic safety and efficiency and reducing environmental impacts. The proposed other valuable research directions can provide a roadmap for the development of MVCC technology and facilitate the realisation of its full potential.

Chapter 4

Distributed Motion Planning for Safe Autonomous Vehicle Overtaking

4.1 Introduction

As the number of private cars and rented vehicles increases rapidly in all countries, traffic congestion, road safety, and environmental pollution are becoming critical issues [165]. The autonomous driving and vehicle platooning strategies offer potential and realistic solutions to these challenges [166], [167]. In addition to reducing human-caused traffic accidents [168], autonomous driving and vehicle platooning may result in better fuel economy [169], reduced traffic congestion [170], improved traffic efficiency [171] and reduced environmental pollution. Extensive research has been done on autonomous vehicles' perception, decision-making, motion control, motion planning, and traffic scheduling [172]–[176]. The current research trend, however, focuses mainly on the self-driving mechanism of single-lane platoons. However, in the case of multi-lane platoons, the vehicles may face conflicting situations while operating at high speed and overtaking other vehicles due to a lack of communication among the vehicles of the different lanes. This hence affects both traffic safety and the efficiency of a large vehicle platoon.

With the advent of heterogeneous vehicle platooning techniques, the self-driving scheme has significantly improved the carrying capacity of the lanes and road safety [101]. Information exchange and sharing, collaborative sensing, and joint operation of the MVS ensure the possibility of cooperation among intelligent vehicles, thus improving the overall driving quality and driving safety [155], [177]. For instance, V2X communication in a MAS connects vehicles with the network of road facility agents. It enables information exchange and coordinated operation among vehicle agents, which significantly reduces traffic congestion in complex roads [171]. An MVS can also achieve a specific formation, i.e., maintain the desired distance between neighbouring vehicles, increase road capacity, reduce congestion, and improve traffic efficiency [178], [179]. Moreover, an MVS may bring more positive possibilities for road rescue, traffic command, and other fields [180]. Despite all these positive factors, no automotive companies have yet deployed autonomous multi-vehicle schemes into practical use.

In recent years, much progress has been made in the study of MVSs, which includes unmanned vehicle formations [181], [182], cooperative navigation of unmanned vehicles [183], and multi-vehicle merging [184], [185]. Among them, the CACC of vehicles is more relevant and will greatly improve the efficiency of existing traffics. However, many research works on such multi-vehicle platoon systems are still limited to the control of vehicle motion in a single dimension, i.e., only the longitudinal motion of the platoon can be controlled. This technique may not fulfill the requirements in most real-world applications as longitudinal motion control alone cannot deal with the situation when there exist vehicles blocking the road. Therefore, to handle unexpected scenarios on the road, safe autonomous overtaking methods should be considered in the protocol design of autonomous vehicles (AVs).

One of the most typical application scenarios of AVs is the overtaking of the MVS in a dynamic environment in which obstacles and vehicles have varying accelerations. The MVS's overtaking is a highly complex scenario, including various traffic scenarios, such as lane-changing, obstacle avoidance, formation, and target tracking. The overtaking of autonomous driving has always been a challenging research topic. In [186]–[191], overtaking decisions, planning, and control have all been studied in depth. Motion planning is an integral part of the overtaking problem which provides a state trajectory with time series for obstacle avoidance, lane-changing and overtaking [192]. MPC plays a vital role in motion planning [186], [193], [194]. All of these methods transform motion planning into a finite-time quadratic programming problem. Thus, a trajectory satisfying the specific constraints is obtained [195]. Then, using some optimisation techniques, a smoother motion trajectory can be obtained [196]. Besides, the graph search-based method [172], sampling-based method [197], and interpolation curve method [198] are also used in motion planning for overtaking scenarios of autonomous vehicles. Moreover, reinforcement learning also provides a potential solution to the overtaking behaviour of autonomous driving [199]–[201]. Deep deterministic strategy gradient method and deep Q-learning network become the mainstream algorithm frameworks [202], [203]. However, these studies of overtaking motion planning are all based on a single vehicle system.

There are fewer research works on the motion planning of the overtaking application of the autonomous MVS. The article [204] proposed an advanced graph-based optimal solution for overtaking scenarios of multi-vehicles. On this basis, [205] proposed another method of automatic vehicle overtaking based on MPC. The graph optimisation algorithm based on that probability provides the path of obstacle avoidance and overtaking. In [206], a unified approach to cooperative path-planning based on nonlinear MPC was proposed for overtaking the application of MVSs. Subsequently, the trajectory prediction of the human driver model was integrated into the framework, such that the behaviours of the other agents were affected by the human-operated vehicles (HVs) [207]. In [71], a distributed control method for coordinating multiple vehicles in the framework of an automated valet parking system was introduced. The main limitation of this approach is to rely on traffic infrastructure, which poses a considerable challenge to the current traffic facilities. The work presented in [208] proposed an integrated route and motion planning approach by considering a set of customer demands and road rules specified in temporal logic. However, vehicles other than navigators cannot interact with other existing vehicles during the overtaking.

This chapter proposes a distributed multi-vehicle motion planning method motivated by the challenges mentioned above in multi-vehicle overtaking. The method presented in this chapter is to transform the overtaking of the automatic driving fleet into multiple dynamic target-tracking problems by assigning a virtual dynamic target for the leader of the fleet. Firstly, a safe and feasible trajectory is planned for the leader AV so as to achieve tracking of the dynamic virtual target and obstacle avoidance of the HVs and other AV fleet members. To solve a dynamic target tracking problem, this chapter introduces the artificial potential field to carry out the motion planning of target tracking. The position field, velocity field, and acceleration field are added between the leader AV and the dynamic virtual target to realise the accurate tracking of the virtual target by the leader AV. Simultaneously, the position and speed repulsion fields are added between the leader AV, the HVs, and other AV fleet members to realise cooperative collision avoidance among the AV fleet members and avoid the HVs in the environment. Secondly, we design a bounded distributed control protocol that can guarantee topology connectivity for the followers. By using this distributed control protocol, the followers can track the lead AV with varying acceleration. Meanwhile, followers can also achieve obstacle avoidance with HVs, road boundaries, and other AV fleet members, and achieve distance stabilisation between followers. By introducing velocity and acceleration fields to achieve overtaking of dynamic HV, the Artificial Potential Field (APF) method, which is widely used for motion planning of a single mobile robot, can be applied to solve the overtaking motion planning problem of MVSs. Furthermore, we introduce a bounded distributed control protocol that achieves speed consistency across the AV fleet and avoids collisions among the vehicles. To the best of the authors' knowledge, such an APF-based motion planning strategy has not been proposed in the literature.

The main contributions of this work can be summarized as follow:

- A distributed motion planning algorithm for the leader AV based on the improved artificial potential field is proposed, which enables the leader AV to complete the overtaking of dynamic human-operated vehicles.
- We design a bounded distributed control protocol to implement the follower's safe tracking of the leader AV. Moreover, we analyze the stability of the MVS with N followers and one leader AV. It is proved that under this control protocol, the velocity of all the followers will be synchronized with the leader AV, and all the AVs will keep a safe distance between them.
- The effectiveness of the proposed strategy for use in autonomous vehicle overtaking scenarios is validated by a realistic simulator, Unreal Engine™.

4.2 Problem statement

We consider using the following double integral dynamical system kinematics equation to approximate the motion of the N vehicles in a 2D space:

$$\begin{cases} \dot{r}_i = v_i \\ \dot{v}_i = a_i, \end{cases} \tag{4.1}$$

where $r_i \in \mathbb{R}^2, v_i \in \mathbb{R}^2$ are, respectively, the position, and velocity vector of vehicle i. We use a time-varying directed graph $G(t) \triangleq (\mathcal{V}, \mathcal{E}(t))$ to describe the network topology between vehicles. where $\mathcal{V} \triangleq \{\mathcal{V}_1, \dots, \mathcal{V}_N,\}$ is set of nodes. and elements of $\mathcal{E}(t) \in N \times N$ are denoted as $(\mathcal{V}_i, \mathcal{V}_j)$ which is termed an edge from $\mathcal{V}_i$ to $\mathcal{V}_j$. $A(t) = [a_{ij}] \in \mathbb{R}^{N\times N}$ is the adjacency matrix of graph $G(t)$. The initial connection of the system is: $\mathcal{E}(0) = \{(i,j) | \|r_i(0) - r_j(0)\| < \rho_c, i, j \in \mathcal{V}\}$, where ρ_c is the communication range of the vehicles.

The AV fleet overtaking scenario can be summarized as a dynamic multi-target tracking problem. We assume that the AV fleet consists of N followers and 1 leader AV. With V2V communication technology [209], vehicle terminals exchange real-time state information directly with each other without the need for forwarding through a base station. AVs need to avoid other HVs actively in the environment; meanwhile, the AVs also need to avoid collisions between each other. We consider setting up one dynamic virtual node representing the target position. The motion parameters of the virtual node need to be determined by perception and mission planning block according to the state information of HVs. The distance between the virtual target and the human-operated vehicle being overtaken needs to be sufficient to accommodate the entire vehicle platoon. The virtual node should always be in front of the HVs and at least have the same velocity and acceleration parameters as the HVs after complete overtaking. Therefore, overtaking tasks can be decoupled into three tasks. Firstly, in a limited time, the leader AV must reach the virtual node. Secondly, the followers in the AV fleet must remain synchronous in the motion parameters with the leader AV. Thirdly, all the AVs must avoid HVs and avoid collisions with members of the AV fleet.

4.2.1 Basic assumptions

- We assume that it takes time τ ($\tau > 0$) seconds for the platoon system to switch the connection topology each time.
- In the current environment, there are $N + 1$ AVs and M human-operated vehicles. Human-operated vehicles appear randomly in the environment.
- The V2V communication function allows vehicles to communicate their position, velocity, and acceleration with each other. The communication range is limited. When other vehicles enter the communication range of vehicle i, vehicle i can receive the status

information of adjacent vehicles.

- During the overtaking, all vehicles are connected by a communication network. The communication network topology is shown in Fig. 4.1. The communication range of each AV is ρ_c. We assume that the initial topology $G(0)$ is connected. The communication between AVs is bidirectional, where AVs can access state information from each other. Note that HVs do not communicate with other vehicles and each HV's state information is obtained by the onboard sensors of nearby AVs. Since the delays and errors can be minimized by the high-performance sensors, this information flow can also be viewed as a unidirectional communication system for analytical purposes, where AVs can access state information from HVs, but HVs will not use any information from AVs.

- Without loss of generality, we assume that each HV has a changing acceleration. The jerk of the vehicle is constant, $\dddot{r} = J$.

- Because of the differences in traffic laws between countries and regions, we assume that it is legal to overtake on the left and the right.

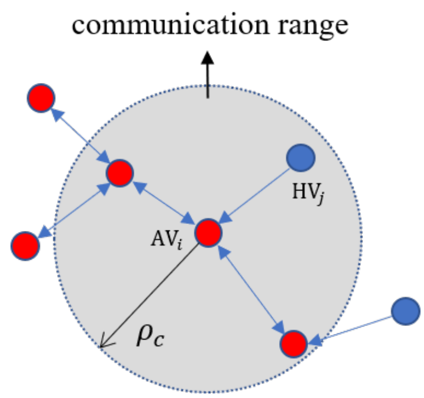

Figure 4.1. The communication network amongst the autonomous vehicles (indicated by Red circles) and human-operated vehicles (indicated by Blue circles).

4.2.2 A specific scenario

In this work, we use the specific scenario shown in Fig. 4.2 to carry out the experiments. Fig. 4.2 depicts a two-lane overtaking scene of an AV fleet, where H1 denotes the human-operated vehicle, L1, F1, and F2, respectively, denote the leader AV, first follower AV, and second follower AV. Red cars are AVs in a particular formation; the blue car is the object to be overtaken, and grey cars represent the desired position of the autonomous vehicles fleet after overtaking. We consider the most common overtaking scenario, in which the AV fleet

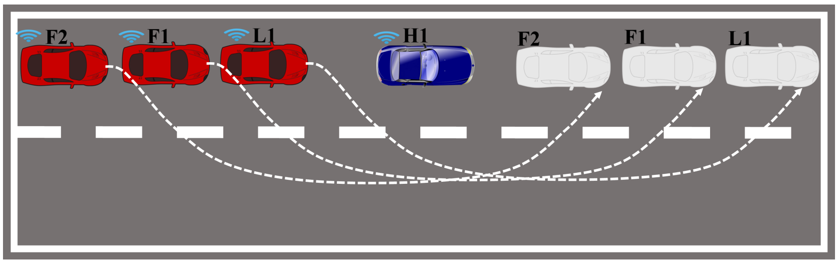

Figure 4.2. A typical overtaking scenario of autonomous vehicles. H1 denotes the human-operated vehicle, L1, F1, and F2, respectively, denote the leader AV, first follower AV, and second follower AV.

changes lanes to overtake, then needs to make a second lane-changing and return to the initial lane. In this scenario, the road is a two-lane straight road segment, and each lane has a fixed width. Additionally, the human-operated vehicle's acceleration in front of the AV fleet is continuously changing during overtaking.

4.2.3 System architecture of automatic driving

This chapter assumes that each AV fleet member has the most commonly used autonomous driving system architecture, making this chapter's method feasible in real autonomous vehicles. Fig. 4.3 describes a general system architecture of automatic driving function. The planning module will generate a position trajectory with a time sequence in each control cycle. The control module will track this trajectory accurately. Motion Planning aims to plan a safe, comfortable, and derivable trajectory for an autonomous vehicle according to the data from the prediction, perception, localisation, high-definition map (HD-Map), and routing module. In this chapter, The AV fleet members can obtain the position, velocity, and acceleration of human-operated vehicles and the other AV fleet members through the perception module. The prediction module will predict the driving intention, position, and velocity changes of the human-operated vehicles and output the human-operated vehicle's predictive motion trajectory in the finite time-domain. In traditional single-vehicle autonomous driving, motion planning during overtaking considers the environment of vehicles and overtaking and lane-changing. While in multi-vehicle autonomous driving, motion planning should also take into account the risk of collisions between AV fleet members and the specific formation requirements of the AV fleet. The main objective of this chapter is to develop algorithms in planning and control blocks to achieve safe overtaking behaviours of the AV fleet. This AV fleet constitutes a typical distributed system. All individual agents in this distributed system are isomorphic autonomous vehicles and use the same autonomous driving system architec-

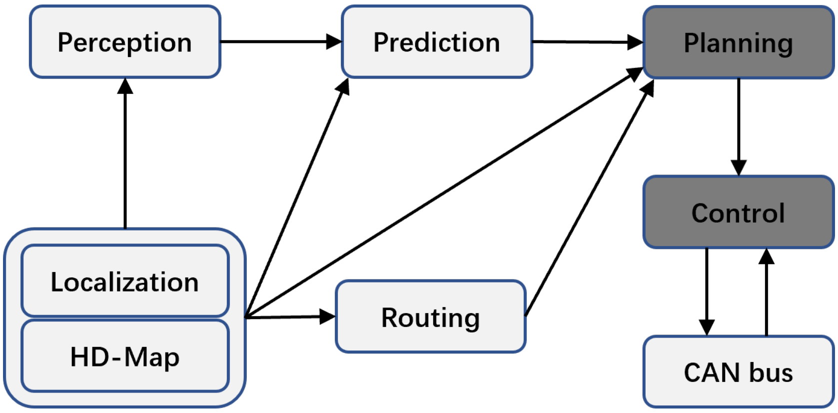

Figure 4.3. Functional block diagram of an intelligent autopilot scheme for autonomous vehicles.

ture shown in Fig. 4.3.

4.3 Distributed motion planning and control design

4.3.1 Motion planning of the navigator

The idea of using artificial potential field methods for path planning has a long history. The basic idea comes from the concept of potential in physics. The obstacles in the environment generate the repulsive force on the robot, the target points generate attraction to the robot, and the robot moves along the direction of minimum potential energy under the resultant force's action. The artificial potential field method is often applied in path planning and multi-agent motion control in recent years [186]. The advantage of this method is that it is simple to calculate and easy to realise real-time control. The traditional artificial potential field method is based on the distance difference between the robot and the target or obstacle to generate the corresponding attractive and repulsive forces. The following functions generate a typical attractive potential field and repulsive potential field [210]:

$$\begin{cases} U_{\text{att}} = \dfrac{1}{2} K_p \, d^2(r) \\ F_{\text{att}} = -\nabla U_{\text{att}}(r) \end{cases} \tag{4.2}$$

and

$$\begin{cases} U_{\text{rep}} = \dfrac{1}{2} \eta_p \left(\dfrac{1}{d(r)} - \dfrac{1}{D} \right)^2 \\ F_{\text{rep}} = -\nabla U_{\text{rep}}(r). \end{cases} \tag{4.3}$$

However, the traditional APF technique is mostly used for path planning in a static environment and may not be effective in a dynamic environment. Hence, it is necessary to modify the traditional APF technique relying on the positional difference.

Let there be M human-operated vehicles in the current scenario. The current position of the leader AV, the k^{th} AV, the j^{th} HV, and the goal position of leader AV are denoted by r_l, r_k, r_j and r_g respectively. Similarly, the velocities and accelerations are denoted by v_l, v_k, v_j, v_g and a_l, a_k, a_j, a_g, respectively. In addition, we define the following variables:

- $d(r_l, r_k)$ is the geometric distance between the leader AV and the k^{th} AV. The relative velocity and relative acceleration between the leader AV and the k^{th} AV in the fleet are symbolized as $d(v_l, v_k)$ and $d(a_l, a_k)$;
- $d(r_l, r_j)$ is the geometric distance between the leader AV and the j^{th} HV. The relative velocity and relative acceleration between the leader AV and the j^{th} HV are symbolized as $d(v_l, v_j)$ and $d(a_l, a_j)$;
- $d(r_l, r_g)$ is the geometric distance between the leader AV and the goal node. The modulus of relative velocity and relative acceleration between the leader AV and the goal node is denoted by $d(v_l, v_g)$, and $d(a_l, a_g)$.

  Hence, the goal node of leader AV is given by the routing block when the decision-making level makes the decision to overtake. This dynamic goal node will change with the state of motion of the HV.

In order to achieve the leader AV's tracking of the virtual target, we define the following artificial potential field.

Attractive quadratic potential fields

We define the following Attractive Quadratic Potential Field (AQPF)

$$U_{\text{att}}(r, v, a) = \frac{1}{2}K_p d^2\left(r_l, r_g\right) + \frac{1}{2}K_v d^2\left(v_l, v_g\right) + \frac{1}{2}K_a d^2\left(a_l, a_g\right) \tag{4.4}$$

between the leader autonomous vehicle and the virtual goal (treated as a node). The attractive force produced by the proposed AQPF technique is given by

$$
\begin{aligned}
F_{\text{att}}(i) &= -\nabla U_{\text{att}}(r, v, a) \\
&= -\frac{\partial U_{\text{att}}(r, v, a)}{\partial r} - \frac{\partial U_{\text{att}}(r, v, a)}{\partial v} - \frac{\partial U_{\text{att}}(r, v, a)}{\partial a} \\
&= -K_p d\left(r_l, r_g\right) - K_v d\left(v_l, v_g\right) - K_a d\left(a_l, a_g\right) \\
&= F_{\text{attP}} + F_{\text{attV}} + F_{\text{atta}},
\end{aligned}
\tag{4.5}
$$

where $K_p > 0$, $K_v > 0$, and $K_a > 0$ denote respectively the position, velocity, and acceleration gain coefficients. Fig. 4.4 shows the vector diagram for calculating the attractive force between a leader AV and its goal node. The F_{attP} aims to make the autonomous vehicle track the position of the goal node. The direction of the force is from the leader AV to the goal node. The F_{attV} aims to make the leader AV track the velocity of the goal node and its direction is the same as the direction of vector $(\overrightarrow{v_g} - \overrightarrow{v_l})$. The F_{atta} aims to complete the acceleration tracking, and its direction is the same as the direction of vector $(\overrightarrow{a_g} - \overrightarrow{a_l})$.

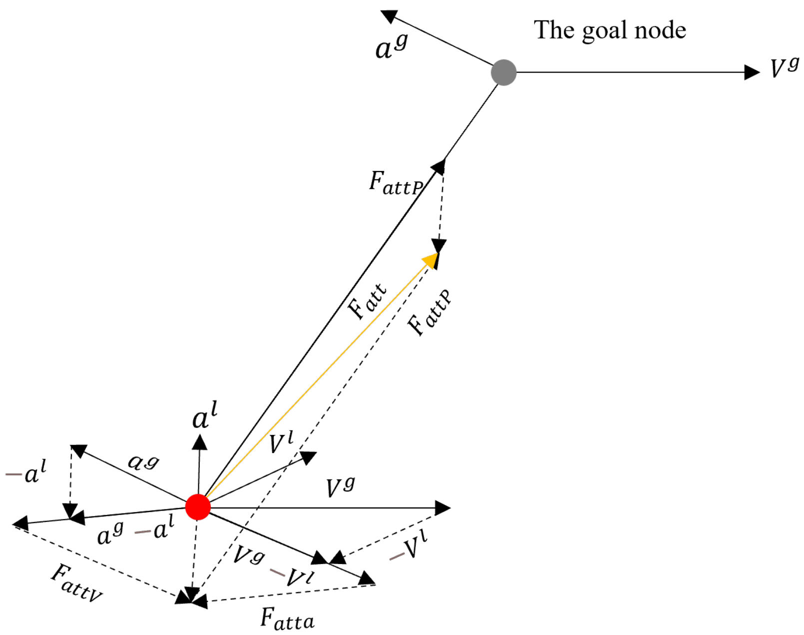

Figure 4.4. The vector diagram has been used for calculating the attractive force between the leader AV (red circle) and its goal node (grey circle).

Repulsive potential field generated by the HVs

Regarding the potential field of HVs, we also consider the potential field caused by position and speed. The distance factor ensures that an autonomous vehicle will not collide with HVs. The speed factor can predict and avoid collisions in advance. We define $\vec{d}\left(v_l, v_j\right)$ and $\vec{d}(r_l, r_j)$ the relative velocity and position vectors of the leader and the HVs. When $\vec{d}\left(v_l, v_j\right) \cdot \vec{d}(r_l, r_j) > 0$, it means that the leader AV will have the risk of collision with the HVs, thus the HVs generate the repulsive force to the leader AV. Hence, we establish the following repulsive potential field:

$$U_{\text{rep(lj)}(r,v)} = \begin{cases} \frac{1}{2}\eta_p \left(\frac{1}{d\left(r_l, r_j\right)} - \frac{1}{D_{\text{max}}} \right)^2 d(r_l, r_g) + \eta_v d\left(v_l, v_j\right), \\ \frac{1}{2}\eta_p \left(\frac{1}{d\left(r_l, r_j\right)} - \frac{1}{D_{\text{max}}} \right)^2 d(r_l, r_g), \\ 0; \end{cases} \tag{4.6}$$

for

$$\begin{cases} d\left(r_j, r_l\right) \leq D_{\text{max}} \text{ and } \vec{d}\left(v_l, v_j\right) \cdot \vec{d}(r_l, r_j) > 0; \\ d\left(r_l, r_j\right) \leq D_{\text{max}} \text{ and } \vec{d}\left(v_l, v_j\right) \cdot \vec{d}(r_l, r_j) \leq 0; \\ d\left(r_l, r_j\right) > D_{\text{max}}. \end{cases}$$

where D_{max} denotes the repulsive area defined by the following elliptical equation:

$$\frac{(x - x_j)^2}{a^2} + \frac{(y - y_j)^2}{b^2} = 1 \qquad \text{(where } a > b > 0). \tag{4.7}$$

The elliptical action area allows the vehicle to avoid obstacles in advance in the longitudinal direction. The region D_{max} defined by formula (4.7) is a variable value.

$$D_{\text{max}} = \sqrt{\frac{a^2 b^2 (1 + k^2)}{b^2 + a^2 k^2}}, \tag{4.8}$$

where $k = \frac{y_i - y_j}{x_i - x_j}$.

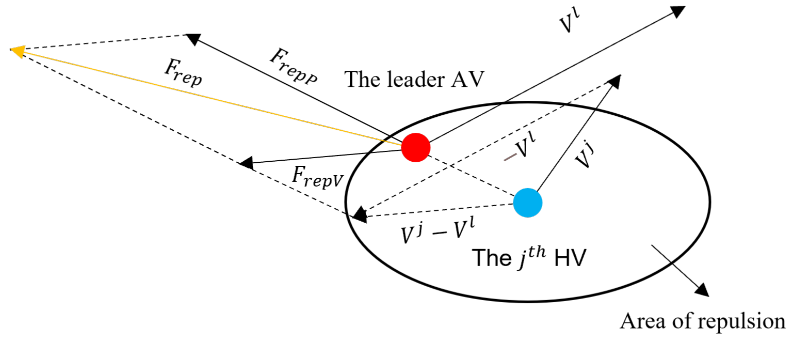

Figure 4.5. Schematic diagram of repulsive force calculation between leader AV (red circle) and HV (blue circle).

We define that the gradient of repulsive potential fields is the repulsive force

$$\begin{aligned} F_{\text{rep}}(lj) &= -\nabla U_{\text{rep}(lj)}(r, v) \\ &= -\frac{\partial U_{\text{rep}(lj)}(r, v)}{\partial r} - \frac{\partial U_{\text{rep}(lj)}(r, v)}{\partial v} \\ &= F_{\text{repP}}(lj) + F_{\text{repv}}(lj). \end{aligned} \tag{4.9}$$

Fig. 4.5 describes the calculation process of the repulsive force between the leader AV and the j^{th} HV. The repulsive force $F_{\text{repP}}(lj)$ generated by the position difference is directed from the obstacle vehicle to the autonomous vehicle. This repulsion trend the AV away from the obstacle vehicle. The repulsive force $F_{\text{repv}}(lj)$ due to the velocity difference is in the same direction as the vector $(\vec{v_j} - \vec{v_l})$. This repulsive force causes the autonomous vehicle to slow down when approaching an obstacle vehicle.

$$F_{\text{rep}}(lj) = \begin{cases} \eta_p \left(\dfrac{1}{d\left(r_l, r_j\right)} - \dfrac{1}{D_{\max}} \right) \dfrac{d(r_l, r_g)}{d^2\left(r_l, r_j\right)} + \dfrac{1}{2}\eta_p \left(\dfrac{1}{d\left(r_l, r_j\right)} - \dfrac{1}{D_{\max}} \right)^2 + \eta_v, \\ \eta_p \left(\dfrac{1}{d\left(r_l, r_j\right)} - \dfrac{1}{D_{\max}} \right) \dfrac{d(r_l, r_g)}{d^2\left(r_l, r_j\right)} + \dfrac{1}{2}\eta_p \left(\dfrac{1}{d\left(r_l, r_j\right)} - \dfrac{1}{D_{\max}} \right)^2, \\ 0, \end{cases} \tag{4.10}$$

for

$$\begin{cases} d\left(r_l, r_j\right) \leq D_{\max} \text{ and } \vec{d}\left(v_l, v_j\right) \cdot \vec{d}(r_l, r_j) > 0; \\ d\left(r_l, r_j\right) \leq D_{\max} \text{ and } \vec{d}\left(v_l, v_j\right) \cdot \vec{d}(r_l, r_j) \leq 0; \\ d\left(r_i, r_j\right) > D_{\max}. \end{cases}$$

Hence, the total repulsive force of human-operated vehicles to the leader AV is:

$$F_{\text{repj}}(l) = \sum_{j=1}^{M} F_{\text{rep}}(lj). \tag{4.11}$$

Repulsive potential field generated by the autonomous vehicles

For the overtaking scenario in this chapter, we should consider avoiding human-operated vehicles and consider collisions between members of the fleet. Similarly, the repulsion field is defined between vehicles within the AV fleet,

$$F_{\text{rep}}(lk) = \begin{cases} \eta_p \left(\dfrac{1}{d\left(r_l, r_k\right)} - \dfrac{1}{D_{\text{max}}} \right) \dfrac{d(r_l, r_g)}{d^2\left(r_l, r_k\right)} + \dfrac{1}{2}\eta_p \left(\dfrac{1}{d\left(r_l, r_k\right)} - \dfrac{1}{D_{\text{max}}} \right)^2 + \eta_v, \\ \eta_p \left(\dfrac{1}{d\left(r_l, r_k\right)} - \dfrac{1}{D_{\text{max}}} \right) \dfrac{d(r_l, r_g)}{d^2\left(r_l, r_k\right)} + \dfrac{1}{2}\eta_p \left(\dfrac{1}{d\left(r_l, r_k\right)} - \dfrac{1}{D_{\text{max}}} \right)^2, \\ 0, \end{cases} \tag{4.12}$$

for

$$\begin{cases} d\left(r_l, r_k\right) \le D_{\text{max}} \text{ and } \vec{d}\left(v_l, v_k\right) \cdot \vec{d}(r_l, r_k) > 0; \\ d\left(r_l, r_k\right) \le D_{\text{max}} \text{ and } \vec{d}\left(v_l, v_k\right) \cdot \vec{d}(r_l, r_k) \le 0; \\ d\left(r_l, r_k\right) > D_{\text{max}}. \end{cases}$$

Moreover, the repulsive force calculation between the leader AV and other members in the AV fleet is the same as shown in Fig. 4.5. The total repulsive force exerted by the other members in the fleet on the leader AV is given by:

$$F_{\text{repk}}(l) = \sum_{k=1}^{N-1} F_{\text{rep}}(lk). \tag{4.13}$$

Repulsive Potential Field generated due to road boundary and the resultant force calculation

In order to make the vehicle drive within a reasonable road range, we define the potential field for the road boundary:

$$U_{\text{rep}}(\text{road}) = \begin{cases} \frac{1}{2}\eta_{\text{road}}\left(\frac{1}{d\left(r_l, r_{\text{road}}\right)} - 1\right)^2, d(r_l, r_{\text{road}}) \leq 1; \\ 0, d(r_l, r_{\text{road}}) > 1; \end{cases} \tag{4.14}$$

and

$$F_{\text{rep}}(\text{road}) = \begin{cases} \eta_{\text{road}}\left(\frac{1}{d\left(r_l, r_{\text{road}}\right)} - 1\right) \times \frac{1}{d^2\left(r_l, r_{\text{road}}\right)}, d(r_l, r_{\text{road}}) \leq 1; \\ 0, \ d(r_l, r_{\text{road}}) > 1, \end{cases} \tag{4.15}$$

where $d(r_l, r_{\text{road}})$ represents the distance between the leader AV and road boundary.

To sum up, the resultant force of the leader AV in the environment is

$$F_{\text{total}}(l) = F_{\text{att}}(l) + F_{\text{repj}}(l) + F_{\text{repk}}(l) + F_{\text{rep}}(\text{road}). \tag{4.16}$$

In addition, the artificial potential field method of motion planning is prone to local minimum potential fields, which prevent the vehicle from moving towards the target if it is in a local minimum potential field. To solve this problem to some extent, a weak random noise is added to the vehicle so that it can move out of the local minimum potential field region. However, this does not completely solve the problem of the local minimum potential field, as it is difficult to identify whether the region is a local minimum potential field or not, and more effort will need to be invested in future research to solve this problem.

4.3.2 Steady-state analysis of leader AV

From the equations (4.10) and (4.12), the repulsive forces generated by a human-operated vehicle have the same form as those generated by other members of the AV fleet. Moreover, the repulsive forces generated by the road boundary exist only within a small range of the boundary, and their direction is parallel to the lateral direction. When analyzing the steady state and stability of the algorithm, we ignore this part of repulsion. Therefore, we unify the repulsive force into the following formula, which is called the interference term:

$$Q = \sum_{f \in \mathcal{N}_l} \eta_p \left(\frac{1}{r_l - r_f} - \frac{1}{D_{\text{max}}} \right) \frac{r_l - r_g}{(r_l - r_f)^2} + \frac{1}{2} \eta_p \left(\frac{1}{r_l - r_f} - \frac{1}{D_{\text{max}}} \right)^2 + \eta_v, \tag{4.17}$$

where r_f denotes the position of vehicles which generate the repulsive force to the leader AV. Considering particle dynamics, the following equation is obtained:

$$\dddot{r}_l = \frac{1}{m} [-K_p(r_l - r_g) - K_v(\dot{r}_l - \dot{r}_g) - K_a(\ddot{r}_l - \ddot{r}_g) + Q]. \tag{4.18}$$

We define the difference between the position of the leader AV and the virtual dynamic node as the control object:

$$\begin{cases} e = r_l - r_g \\ \dot{e} = \dot{r}_l - \dot{r}_g \\ \ddot{e} = \ddot{r}_l - \ddot{r}_g \\ \dddot{e} = \dddot{r}_l - \dddot{r}_g. \end{cases} \tag{4.19}$$

The closed loop dynamic model is updated to:

$$\begin{aligned} \dddot{e} =& \frac{1}{m} [-K_p e - K_v \dot{e} - K_a \ddot{e} \\ &+ \sum_{f \in \mathcal{N}_l} \eta_p \left(\frac{1}{e + r_g - r_f} - \frac{1}{D_{\text{max}}} \right) \frac{e}{(e + r_g - r_f)^2} \\ &+ \frac{1}{2} \eta_p \left(\frac{1}{e + r_g - r_f} - \frac{1}{D_{\text{max}}} \right)^2 + \eta_v] - \dddot{r}_g. \end{aligned} \tag{4.20}$$

Defining $B_f := r_g - r_f$ and the following equation can be obtained:

$$\begin{aligned} \dddot{e} =& \frac{1}{m} [-K_p e - K_v \dot{e} - K_a \ddot{e} \\ &+ \sum_{f \in \mathcal{N}_l} \eta_p \left(\frac{1}{e + B_f} - \frac{1}{D_{\text{max}}} \right) \frac{e}{(e + B_f)^2} \\ &+ \frac{1}{2} \eta_p \left(\frac{1}{e + B_f} - \frac{1}{D_{\text{max}}} \right)^2 + \eta_v] - \dddot{r}_g. \end{aligned} \tag{4.21}$$

The equilibrium state of system is obtained by setting $\dddot{e} = \ddot{e} = \dot{e} = 0$, which results in the following equations:

$$\begin{aligned}&\frac{1}{m}[-K_pe + \sum_{f\in\mathcal{N}_l} \eta_p \left(\frac{1}{e+B_f} - \frac{1}{D_{\max}}\right) \frac{e}{(e+B_f)^2} \\ &+ \frac{1}{2}\eta_p \left(\frac{1}{e+B_f} - \frac{1}{D_{\max}}\right)^2 + \eta_v] - \dddot{r}_g = 0.\end{aligned} \tag{4.22}$$

The solution is as follows:

$$e = F(B_1, B_2, \cdots, B_f, \dddot{r}_g). \tag{4.23}$$

Whether there are variables B_f depends on whether the vehicle is subject to interference item. f is the number of obstacles vehicles and other fleet members which are generating repulsive force to the leader AV. Variable $\dddot{r}_g$ is the jerk of the virtual target. Therefore, one of the necessary conditions for the steady state of the system is that $\dddot{r}_g$ is constant. This is consistent with our previous basic assumption that dynamic virtual targets have varying accelerations. In general, in the case of small changes in acceleration, we can think about jerk as zero. Therefore, the steady state of the system under the disturbance term depends on the value of B_f. Therefore, when B_f is also constant, the system is purely in a steady state. In this case, the vehicle is likely to enter a local steady-state formed by B_f, which prevents tracking of the virtual target node. Its steady state value is given in equation (4.23). However, this does not meet our requirements when modelling the overtaking problem. We expect that the vehicle will not enter a steady state when approaching the obstacle. To solve this problem, we randomly add noise w_f to the repulsive force field of obstacles, so that the vehicle will not enter a steady state:

$$\begin{aligned}\dddot{e} = &\frac{1}{m}[-K_pe - K_v\dot{e} - K_a\ddot{e} \\ &+ \sum_{f\in\mathcal{N}_l} \eta_p \left(\frac{1}{e+r_g-r_f} - \frac{1}{D_{\max}}\right) \frac{e}{(e+r_g-r_f)^2} \\ &+ \frac{1}{2}\eta_p \left(\frac{1}{e+r_g-r_f} - \frac{1}{D_{\max}}\right)^2 + \eta_v + w_f] - \dddot{r}_g.\end{aligned} \tag{4.24}$$

In addition, the addition of random noise follows the following rule:

$$\begin{cases} w_f = 0 & \text{if } \mathcal{N}_l = \emptyset \\ w_f \neq 0 & \text{if } \mathcal{N}_l \neq \emptyset \end{cases}. \tag{4.25}$$

Then equation (4.23) is updated to:

$$e = F(B_1, B_2, \cdots, B_f, w_f, \dddot{r}_g). \tag{4.26}$$

When the vehicle is affected by the interference term, it will not enter the steady state because of the noise w_f but will leave the repulsive region because of the repulsive force. The vehicle will then enter an attractive field with no interference terms. Essentially, according to equation (4.25), w_f will be eliminated when the vehicle is not affected by the interference term. Thus, when the vehicle converges to the steady state without disturbance terms, equation (4.24) is then updated to:

$$\dddot{e} = \frac{1}{m}[-K_p e - K_v \dot{e} - K_a \ddot{e}] - \dddot{r}_g. \tag{4.27}$$

The steady state can be solved by the following equation:

$$\dddot{r}_g + \frac{1}{m} K_p \, e = 0. \tag{4.28}$$

The set of equilibrium states $\mathbb{E}$ is therefore obtained as

$$\mathbb{E} = \left\{ \ddot{e}, \dot{e}, e \mid e = -\frac{m\dddot{r}_g}{K_p}, \ddot{e} = \dot{e} = 0 \right\}. \tag{4.29}$$

According to the above analysis, the velocity and acceleration parameters of leader AV will converge to those of the virtual target, and its position will converge to $(r_g - \frac{m\dddot{r}_g}{K_p})$.

Relying on the above analysis, we can conclude that an autonomous vehicle can dynamically track a virtual target following the proposed algorithm. However, the vehicle cannot completely converge to the position of the virtual target. There exists a positional difference between them, the value of which depends on the jerk of the virtual target $\dddot{r}_g$ and the constant parameters K_p, m. Therefore, the algorithm is suitable for a dynamic target with a small jerk. However, this algorithm is not useful for dynamic targets whose acceleration varies significantly. In a real-world scenario, due to the unpredictable road conditions, obstacles, and nonuniformities of the vehicles, different driving styles of human drivers lead to frequent acceleration changes. Hence, the previous algorithm needs to be modified to enable a vehicle to track unforeseen circumstances (modelled as dynamic targets/obstacles) during the course of motion. In order to eliminate the influence of the jerk of the target node on the steady-state error of the position, we consider introducing the jerk of the target node into the closed-loop control:

$$F_{\text{att}}(l) = -K_p\left(r_l - r_g - \frac{m\dddot{r}_g}{K_p}\right) - K_v(\dot{r}_l - \dot{r}_g) - K_a(\ddot{r}_l - \ddot{r}_g). \tag{4.30}$$

We will now use the same analysis to obtain the third-order system model of an autonomous vehicle as follows:

$$\begin{aligned}\dddot{e} = \frac{1}{m}\Bigg[&-K_p\left(e - \frac{m\dddot{r}_g}{K_p}\right) - K_v\dot{e} - K_a\ddot{e} \\ &+ \sum_{f\in\mathcal{N}_l}\eta_p\left(\frac{1}{e + r_g - r_f} - \frac{1}{D_{\max}}\right)\frac{e}{(e + r_g - r_f)^2} \\ &+ \frac{1}{2}\eta_p\left(\frac{1}{e + r_g - r_f} - \frac{1}{D_{\max}}\right)^2 + \eta_v + w_f\Bigg] - \dddot{r}_g.\end{aligned} \tag{4.31}$$

Without being affected by the interference term, the state space expression of the closed-loop control system can be expressed as

$$\begin{bmatrix}\dot{e}\\ \ddot{e}\\ \dddot{e}\end{bmatrix} = \begin{bmatrix}0 & 1 & 0\\ 0 & 0 & 1\\ -\frac{K_p}{m} & -\frac{K_v}{m} & -\frac{K_a}{m}\end{bmatrix}\begin{bmatrix}e\\ \dot{e}\\ \ddot{e}\end{bmatrix}. \tag{4.32}$$

The set of steady-state operating points of the above system is obtained as

$$\mathbb{E} = \{\ddot{e}, \dot{e}, e \mid \ddot{e} = \dot{e} = e = 0\}. \tag{4.33}$$

The set $\mathbb{E}$ signifies that the position, velocity, and acceleration of leader AV converges to the motion parameters corresponding to the virtual target. The stability of closed-loop control systems can be determined by the A matrix, where

$$A = \begin{bmatrix} 0 & 1 & 0 \\ 0 & 0 & 1 \\ -\frac{K_p}{m} & -\frac{K_v}{m} & -\frac{K_a}{m} \end{bmatrix}. \tag{4.34}$$

Let $|\lambda E - A| = 0$, Characteristic equation is:

$$\lambda^3 + \frac{K_a}{m}\lambda^2 + \frac{K_v}{m}\lambda + \frac{K_p}{m} = 0, \tag{4.35}$$

where $\frac{K_p}{m} > 0$, $\frac{K_v}{m} > 0$, $\frac{K_a}{m} > 0$. It's easy to conclude that the characteristic equation has no solution greater than or equal to zero. Therefore, the matrix A must be negative definite or semi-negative definite. In conclusion, the closed-loop control system is Lyapunov stable or Lyapunov asymptotically stable.

4.3.3 Trajectory generation and optimisation

Trajectory generation

On the premise of not affecting the algorithm itself, we consider using a particle dynamics model for trajectory prediction. Select state vector S:

$$S_l = \begin{bmatrix} r_l \\ v_l \\ a_l \end{bmatrix}, \tag{4.36}$$

and equation of state for the system:

$$\dot{S}_l = AS_l + BU_l, \tag{4.37}$$

where,

$$A = \begin{bmatrix} 0 & 1 & 0 \\ 0 & 0 & 1 \\ 0 & 0 & 0 \end{bmatrix}, \quad B = \begin{bmatrix} 0 \\ 0 \\ \frac{1}{m} \end{bmatrix}.$$

Use the forward Euler method to discretize the equation of state:

$$\dot{S}_l \approx \frac{S_l(t+1) - S_l(t)}{T} = AS_l(t) + BU_l(t), \tag{4.38}$$

where T is the control period. The equation of state after discretisation is

$$\begin{aligned} S_l(t+1) &= (I + TA)S_l(t) + TBU_l(t) \\ &= \overline{A}S_l(t) + \overline{B}U_l(t), \end{aligned} \tag{4.39}$$

where

$$\overline{A} = \begin{bmatrix} 1 & T & 0 \\ 0 & 1 & T \\ 0 & 0 & 1 \end{bmatrix}, \quad \overline{B} = \begin{bmatrix} 0 \\ 0 \\ \frac{T}{m} \end{bmatrix}.$$

In the finite time-domain, the predicted trajectory and state of the vehicle can be obtained by:

$$\begin{aligned} U_l(t) =& mJ_g(t) - K_p(r_l(t) - r_g(t)) \\ & - K_v(v_l(t) - v_g(t)) - K_a(a_l(t) - a_g(t)), \end{aligned} \tag{4.40}$$

where $J_g(t)$ is the jerk of target node. $U_l(t)$ is a discrete-time signal where $t = 0, 1, 2, ...$ denotes the discrete time instants.

In addition, the traffic speed limit and the power limit of the vehicle are also taken into account. The acceleration and velocity constraints are defined as

$$a_l(t+1) = \begin{cases} a_l(t) + \frac{T}{m}U_l(t), & \left|a_l(t) + \frac{T}{m}U_l(t)\right| < a_{\max} \\ a_{\max}, & \left|a_l(t) + \frac{T}{m}U_l(t)\right| \geq a_{\max} \end{cases} \tag{4.41}$$

and

$$v_l(t+1) = \begin{cases} v_l(t) + Ta_l(t), & |v_l(t) + Ta_l(t)| < v_{\max} \\ v_{\max}, & |v_l(t) + Ta_l(t)| \geq v_{\max} \end{cases}. \tag{4.42}$$

Trajectory optimisation

The trajectory generated by the APF technique satisfies the vehicle's barrier avoidance constraints and the motion tracking of the target point. However, the resulting trajectory does not guarantee sufficient smoothness in the event of curvature changes and acceleration changes. In the literature, there are a variety of local trajectory optimisation techniques. For instance, the idea of optimal control for local rolling optimisation is often considered. In the longitudinal direction, to minimize the jerk and thereby increase the passengers' comfort, the following optimisation problem

$$\begin{aligned} &\min_{j_x(t)} J_x = \int_t^{t+q} \frac{1}{2} j_x^2(t) \mathrm{d}t \\ &\text{such that } \dot{x}(t) = v_x(t), \dot{v}_x(t) = a_x(t), \dot{a}_x(t) = j_x(t). \end{aligned} \tag{4.43}$$

can be solved taking the inspiration from [211]. According to Pontryagin's maximum principle, the optimal longitudinal displacement trajectory $x(t)$ can be obtained. In equation (4.43), the position constraint must be added to meet the obstacle avoidance requirements. Meanwhile, the velocity and acceleration constraints at the endpoints need to be introduced to ensure the smoothness of the generated trajectories. Similarly, in the lateral direction, the objection function is established as followed [211]:

$$\begin{aligned} &\min_{j_y(t)} J_y = \int_t^{t+q} \frac{1}{2} j_y^2(t) \mathrm{d}t \\ &\text{such that } \dot{y}(t) = v_y(t), \dot{v}_y(t) = a_y(t), \dot{a}_y(t) = j_y(t). \end{aligned} \tag{4.44}$$

The two optimal problems above end up with two high-order curves, which ensure the requirement of avoiding obstacles and the smoothness of the acceleration change.

Another local optimisation method, high-order Bessel curve fitting [212], is also adopted in this chapter. It can obtain locally smoother trajectories but may not obtain the optimal solution. We consider using the fifth-order Bessel curve to carry out rolling optimisation on the obtained trajectory to obtain a trajectory that is as smooth as possible in the finite time-domain.

Given $(n+1)$ space vectors $P_i \in R^3$, where $i \in \{0, 1, 2, \ldots, n\}$, the n-th Bessel curve can be defined as

$$P(t) = \sum_{i=0}^{n} P_i B_i^n(t) \qquad \forall t \in [0, 1], \tag{4.45}$$

where P_i are the control points and $B_i^n(t)$ is given by:

$$B_i^n(t) = C_n^i t^i (1-t)^{n-i} \qquad \forall i \in \{0, 1, \ldots, n\}. \tag{4.46}$$

The fifth-order Bessel curve has a very smooth curvature and the corresponding changes in the turning angle and angular velocity are relatively gentle. In the terminology of vehicular control, this signifies that the curvature of turning of a vehicle will be smoother.

Motion planning algorithm

After the decision of overtaking is made by the leader AV of the MVS, the leader needs to generate a virtual target node. Virtual target nodes are generated according to Algorithm 1. Let $S_j = [r_j, v_j, a_j]^T$ and $S_g = [r_g, v_g, a_g]^T \in \mathrm{R}^3$ represent the state vector of the j^{th} HV and the goal node, respectively. Note that this static coupling can be described as $S_g = S_j + \Delta d$, where $\Delta d = [C + \mu, 0, 0]^T$, C is the platoon length and μ is the desired distance between HV and the platoon. $S_l(p)$ in this algorithm represents the leader AV's state vector at time step p, which includes position, velocity, and acceleration. In the actual self-driving vehicle, the motion planning needs to be updated in real-time and sent to the control module. Algorithm 2 provides a reference trajectory for the leader AV to avoid the dynamic vehicle. The algorithm is updated dynamically in real-time, each update calculates the motion trajectory in the finite time-domain.

4.3.4 Distributed control protocol for followers

In practical applications, due to the large size of the vehicle structure, we expect that the vehicle can achieve the one-to-one following, which is more conducive to the AV fleet to

Algorithm 1 Virtual target node generation algorithm

Input: The current state variables of autonomous vehicle fleet members, human-operated vehicles $S_l(p)$, $S_j(p)$. Prediction state of human-operated vehicles in p time-domain, $S_j(p)$, $S_j(p+1)$, ···, $S_j(p+q)$.
Output: The target node's lane number L_g and the target node's motion parameters S_g.

```
Initialize basic parameters, control period T, and prediction time-domain q.
for each control cycle.
    Leader AV receives the lane number of itself, L_l.
    Leader AV receives the predictive states S_j(p+1), ···, S_j(p+q) from prediction module.
    Find vehicle HV_g with max(S_j).
    L_g = L_l;
    S_g=max(S_j) + Δd.
    Leader AV calculates the state of the virtual target node in the proactive time-domain.
End for
Return S_g(p), S_g(p+1), ···, S_g(p+q).
```

Algorithm 2 Overtaking motion planning algorithm for autonomous vehicles in a dynamic environment

Input: The current state variables of leader AV, human-operated vehicles, and, goal node, $S_l(p)$, $S_j(p)$, $S_g(p)$. Prediction state of human-operated vehicles and goal nodes in p time-domain, $S_j(p)$, $S_j(p+1)$, ···, $S_j(p+q)$, $S_g(p)$, $S_g(p+1)$, ···, $S_g(p+q)$.
Output: $S_l(p)$, $S_l(p+1)$, ···, $S_l(p+q)$.

```
Initialize basic parameters, control period T, and prediction time-domain q.
While |d(S_l(p), S_g(p))| > threshold value
    Receive the current position and velocity S_l(p), S_j(p),S_g(p).
    Receive the predictive states S_j(p+1), ···, S_j(p+q) from prediction module.
    For each predictive time sequence ∈ q
        Calculate the artificial potential force U_l(p).
        Calculate and save the next state S_l(p+1) of autonomous vehicle relying on equation (4.39).
    End for
    Return S_l(p), S_l(p+1), ···, S_l(p+q).
    Use the high-order Bessel curve for trajectory optimisation based on equation (4.45). Or use optimal
control for trajectory optimisation based on equation (4.43) and equation (4.44).
    Send the optimised trajectory sequence S_l(p), S_l(p+1), ···, S_l(p+q) to control module.
End while
```

complete overtaking on the road with limited width and will not occupy too many road resources. Hence, we define a new control connection topology $\mathcal{G}(t) = \left(\bar{\mathcal{V}}, \bar{\mathcal{E}}(t)\right)$. $\bar{A}(t) = \left[\bar{a}_{ij}\right] \in \mathbb{R}^{N\times N}$ is the adjacency matrix of graph $\mathcal{G}(t)$. Define for each i node a neighbour:

$$\bar{\mathcal{N}}_i = \begin{Bmatrix} j \in N : \left\|r_i(t) - r_j(t)\right\| \leq R_j, \mathrm{Min}\left\|r_i(t) - r_j(t)\right\|, \\ r_j(t) \geq r_i(t) \end{Bmatrix}.$$

We consider using a leader AV to guide the cluster movement of the AV fleet. Define r_l, v_l as, respectively, the position, and velocity vector of leader AV. We define two classes of bounded potential field functions V_{ij}, V_{il}, V_{ik} and V_{en}, where V_{ij} and V_{il} are the same type of potential field function, V_{ik} and V_{en} are the other one type of potential field function.

- V_{ij} is a bounded potential field function between vehicles, which mainly solves the following problems: Collision avoidance, distance stabilisation, and connectivity keeping.

- V_{il} is the bounded potential field function between followers and leader AV, which ensures that the follower can continuously follow the leader AV.
- V_{ik} is the potential field between the followers and human-operated vehicle k, which ensures there is a safe distance between AV and human-operated vehicle.
- V_{en} is the potential field formed by the structured road environment, which ensures that the vehicle travels within the desired road range.

Inspired by reference [213], the control protocol we designed is as follows:

$$
\begin{aligned}
a_i = & - \sum_{j \in \bar{\mathcal{N}}_i} \nabla_{r_i} V(\|r_{ij}\|) - h_i \nabla_{r_i} V(\|r_{il}\|) \\
& - \nabla_{r_i} V(\|r_{en}\|) - \sum_{k \in \bar{\mathcal{N}}_i} \nabla_{r_i} V(\|r_{ik}\|) \\
& - \alpha \sum_{j \in \bar{\mathcal{N}}_i} \bar{a}_{ij} \left\{ \text{sgn} \begin{bmatrix} \sum\limits_{p \in \bar{\mathcal{N}}_i} \bar{a}_{ip}(v_i - v_j) \\ + h_i(v_i - v_l) \end{bmatrix} \right\} \\
& + \alpha \sum_{j \in \bar{\mathcal{N}}_i} \bar{a}_{ij} \left\{ \text{sgn} \begin{bmatrix} \sum\limits_{p \in \bar{\mathcal{N}}_j} \bar{a}_{jp}(v_j - v_p) \\ + h_j(v_j - v_l) \end{bmatrix} \right\},
\end{aligned}
\tag{4.47}
$$

where $h_i(t) = \begin{cases} 1 & i \in \mathcal{N}_l(t) \\ 0 & others \end{cases}$, α is control gain.

Define a semi-positive definite energy function:

$$
\begin{aligned}
Q(x, v, r_l, v_l) = & \sum_{i=1}^{N} \Big(\sum_{j \in \bar{\mathcal{N}}_i} V(\|r_{ij}\|) + h_i V(\|r_{il}\|) \\
& + V(\|r_{en}\|) + \sum_{k \in \bar{\mathcal{N}}_i} V(\|r_{ik}\|) \Big) \\
& + \frac{1}{2} \sum_{i=1}^{N} (v_i - v_l)^T (v_i - v_l).
\end{aligned}
\tag{4.48}
$$

Based on this energy function, we define a maximum of the energy function Q_{max}:

$$\begin{aligned} Q_{max} =& \frac{N(N-1)}{2} V_{max}(\|r_{ij}\|) + MNV_{max}(\|r_{ik}\|) \\ &+ NV_{max}(\|r_{en}\|) + NV_{max}(\|r_{il}\|)) \\ &+ \frac{1}{2}\sum_{i=1}^{N}(v_i(0) - v_l(0))^T(v_i(0) - v_l(0)). \end{aligned} \tag{4.49}$$

In order to ensure the boundedness of the control input, realise collision avoidance, and maintain connectivity, we adopt the following interaction potential function [214]:

$$\begin{aligned} V_{ij}(\|r_{ij}\|) =& \frac{(\|r_{ij}\| - d)^2(R_j - \|r_{ij}\|)}{\|r_{ij}\| + \frac{d^2(R_j - \|r_{ij}\|)}{c_1 + Q_{max}}} \\ &+ \frac{\|r_{ij}\|\left(\|r_{ij}\| - d\right)^2}{(R_j - \|r_{ij}\|) + \frac{\|r_{ij}\|(R_j - d)^2}{c_2 + Q_{max}}}, \end{aligned} \tag{4.50}$$

where d is the desired distance between vehicles, and R_j is the communication range of vehicle j.

In addition, in order to ensure that the vehicle is always within the road boundary while being able to avoid human-operated vehicles in the environment. $V_{ik}(\|r_{ik}\|)$ and $V_{en}(\|r_{en}\|)$ should satisfy the following conditions: $V_{ik}(\|r_{ik}\|)$ and $V_{en}(\|r_{en}\|)$ are continuous, differentiable, monotonically decreasing over the interval $\|r_{ik}\|, \|r_{en}\| \in (0, d_{ek}]$, where d_{ek} denotes the minimum distance allowed between the vehicle i and the road boundary or human-operated vehicles. Additionally, these two interaction potential fields also need to meet the following conditions:

$$\begin{aligned} &V_{ik}(0) = c_3 + Q_{max}, \\ &V_{en}(0) = c_4 + Q_{max}, \\ &V_{ik}(d_{ek}) = 0, \\ &V_{en}(d_{ek}) = 0. \end{aligned} \tag{4.51}$$

V_{ik} and V_{en} are also similar potential field functions of equation (4.50). Their parameters will be adjusted according to the actual application. Moreover, these two interaction potential functions only work on the interval $(0, d_{ek}]$. This is because the human-operated vehicles and the road boundary exert only repulsive forces on the AV fleet members.

4.3.5 Stability analysis

To consider an MVS consisting of N follower vehicles and one leader AV, the dynamic models of both the leader AV and the followers satisfy equation (5.1), we design the control protocol equation (4.47) for all follower vehicles. We assume that the lateral and longitudinal accelerations of all vehicles have maximum values, and $\|\dot{v}_l\|_1 \leq a_{max}$. When the initial connection topology $G(0)$ is connected, and the initial energy $Q(0)$ is limited if the control gain $\alpha > \frac{a_{max}}{2}$, the connection of the whole MVS will be kept, all followers will gradually synchronize velocity with the leader AV and achieve obstacle avoidance.

Define a position difference vector $\tilde{r}_i = r_i - r_l$ and velocity difference vector $\tilde{v}_i = v_i - v_l$ between the vehicle i and leader AV. We can get the following equations:

$$
\begin{aligned}
\dot{\tilde{r}}_i &= \tilde{v}_i \\
\dot{\tilde{v}}_i &= -\sum_{j \in \bar{\mathcal{N}}_i} \nabla_{\tilde{r}_i} V(\|r_{ij}\|) - h_i \nabla_{\tilde{r}_i} V(\|r_{il}\|) \\
&\quad - \nabla_{\tilde{r}_i} V(\|r_{en}\|) - \sum_{k \in \bar{\mathcal{N}}_i} \nabla_{\tilde{r}_i} V(\|r_{ik}\|) - \dot{v}_l \\
&\quad - \alpha \sum_{j \in \bar{\mathcal{N}}_i} \bar{a}_{ij} \left\{ \operatorname{sgn} \begin{bmatrix} \sum_{p \in \bar{\mathcal{N}}_i} \bar{a}_{ip} (\tilde{v}_i - \tilde{v}_p) \\ + h_i \tilde{v}_i \end{bmatrix} \right\} \\
&\quad + \alpha \sum_{j \in \bar{\mathcal{N}}_i} \bar{a}_{ij} \left\{ \operatorname{sgn} \begin{bmatrix} \sum_{p \in \bar{\mathcal{N}}_j} \bar{a}_{jp} (\tilde{v}_j - \tilde{v}_p) \\ + h_j \tilde{v}_j \end{bmatrix} \right\}.
\end{aligned} \tag{4.52}
$$

Energy function equation (4.48) can be redefined as:

$$
\begin{aligned}
Q(\tilde{r}, \tilde{v}) = &\sum_{i=1}^{N} \Big(\sum_{j \in \bar{\mathcal{N}}_i} V(\|r_{ij}\|) + h_i V(\|r_{il}\|) \\
&+ V(\|r_{en}\|) + \sum_{k \in \bar{\mathcal{N}}_i} V(\|r_{ik}\|) \Big) \\
&+ \frac{1}{2} \sum_{i=1}^{N} \tilde{v}_i^T \tilde{v}_i.
\end{aligned} \tag{4.53}
$$

In the interval $[t_0, t_1)$, control connection topology $\mathcal{G}(t)$ will not update. We take the first derivative of the energy function (4.53) with respect to time:

$$
\begin{aligned}
\dot{Q}(\tilde{r},\tilde{v}) = &\sum_{i=1}^{N}\Big(\sum_{j\in\tilde{\mathcal{N}}_i} v_i \nabla_{\tilde{r}_i} V(\|r_{ij}\|) + h_i v_i \nabla_{\tilde{r}_i} V(\|r_{il}\|) \\
&+ v_i \nabla_{\tilde{r}_i} V(\|r_{en}\|) + \sum_{k\in\tilde{\mathcal{N}}_i} v_i \nabla_{\tilde{r}_i} V(\|r_{ik}\|)\Big) \\
&+ \sum_{i=1}^{N} \tilde{v}_i \dot{\tilde{v}}_i .
\end{aligned} \tag{4.54}
$$

Substituting equation (5.16), equation (4.55) can be obtained,

$$
\begin{aligned}
\dot{Q}(\tilde{r},\tilde{v}) &= \sum_{i=1}^{N} \tilde{v}_i^T \alpha \sum_{j\in\bar{\mathcal{N}}_i} \bar{a}_{ij} \left\{ \text{sgn}\left[\sum_{p\in\bar{\mathcal{N}}_j} \bar{a}_{jp}(\tilde{v}_j - \tilde{v}_p) + h_j \tilde{v}_j \right] \right\} \\
&\quad - \sum_{i=1}^{N} \tilde{v}_i^T \alpha \sum_{j\in\bar{\mathcal{N}}_i} \bar{a}_{ij} \left\{ \text{sgn}\left[\sum_{p\in\bar{\mathcal{N}}_i} \bar{a}_{ip}(\tilde{v}_i - \tilde{v}_p) + h_i \tilde{v}_i \right] \right\} - \sum_{i=1}^{N} \tilde{v}_i^T \dot{\tilde{v}}_l \\
&= -\alpha \tilde{v}^T (\bar{L}(t_0) + H(t_0)) \text{sgn}\left[\bar{L}(t_0) + H(t_0)\tilde{v}\right] - \sum_{i=1}^{N} \tilde{v}_i^T \dot{\tilde{v}}_l \\
&\le \|\dot{v}_l\|_1 \|\tilde{v}\|_1 - \alpha \left\|\bar{L}(t_0) + H(t_0)\right\|_1 \|\tilde{v}\|_1 \\
&\le (a_{max} - \alpha \left\|\bar{L}(t_0) + H(t_0)\right\|_1) \|\tilde{v}\|_1 \\
&\le (a_{max} - \alpha \cdot \min \left\|\bar{L}(t_0) + H(t_0)\right\|_1) \|\tilde{v}\|_1 .
\end{aligned} \tag{4.55}
$$

where $H(t_0) = \text{diag}\{h_1, h_2, \dots, h_N\}$. By the definition of the Laplace matrix, $\bar{L}(t) = \bar{D}(t) - \bar{A}(t)$. $\bar{D} = \text{diag}\{d_i\}$, where d_i is the in-degree of the node i. For the control connection topology $\mathcal{G}(t)$, $\min(d_i) = 1$. Since the initial topology of an MVS is connected, $\exists h_i = 1$. Hence, $\min\left\|\bar{L}(t_0) + H(t_0)\right\|_1 = 2$. According to the assumption $\alpha > \frac{a_{max}}{2}$, Equation (4.55) can be transformed into:

$$
\begin{aligned}
\dot{Q}(\tilde{r},\tilde{v}) &\le (a_{max} - 2\alpha) \|\tilde{v}\|_1 \\
&\le 0, \forall t \in [t_0, t_1) .
\end{aligned} \tag{4.56}
$$

The equation (4.56) indicates that $Q(t) \le Q(t_0) < Q_{max}, \forall t \in [t_0, t_1)$, which means:

- The distance between vehicle i and the road boundary will not be zero.
- The distance between vehicle i and human-operated vehicles will not be zero.
- The length of communication connection between vehicle i and vehicle j will not be

zero and will not equal R_j.

Therefore, $\forall t \in [t_0, t_1)$, the vehicle will not reach the road boundary, and will not lose the communication connection with other vehicles. Meanwhile, the MVS will not collide, nor will it collide with human-operated vehicles.

Without loss of generality, we assume that the control connection topology switches at t_{n-1}. The newly formed connection topology consists of N_f follower-follower connections and N_l follower-leader connections. According to the definition of $\mathcal{G}(t)$, it follows that:

$$\begin{aligned} &1 \leq N_l \leq N \\ &N-1 \leq N_f \leq \frac{N(N-1)}{2}. \end{aligned} \tag{4.57}$$

Therefore,

$$\begin{aligned} Q(t_{n-1}) \leq\ & N_f V_{max}(\|r_{ij}\|) + MNV_{max}(\|r_{ik}\|) \\ & + NV_{max}(\|r_{en}\|) + N_l V_{max}(\|r_{il}\|)) \\ & + \frac{1}{2}\sum_{i=1}^{N}(v_i(0) - v_l(0))^T(v_i(0) - v_l(0)) \\ & \leq Q_{max}. \end{aligned} \tag{4.58}$$

In the interval $[t_{n-1}, t_n)$, taking the first derivative of the energy function with respect to time:

$$\begin{aligned} \dot{Q} &\leq (a_{max} - \alpha \left\|\bar{L}(t_{n-1}) + H(t_{n-1})\right\|_1) \left\|\tilde{v}\right\|_1 \\ &\leq (a_{max} - \alpha \cdot \min \left\|\bar{L}(t_{n-1}) + H(t_{n-1})\right\|_1) \left\|\tilde{v}\right\|_1 \\ &\leq (a_{max} - 2\alpha) \left\|\tilde{v}\right\|_1 \\ &\leq 0, \forall t \in [t_{n-1}, t_n). \end{aligned} \tag{4.59}$$

Hence, $\forall t \in [t_{n-1}, t_n)$, the energy function follows that:

$$Q(t_n) \leq Q(t_{n-1}) \leq Q_{max}, \tag{4.60}$$

which means that when the MVS switches the network topology, the control protocol can still ensure that there will be no collision. Hence, the vehicle will not exceed the road boundary and will not collide with the HVs. In addition, according to the definition of control connection topology $\mathcal{G}(t)$, when the system switches the control connection topology, although the original control connections may disappear, new control connections will be generated to ensure the connectivity of the whole system.

Similarly, at any time t_n of control connection topology switching, the number of control connections in the new topology $\mathcal{G}(t_n)$ is always limited, and the range of its number also satisfy equation (4.57). We define the following set:

$$\mathrm{S} = \left\{ \tilde{r} \in D_1, \tilde{v} \in \mathbb{R}^{2N} | Q(\tilde{r}, \tilde{v}) \leq Q_{max} \quad \right\}, \tag{4.61}$$

where $D_1 = \begin{Bmatrix} \tilde{r} = \mathbb{R}^{N^2} | \left\| \tilde{r}_i - \tilde{r}_j \right\|_2 \in \left[0, V_{ij}^{-1}(Q_{max})\right] \\ \forall (i,j) \in \mathcal{G}(t_n) \end{Bmatrix}$.

According to LaSalle's invariance principle, the state trajectory of this multi-vehicles system will converge to the following set:

$$\mathrm{S}_{\text{end}} = \left\{ \tilde{r} \in D_1, \tilde{v} \in \mathbb{R}^{2N} | \dot{Q}(\tilde{r}, \tilde{v}) = 0 \quad \right\}. \tag{4.62}$$

Therefore, when the MVS enters the steady state, we can get $\dot{Q}(\tilde{r}, \tilde{v}) = 0$. According to the equation (4.59), we can calculate: $\left\| \tilde{v} \right\|_1 = 0$, which means the velocity of the follower vehicles will eventually synchronize with the leader AV. Moreover, for each $\mathcal{G}(t_n)$, all the follower vehicles will form a connected traffic flow with the leader AV.

4.4 Experiments

In this section, we verify the effectiveness of the proposed algorithm through a very representative overtaking scenario. Unreal Engine and Matlab are used in the simulation experiments. Unreal Engine is a powerful game physics engine that can be used to build very realistic autopilot scenarios that are closer to real-world driving environments. Matlab is used for algorithm development. Through the combination of Unreal Engine and Matlab, the overtaking scene of the autonomous driving team can be simulated more realistically and the overtaking process can be observed more intuitively.

4.4.1 Parameters and variables setting

As for the motion planning algorithm of leader AV, we set the following experimental parameters and variables (shown in Table 4.1).

Table 4.1. Simulation parameters and variables of motion planning algorithm of leader AV

Parameter and variable names	Value
Initial position of Leader	(12, -2.875) m
Initial velocity of Leader	5 m/s
Initial acceleration of Leader	0 m/s^2
Initial position of human-operated vehicle	(32, -3) m
Initial velocity of human-operated vehicle	10 m/s
Initial acceleration of human-operated vehicle	0.1 m/s^2
The jerk of human-operated vehicle	0.01 m/s^3
Attractive force gain (K_p, K_v, K_a)	(500,2000,2000)
Repulsive force gain of vehicles (η_p, η_v)	(100, 200)
Repulsive force gain of road boundary	4000
Mass of Leader	1000 kg
Sampling time	0.1 s
Maximum velocity in longitudinal	33 m/s
Maximum velocity in lateral	5 m/s
Maximum acceleration in longitudinal	5 m/s^2
Maximum acceleration in lateral	1.3 m/s^2

For the distributed control topology, We set the following simulation conditions:

- Assume that the velocity of all vehicles is randomly selected in $[0, 33]$ m/s.
- In order to reflect the complete lane-changing and overtaking process, we assume that the AV fleet and the human-operated vehicle are in the same initial lane.
- The maximum acceleration of the vehicle is 5 m/s^2. According to the conditions of distributed control protocol, we set control gain $\alpha = 5 > \frac{a_{max}}{2}$.
- V2V topology connection communication range is 8 m.
- The desired distance of the vehicle in the longitudinal direction and lateral direction are, respectively, 6 m and 0 m.
- The minimum distance allowed between the vehicle i and the road boundary or obstacles $d_{ek} = 1$.

We add an additive hysteresis constant ε_0 to all potential field functions to prevent vehicle connection topology disconnection in the discrete time-domain. Hence, $V_{max}(\|r_{ij}\|) = V_{r_{ij}}(R-\varepsilon_0)$. $V_{max}(\|r_{ik}\|) = V_{r_{ik}}(\varepsilon_0)$. $V_{max}(\|r_{en}\|) = V_{r_{en}}(\varepsilon_0)$. $V_{max}(\|r_{il}\|) = V_{r_{il}}(R_l - \varepsilon_0)$. According to equation (4.49), Q_{max} can be calculated as:

$$
\begin{aligned}
Q_{max} \leq \frac{N(N-1)}{2} & V_{r_{ij}}(R-\varepsilon_0) + MNV_{max}V_{r_{ik}}(\varepsilon_0) \\
& + NV_{r_{en}}(\varepsilon_0) + NV_{r_{il}}(R_l - \varepsilon_0) \\
& + \frac{N}{2}(v_{max}^T v_{max}).
\end{aligned} \tag{4.63}
$$

Here, we set $N = 2$, and $\varepsilon_0 = 0.5$. Q_{max} can be determined by the upper bound of the vehicle velocity. It is calculated that: $Q_{max} \leq 1153$. $c_1 = c_2 = c_3 = c_4 = 50$. Substituting the parameters into equation (4.50), we can obtain the specific form of the interaction potential function.

4.4.2 Results and analysis

Overtaking performance

In this scenario, the leader AV needs to complete the planning of overtaking trajectory and lead the follower AVs to complete the overtaking of human-driven vehicles in front. The follower AVs need to track the leader AV and maintain a safe distance from other vehicles. We simulated the overtaking scenario with Unreal Engine. In this engine, we can clearly observe the detailed process of the overtaking of the AV fleet. Fig. 4.6 shows the process of autonomous overtaking and lane-changing of the AV fleet. At $t = 2$ s, the AV fleet and the H1 were in the same lane. When $t = 6$ s, the AV fleet was in the process of lane-changing, from the right lane to the left lane. After the AV fleet finished lane-changing, it began to approach and overtook the H1 (as shown in Fig. 4.6(c)). At $t = 9$ s, the AV fleet began to accelerate to overtake the H1 on the right lane. By $t = 10$ s, the L1 and F1 completely overtook the H1. In Fig. 4.6(f), the whole AV fleet completed the overtaking and began to switch to the initial lane. Then, the vehicle returned to the initial lane at $t = 20$ s and the overtaking and lane-changing process were finished. During the whole overtaking process, there was no collision and no driving out of the road boundary. The corresponding motion trajectory can be clearly shown in Fig. 4.7. It can be seen that in the process of overtaking and lane-changing, the trajectories of all AVs are smooth. In particular, in Fig. 4.7(d) and (e), the trajectories of F1 and F2 show lateral fluctuations, which is the obstacle avoidance behaviour of vehicles. After

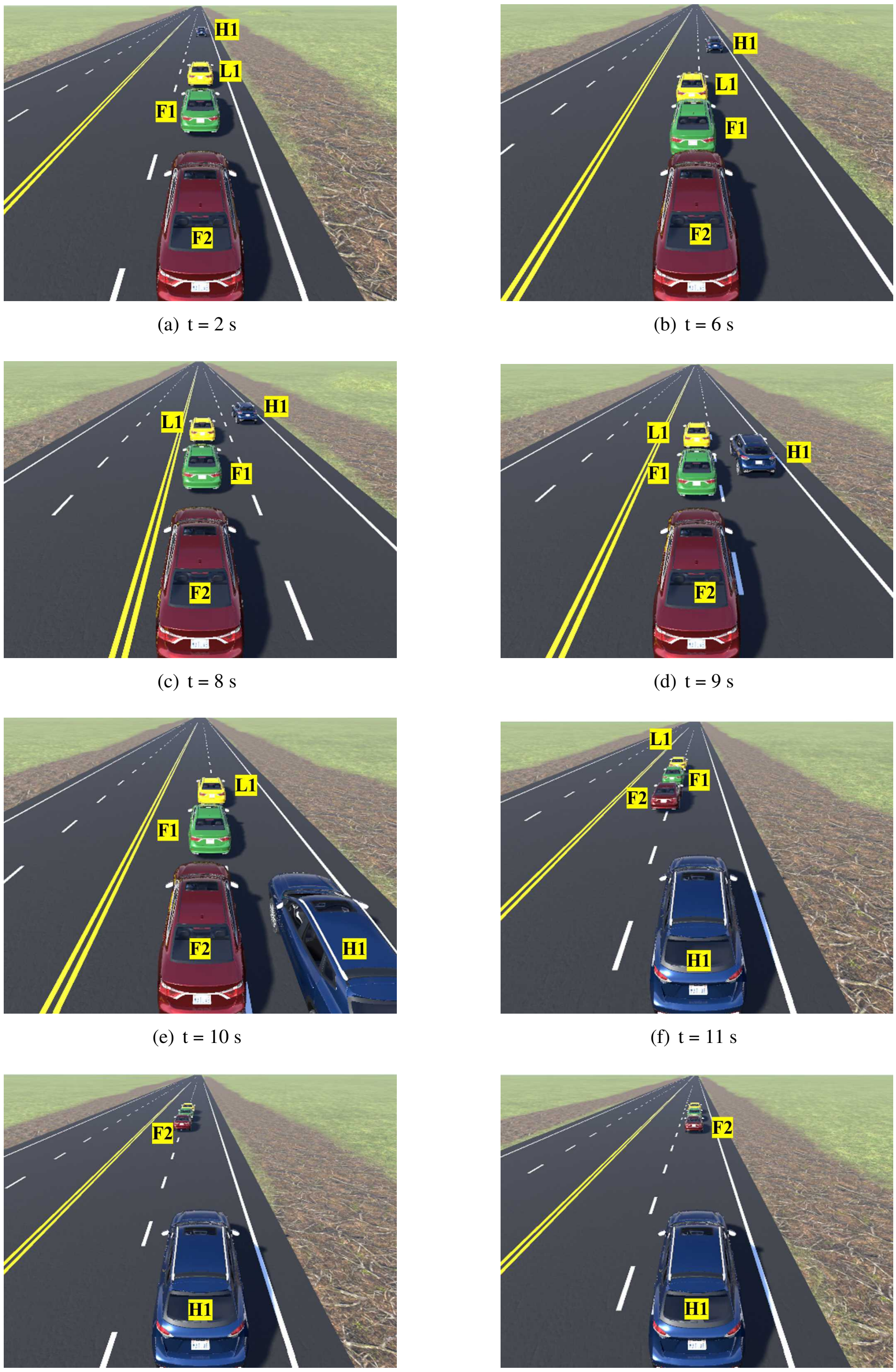

(a) t = 2 s (b) t = 6 s (c) t = 8 s (d) t = 9 s (e) t = 10 s (f) t = 11 s (g) t = 14 s (h) t = 20 s

Figure 4.6. The process of lane-changing and overtaking in Unreal Engine. H1 denotes the human-operated vehicle. L1, F1, and F2, respectively, denote the leader AV, first follower AV, and second follower AV.

completing obstacle avoidance, F1 and F2 can still follow the leader AV. It shows that in the control protocol designed in this chapter, the human-operated vehicles will not cut off the connection topology of the AV fleet.

We discuss the leader VA's motion planning algorithm in this chapter independently. Fig. 4.8 is the position and velocity curve of the leader AV. As can be seen from the figure, the lateral

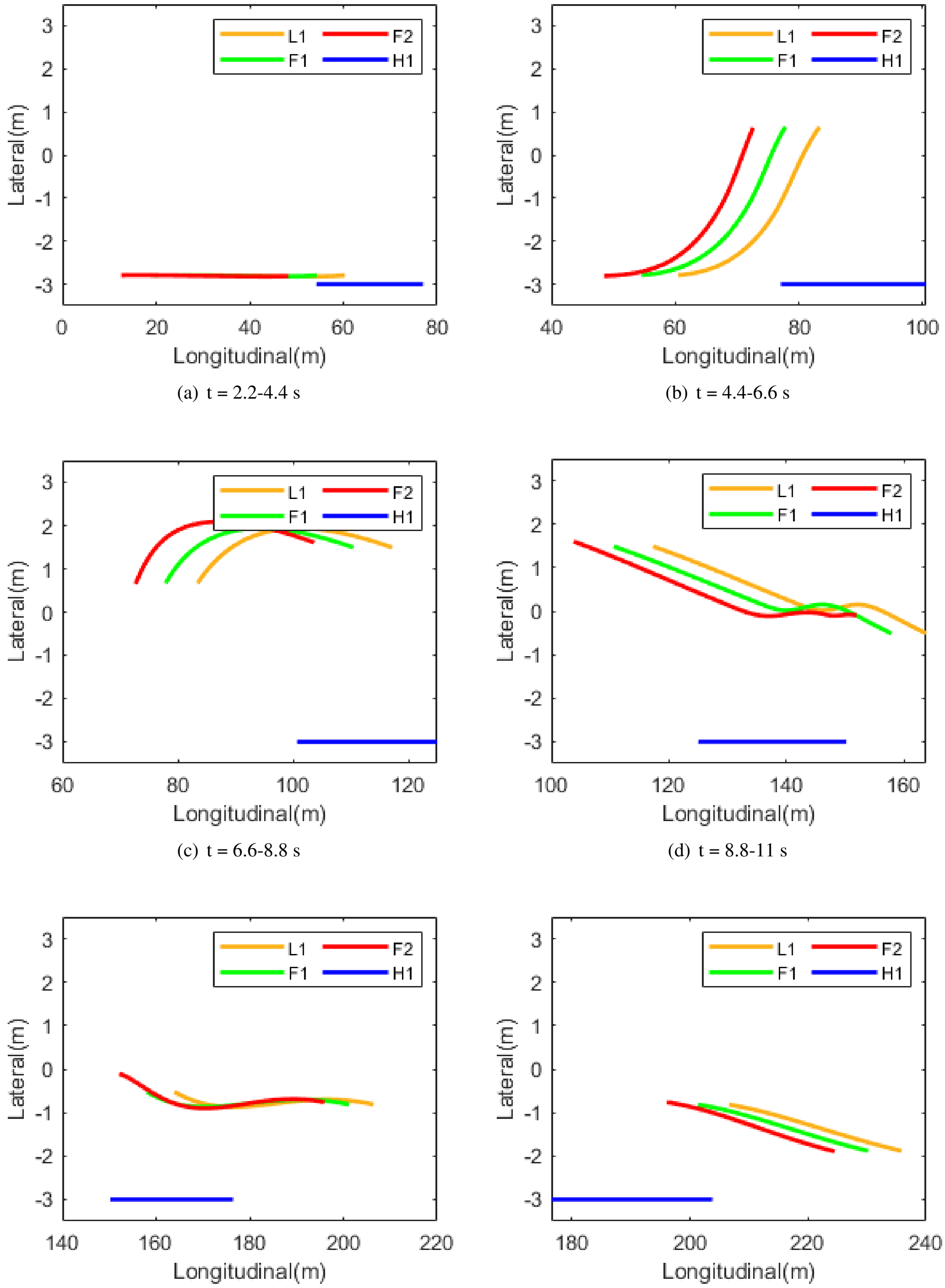

(a) t = 2.2-4.4 s

(b) t = 4.4-6.6 s

(c) t = 6.6-8.8 s

(d) t = 8.8-11 s

(e) t = 11-13.2 s

(f) t = 13.2-15.4 s

Figure 4.7. Detailed autonomous overtaking process of autonomous vehicles fleet with one leader AV

and longitudinal velocity of the vehicle converges to the same value as the velocity of the HV. The position difference between the leader AV and the HV converges to a constant value. This constant position difference is given by the vehicle's decision module, and this constant position difference will be adjusted according to the size of the fleet.

Fig. 4.9 and Fig. 4.10, respectively, represent the position difference and speed difference curves between AV fleet members F1, F2, and L1. In the longitudinal direction, the distance

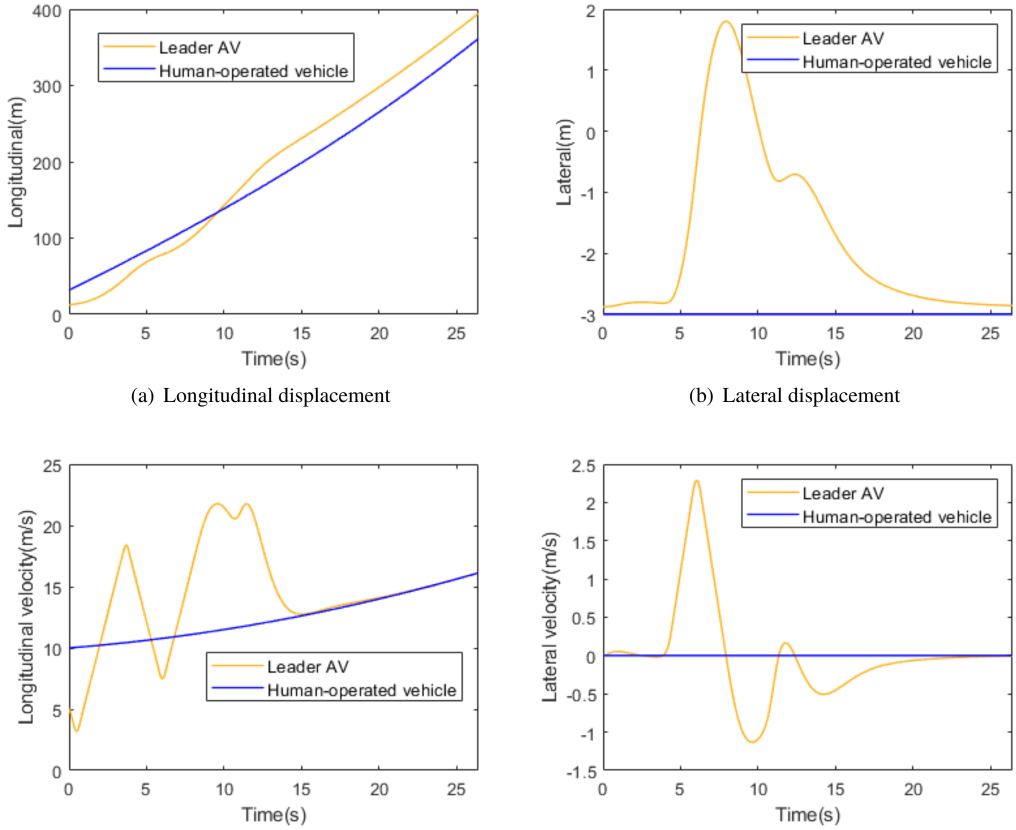

(a) Longitudinal displacement

(b) Lateral displacement

(c) Longitudinal velocity

(d) Lateral velocity

Figure 4.8. The displacement and velocity curves of leader AV and human-operated vehicle

between vehicles fluctuates greatly in the process of overtaking. However, this fluctuation does not cause collisions between vehicles, nor does it sever the topological connection between vehicles. After overtaking, the distance between vehicles converges to an expected value. In the lateral direction, similar results can be achieved. As for the velocity difference, in the process of lane-changing and overtaking, the velocity difference between vehicles changes dramatically. This is caused by the AV's autonomous obstacle avoidance. After overtaking, the velocity difference between vehicles converges to zero, which means that the velocity of the whole AV fleet is synchronized.

Robustness verification

We verify the robustness of the algorithm by randomly setting the speed of H1 and the initial speed of the AV fleet members. The rest of the simulation settings remain the same as Table 4.1. Therefore, we defined three different cases, including Case-1 where the initial velocities of F1, F2, L1, and H1 are 1 m/s, 2 m/s, 5 m/s, and 10 m/s, Case-2 where the initial velocities of F1, F2, L1, and H1 are 1 m/s, 2 m/s, 4 m/s, and 7 m/s, and Case-3 where the

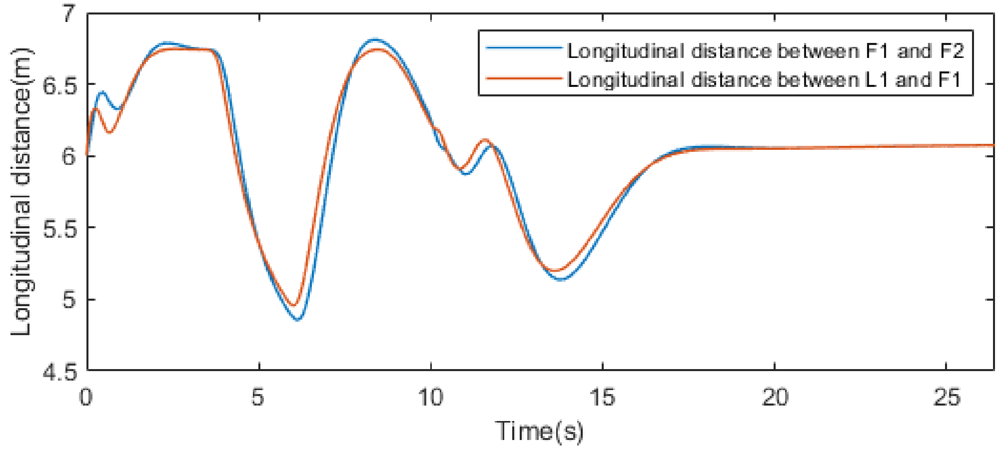

(a) Longitudinal distance

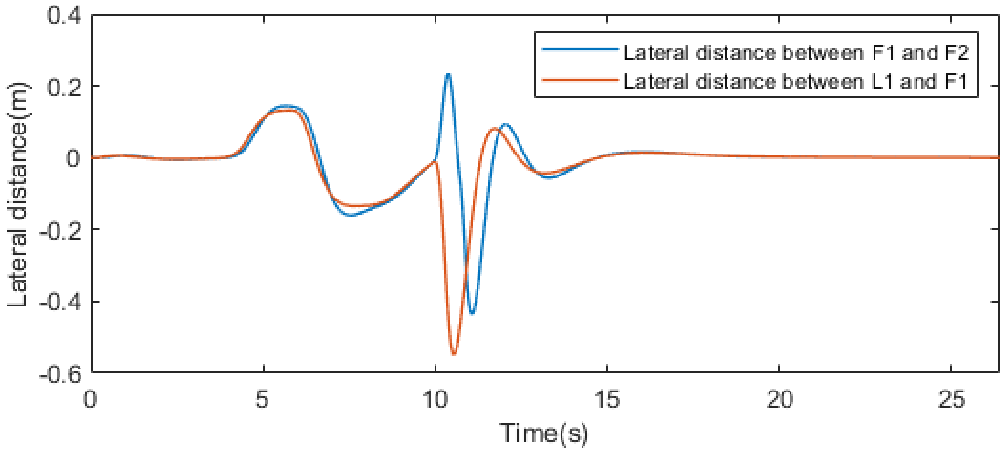

(b) Lateral distance

Figure 4.9. The displacement distance curve between the members of the autonomous vehicles fleet

initial velocities of F1, F2, L1, and H1 are 2 m/s, 3 m/s, 6 m/s, and 9 m/s. As illustrated in Fig. 4.11, the automatic overtaking was completed at different initial speeds for both AVs and H1. Additionally, in real-world applications, the information obtained via V2V is not completely accurate. Similar to [215], we assume that both the position, velocity, and acceleration information obtained from each V2V communication is subject to a random error that ranges from -3% to 3%. We additionally run the simulation experiment with simulation settings in Table 4.1 and obtain the results considering V2V communication errors. As depicted in Fig. 4.12, after adding the random communication error, the trajectory of the AV fleet shifts slightly compared to Fig. 4.11(a). As a result, the overtaking and lane-changing are completed safely, which shows that the proposed algorithm is robust in the presence of communication errors.

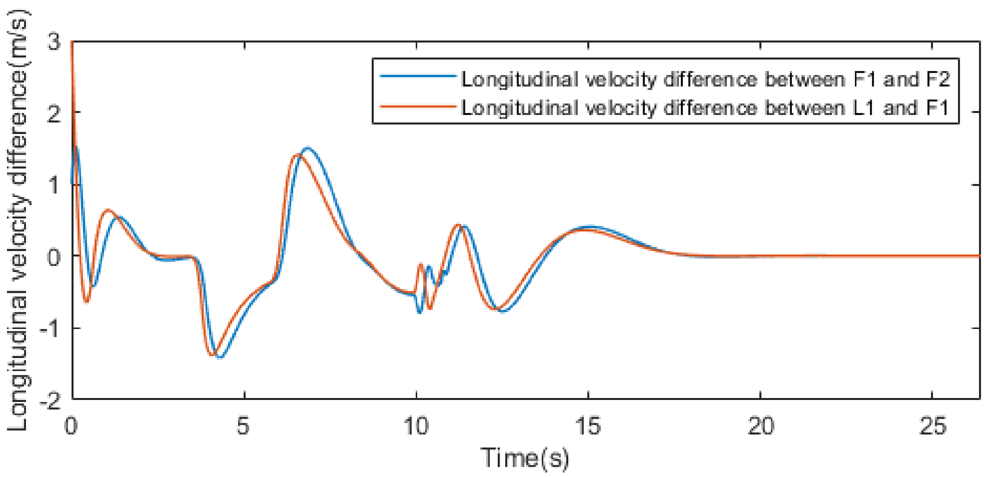

(a) Longitudinal velocity difference

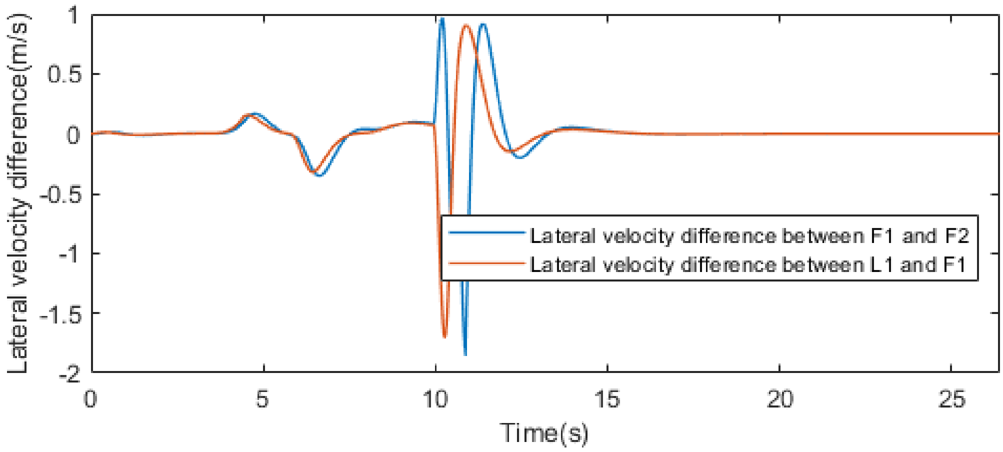

(b) Lateral velocity difference

Figure 4.10. The velocity difference curve between the members of the autonomous vehicle fleet

Comparison

There are many studies on overtaking of AV, e.g., [204] proposes a probability-based approach in the background of the graph-based route selection optimisation, with which the motions of the HVs are predicted. This study considers HVs and aims to search for an overtaking path with the lowest collision probability through the probability distribution of vehicle speed and acceleration. However, this method is only applicable to individual vehicle overtaking and not to MVSs, as the method does not require cooperative control between AVs. In our proposed control strategy, not only HVs are considered, but also a cooperative control protocol is designed to ensure an MVS with good group performance. In [191], a novel swarm intelligence-based algorithm is proposed for producing the multi-objective optimal overtaking trajectory of autonomous ground vehicles, which obtains good overtaking and obstacle avoidance trajectories. However, this approach is still not applicable to MVSs. Moreover, in this study, the object to be overtaken is modelled as a static obstacle. Therefore the validity

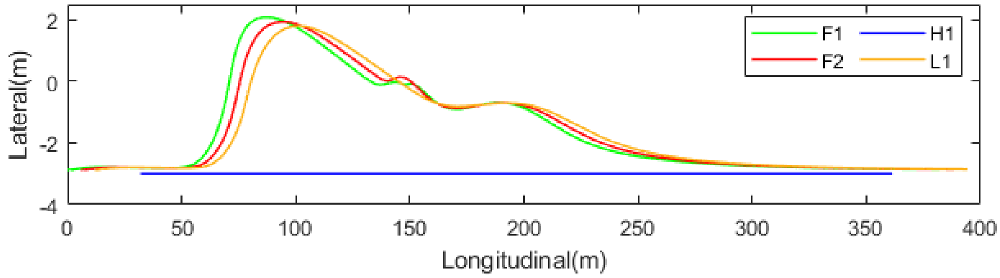

(a) Case1: the initial velocities of F1, F2, L1, and H1 are 1 m/s, 2 m/s, 5 m/s, and 10 m/s, respectively.

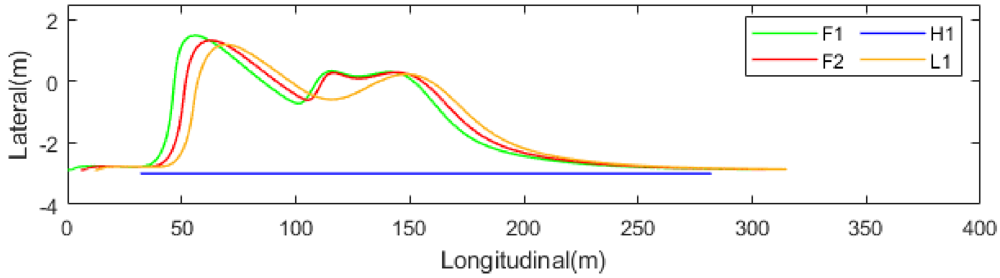

(b) Case2: the initial velocities of F1, F2, L1, and H1 are 1 m/s, 2 m/s, 4 m/s, and 7 m/s, respectively.

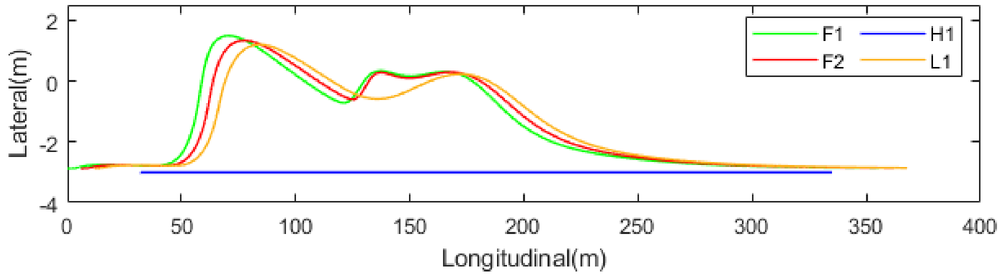

(c) Case3: the initial velocities of F1, F2, L1, and H1 are 2 m/s, 3 m/s, 6 m/s, and 9 m/s, respectively.

Figure 4.11. The process of overtaking and changing lanes of AV fleet in different cases.

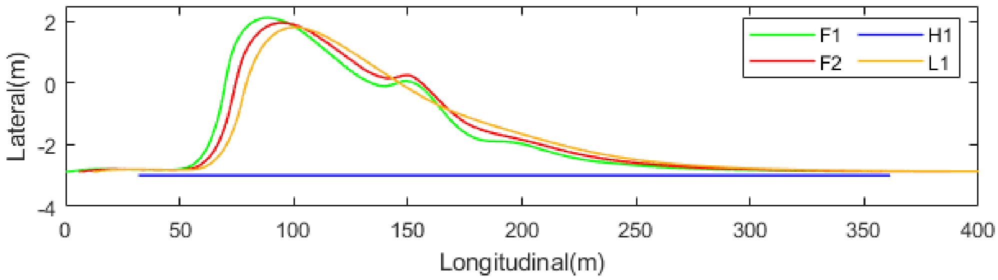

Figure 4.12. The result shows the trajectory of the AV fleet when V2V communication has a random error of 3%. The initial velocities of F1, F2, L1, and H1 are 1 m/s, 2 m/s, 5 m/s, and 10 m/s, respectively.

of the method for dynamic HVs is not guaranteed. In our overtaking control strategy, we consider HVs while focusing on the cooperative control of MVSs, which enables the vehicle platoon to complete safe overtaking while ensuring the stability of the platoon. In this chapter, the overtaking problem of an MVS is transformed into a dynamic target tracking problem of a MAS. A similar study has also been conducted in [216], in which a distributed control framework is used to dynamically track wildfire spreading by drones. However, based on this strategy, the speeds of drones cannot be synchronized with the spread of dynamic wildfires. In our study, the speed synchronisation of multi-agent with the dynamic target is realised. In Fig. 4.13, velocity curves for the target node and all AV fleet members are displayed. For a

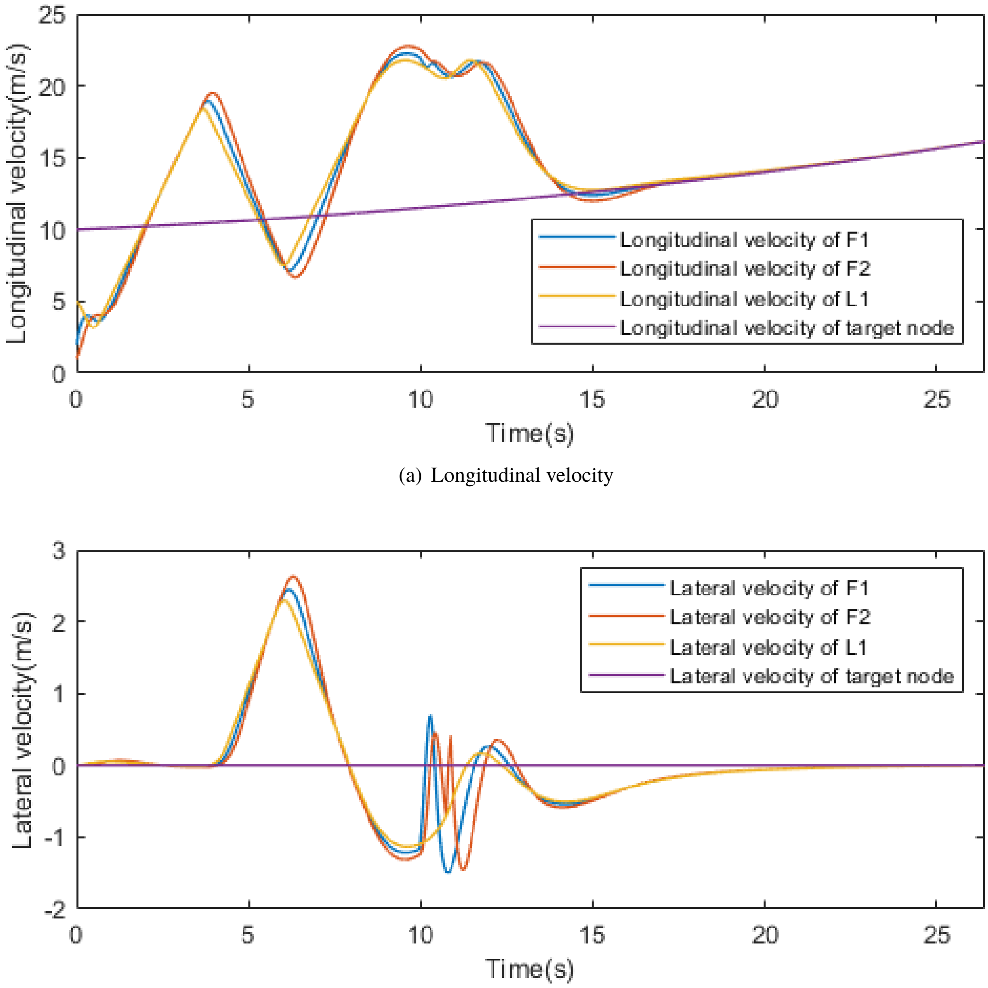

(a) Longitudinal velocity

(b) Lateral velocity

Figure 4.13. Velocity curves of AV fleet members and target node

dynamic target node with varying acceleration, the leader AV and the followers can accurately track the dynamic target node and achieve speed synchronisation. This is due to the utilisation of the proposed control strategy, where the leader AV uses a separate motion planning algorithm and the rest of the followers use a distributed cluster control. Under this strategy, each follower does not need to be equipped with an acceleration sensor. It is only the leader AV which gets the acceleration information of the HV. This greatly reduces the cost of hardware implementation and communication. As the bounded distributed control protocol is used in this chapter, the control output of the follower vehicle is bounded, which is very beneficial to the application of the algorithm in real-world scenarios.

4.5 Summary

This chapter addresses the distributed motion control problem of autonomous vehicles operating in a complex multi-lane, heterogeneous vehicle platoon. The proposed algorithm also includes an effective mechanism for safe autonomous overtaking when the platoon consists of autonomous and human-operated vehicles. This chapter introduces the Velocity Difference Potential Field (VDPF) and Acceleration Difference Potential Field (ADPF) techniques, which are the improved versions of the conventional Artificial Potential Field (APF) method. The overtaking problem of unmanned vehicles in a multi-lane platoon has been formulated as a formation tracking problem, in which human-operated vehicles are set as targets. The proposed technique can effectively handle situations where the acceleration of a leader vehicle changes suddenly due to approaching an obstacle or neighbouring vehicles. It also ensures that the follower unmanned vehicles achieve speed synchronisation with the leader vehicle having variable acceleration. In addition, the follower vehicles of the platoon also avoid obstacles while complying with the desired formation tracking objectives. The chapter has used Matlab and Unreal Engine software simulation platforms to test the usefulness and feasibility of the proposed algorithm. The simulation results show that a group of autonomous vehicles operate safely in a complex, heterogeneous multi-lane platoon, exhibiting safe overtaking, changing lanes, obstacle avoidance, and dynamic target tracking. To further increase the comfort of the proposed method, optimisation-based techniques may need to be integrated into the protocol design, which will be explored in our future works.

Chapter 5

Cooperative Adaptive Cruise Control for Connected Autonomous Vehicles

5.1 Introduction

CACC enables longitudinal automation of connected vehicle platoons by utilizing inter-vehicle distances and vehicle state information, which can be obtained by equipped radars and V2V communication modules [117], [217]. This technique is able to maintain a suitable inter-vehicle distance to alleviate traffic congestion, and improve safety, fuel economy, and traffic throughput [75], [159], [218], [219].

In recent years, a large number of scholars have conducted research on CACC with remarkable success. The traditional proportional-integral-derivative control design has been widely used as an effective method in ACC and CACC, which is also the control scheme now used by most mainstream automobile original equipment manufacturers [217], [220]. In the implementation of the proportional-integral-derivative control, the control input (such as acceleration or velocity) of an individual vehicle is obtained by a nonlinear function, using either the constant spacing strategy or the constant time headway strategy [76], [221]. MPC is also widely adopted in CACC schemes. These control methods not only take V2V spacing as a control objective, but also consider more optimisation indicators such as energy consumption [16], [222], comfort [223], and traffic efficiency [224]. Nowadays, a more mainstream approach is to combine distributed mechanism with MPC [225]–[228]. Other control methods are also being investigated, in [229], the stochastic optimal control strategy can produce smoother vehicle control input signal with small system disturbances and large measurement disturbances. In [230], a new control structure with optimal control and online learning is used to find the optimal error feedback, as well as seek the minimum headway values. In addition, control methods based on a combination of data-driven and optimisation are gaining more and more attention from researchers, where reinforcement learning-based techniques have been utilised in many studies [203], [231], [232] as a potential solution to achieve CACC. However, these optimisation-based control algorithms and data-driven approaches place enormous demands on the computing capacity of autonomous vehicles.

CACC is a framework that relies heavily on V2V communication. If the V2V communication is attacked or lost, CACC will degrade to ACC, thus increasing the risk of vehicle collisions [233], [234]. Numerous experimental results have shown that ACC has a negative impact on the traction energy consumption of the vehicle [235], [236]. In addition, more real vehicle experiments and empirical data are needed to support the improvement and optimisation of the ACC model [237]. To overcome this issue, some preliminary results have been obtained by researchers in recent years. In [238], by incorporating statistical learning with the physical laws of kinematics, a real-time anomaly detection mechanism is proposed which has been shown to be effective in detecting forgery attacks in CACC. Besides, the association between multiple motion parameters concerning both individual and consecutive vehicles is used to assess the credibility of the information provided by the connected members [239]. The security of V2V communications has been assured with the emphasis placed on cyber security by original equipment manufacturers [240], such as by introducing secure onboard communication [241]. These encrypted communications protect the authenticity of communication messages to a large extent. Hence, communication loss has now become the leading cyber security issue in CACC. In order to completely avoid the communication loss problem, it is necessary to expand the communication infrastructure and reduce the failure rate of the onboard communication modules. However, for the CACC algorithm, improving the algorithm to reduce or eliminate the negative effect of communication loss may be more feasible and efficient [124]. In [122], the researchers model communication losses as independent random events. By applying H_∞ control tools to both plant stability and string stability of the average error dynamics and minimizing the variance of the trajectories, the effect of the communication losses can be effectively mitigated. A disturbance observer-based sliding mode control is proposed in [242], which estimates the uncertainty present in the actuator dynamics and the acceleration of the preceding vehicle as a lumped disturbance. In addition, state estimation is considered to be an effective solution to temporary loss of communication

[243]. When the V2V communication is temporarily lost, [123] utilises an adaptive Kalman filter to estimate the acceleration of a preceding vehicle, and the estimated acceleration is implemented as a feedforward signal in the ego-vehicle CACC design. However, most of these solutions are simply finding an estimate for the vehicle to use as a feedback input to achieve CACC. When the number of vehicles experiencing a loss of communication increases, it will bring more difficulties for these methods to secure the system.

Motivated by the aforementioned challenges, we aim to propose a reliable CCAC framework by using SDEM and distributed mechanisms. Different from [123], [244], [245], in our solution, we do not perform state estimation in the case of communication loss. Instead, we aim to design a more generalized CACC algorithm, i.e. one applicable to CACC and equally applicable to ACC. In addition to achieving basic obstacle avoidance and vehicle speed consistency, the proposed control design can also achieve the boundedness of the control input and maintain the connectivity of the topology. To the best of the authors' knowledge, such an SDEM-based distributed control strategy has not been developed in the literature. This chapter draws on the network model presented in [243], [246]. On-board sensors can acquire information about the movement of the closet front vehicle, while V2V communication can obtain state information about the movements of all vehicles within the communication range. The main contributions of the chapter are as follows:

- We innovatively use a specially defined SDEM to construct a robust self-driving vehicle platoon system. This model ensures the internal stability of the platoon system, the stability of the topology connections, and the consistency of the platoon velocity.
- A special nonlinear spring is designed to describe the V2V interaction, which can ensure that no collision occurs within the platoon. Besides, the desired speed can be maintained in the presence of sudden acceleration or deceleration by the leading vehicle.
- Based on the proposed energy model, a distributed control protocol is proposed, which only relies on state information from neighbouring vehicles. The string stability of the vehicle system under this control protocol is proved. Also, this generalized control protocol can be applied to both CACC and ACC cases.
- The effectiveness of the proposed strategy under several scenarios (including merging and separating) is verified by realistic simulation experiments, which lays the foundation

for implementing it on a real vehicle platoon in the future.

The rest of this chapter is structured as follows: Preliminaries and problem statements are shown in Section II. We propose the distributed control protocol based on the SDEM and prove the stability of the control protocol in Section III. The simulation results are analyzed and discussed in SectionIV. Finally, we conclude this work in SectionV.

5.2 Problem formulation

5.2.1 Dynamics model

In the current studies on CACC, the linearisation technique is commonly applied to deal with the upper-level longitudinal nonlinear dynamics [247]–[249]. Since we mainly focus on developing high-level multi-vehicle coordination strategies in this chapter, to simplify the dynamics model, the air drag, rolling resistance, and actuator delay in the vehicle dynamics model are ignored. The second-order differential model can be described using ordinary differential equations (ODE) following [14], [226]:

$$\begin{cases} \dot{x}_i = v_i \\ \dot{v}_i = u_i \end{cases}, \tag{5.1}$$

where x_i, v_i and u_i are the position, velocity and control input of vehicle i, respectively.

5.2.2 Communication topology and vehicle platoon

A time-varying directed graph $\mathcal{G}(t) \triangleq (\mathcal{V}, \mathcal{E}(t))$ is used to describe the network topology among the vehicles within the platoon, where $\mathcal{V} \triangleq \{\mathcal{V}_1, \ldots, \mathcal{V}_N\}$ is set of nodes. And the element of $\mathcal{E}(t) \in N \times N$ is denoted as $(\mathcal{V}_i, \mathcal{V}_j)$, which is termed an edge from $\mathcal{V}_i$ to $\mathcal{V}_j$. $A(t) = [a_{ij}] \in \mathbb{R}^{N\times N}$ is the adjacency matrix of graph $\mathcal{G}(t)$. $a_{ij} = 1$, if $\|x_i(t) - x_j(t)\| < \rho$, otherwise, $a_{ij} = 0$. $a_{ij} = 1$ means that the vehicles i can receive the information from vehicle j through V2V communication or on-board sensors. In this chapter, we suppose that the initial connection topology of the vehicle platoon is connected. The initial connection of

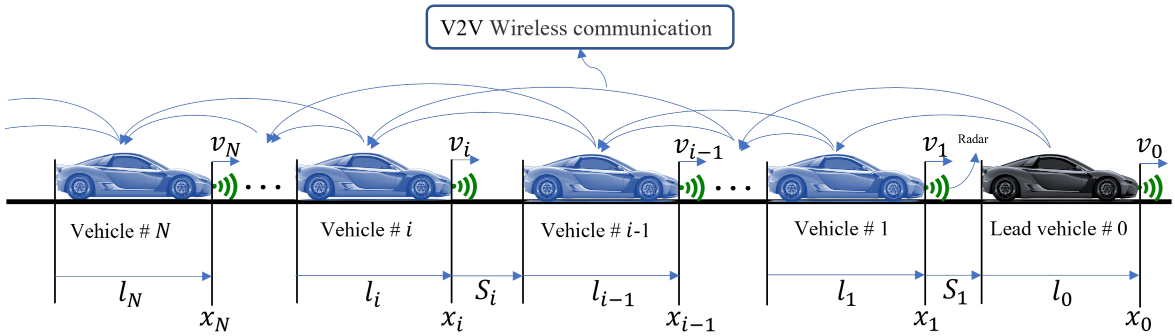

Figure 5.1. Network topology model for autonomous vehicle platoon

the system is: $\mathcal{E}(0) = \{(i,j), | \|x_i(0) - x_j(0)\| < \rho, i, j \in \mathcal{V}\}$.

We consider a platoon of $N+1$ vehicles with an index from 0 to N as shown in Fig. 5.1. The index 0 represents the leader and the index 1 to N denote the followers. l_i is the body length of vehicle i. x_i and v_i, respectively, are the position and velocity of the front bumper of vehicle i. $S_i := x_i - x_{i-1} - l_{i-1}$ is the distance between the front bumper of vehicle i and the back bumper of the vehicle $i-1$. The vehicle can obtain the motion state of the nearest vehicle in front by the ob-board sensors (e.g., radar) and the V2V communication, including position and speed information, and obtain the motion state of the vehicles beyond the radar field of vision through V2V communication. Define a variable to denote the desired distance between vehicle i and vehicle j:

$$\hat{S}_{ij} = \sum_{k=j+1}^{i} S_k + \sum_{k=j}^{i-1} l_k \quad \forall i > j \geq 0 \, , \tag{5.2}$$

where S_k represents the desired distance between the vehicle k and vehicle $k-1$. In addition, suppose that the V2V communication radius is ρ, therefore, the number of vehicles that are within the communication range of vehicle i is limited. Assume that this limited number is m. In the proposed algorithm in this chapter, we assume that the connection topology between the vehicle platoon is directional. This means that vehicle i can use the state information from vehicle j, while vehicle j does not use the state information from vehicle i, $\forall i > j \geq 0$.

5.2.3 Control objectives

There are two mainstream strategies, the dynamic spacing policy, and the constant spacing policy. We chose the latter because it is easy to implement [77] and has the advantages like low computation load [250] and high traffic capacity [251]. For a vehicle platoon with a leader having constant velocity v_o when the initial connection topology is connected, the objective is listed as follows:

- To achieve the following steady state:

$$\begin{cases} \lim_{t\to\infty} \|x_i(t) - x_j(t)\| = \sum_{k=j+1}^{i} S_k + \sum_{k=j}^{i-1} l_k \\ \lim_{t\to\infty} \|v_i(t) - v_0(t)\| = 0 \end{cases} \tag{5.3}$$

$$\forall i > j \geq 0.$$

  This control objective implies that the following distance and speed of all vehicles within the platoon need to converge to the desired value.

- From the perspective of functional security, the temporary loss of V2V communication may lead to platoon collision. Therefore, another important control objective is that when V2V communication is lost, the connection topology of the platoon does not completely disconnect and the vehicle platoon continues to converge to the desired steady state.

- Topology connectivity within the platoon can be guaranteed despite sudden acceleration or deceleration by the leading vehicle. And the vehicle platoon system can re-enter the steady state within a finite time.

5.2.4 Basic lemmas

To facilitate further proof, we introduce the following lemma.

Lemma 5.1 ([252]). *L has rank $N-1$, i.e., $\lambda_1 = 0$, if and only if graph $\mathcal{G}$ has a spanning tree. Where L is the Laplace matrix of $\mathcal{G}$, and λ_1 is the first eigenvalue of L.*

Lemma 5.2 ([253]). *For symmetric matrices $A, B \in \mathbb{R}^{N\times N}$, if their eigenvalue sequences satisfy $\lambda_1(A) \leq \cdots \leq \lambda_N(A), \lambda_1(B) \leq \cdots \leq \lambda_N(B)$, the following conclusions can be drawn:*

$$\lambda_{i+j-1}(A+B) \geq \lambda_i(A) + \lambda_j(B), \tag{5.4}$$

where $i + j \leq N + 1, 1 \leq i, j \leq N$.

Lemma 5.3 ([253]). *If the graph $\mathcal{G}$ is connected, there exists left eigenvector $y > 0$ of $L(\mathcal{G})$ such that $L^T(\mathcal{G})y = 0$, $y^T 1_N = 1$.*

Additionally, we define the following lemma:

Lemma 5.4. *For a connected graph $\mathcal{G}$, define:*

$$\begin{aligned} P &= \text{diag}\{p_i\} \in \mathbb{R}^{N\times N} \\ Q &= PL(\mathcal{G}) + L^T(\mathcal{G})P, \end{aligned} \tag{5.5}$$

where $p = [p_1, p_2, \dots, p_N]$ is the left eigenvector corresponding to the zero eigenvalue of $L(\mathcal{G})$, such that $Q \geq 0$, Q has rank $N-1$.

Proof: According to the definition of the Laplace matrix, we can get:

$$\begin{aligned} L(\mathcal{G}) &= \text{diag}\{d_i\} - A \\ L^T(\mathcal{G}) &= \text{diag}\{d_i\} - A^T, \end{aligned}$$

where A and diag $\{d_i\}$ are, respectively, the adjacency matrix and in-degree matrix of graph $\mathcal{G}$. Hence,

$$PL(\mathcal{G}) + L^T(\mathcal{G})P = \text{diag}\{2d_i p_i\} - (PA + A^T P).$$

The sum of i^{th} row is $2d_i p_i + \sum_{j=1}^{N}(a_{ij}p_i + a_{ji}p_j)$. Because $L^T(\mathcal{G})p = 0$, $d_i + \sum_{j=1}^{N} a_{ji}p_j = 0$, we can obtain that the sum of i^{th} row is 0:

$$Q \begin{pmatrix} 1 \\ \vdots \\ 1 \end{pmatrix}_N = \begin{pmatrix} 0 \\ \vdots \\ 0 \end{pmatrix}_N .$$

Due to $Q^T = Q$, we also get:

$$(1, \dots, 1)_N Q = (0, \dots, 0)_N.$$

Hence, Q is the Laplace matrix of graph $\bar{\mathcal{G}}$, the weighted mirror graph of a connected directed graph $\mathcal{G}$. The weight of edge (i, j) is $\bar{a}_{ij} = p_i a_{ij} + a_{ji}p_j$. We can conclude that $\bar{\mathcal{G}}$ is a strongly connected undirected graph. The rank of Q is $N-1$, and $Q \geq 0$. Thus, the proof is done. [Done]

5.3 Cooperative adaptive cruise control design

In this section, we design a distributed cooperative control protocol for the vehicle platoon system from the perspective of system energy. This novel control design is capable of achieving all our pre-specific control objectives.

5.3.1 Spring damping energy model

In this chapter, we consider a platoon system from a very novel perspective, i.e., system energy. We start by constructing a single spring damping energy system, such as the subsystem in Fig. 5.2, consisting of A_1, A_2, K_{12}, and c_{12}. Define A, c, and K as, respectively, the agents, damping elements, and spring elements. Instead of using physical springs and dampers to connect the vehicle platoon, virtual springs and dampers units are used to connect the vehicle when building the platoon. The specific form of these virtual springs and dampers will be reflected in the vehicle's control protocol. Furthermore, it is assumed that the difference in speed of the vehicle will cause the spring unit to deform and store potential energy so that the kinetic energy generated by the speed and the potential energy stored in the spring unit can be transferred to each other. At the same time, this energy is also consumed by the damping unit when the speed difference between the vehicles is generated. Therefore, we define energy in the energy model as follows:

$$\begin{aligned} E_A(t) &= \frac{1}{2}v(t)^2 \\ E_K(t) &= g(\Delta l_A(t)) \\ E(t) &= E_A(t) + E_K(t), \end{aligned} \tag{5.6}$$

where $E_A(t)$, $E_K(t)$, and $E(t)$ are, respectively, the kinetic energy of agents, potential energy stored in the spring, and total current energy of the system. $\Delta l_A(t)$ denotes the distance between agents, and g is a function of $\Delta l_A(t)$.

Lemma 5.5. *For the energy system defined above, assume that the system has finite initial energy, the system will converge to a state where the velocity difference of vehicles is zero in the absence of external energy input.*

Proof: The time-varying energy function of the system is as follows:

$$E(t) = \frac{1}{2}v_1(t)^2 + \frac{1}{2}v_2(t)^2 + g(\Delta l_A). \tag{5.7}$$

In this spring damping system, the damping unit and the spring unit together provide acceleration to the agents, which satisfies the following equation

$$a = -\nabla g - c\Delta v, \tag{5.8}$$

where $c > 0$ is the damping coefficient. The derivative of this function with respect to time gives:

$$\begin{aligned} \dot{E}(t) &= v_1(-\nabla g - c\Delta v) + v_2(+\nabla g + c\Delta v) + \Delta v \nabla g \\ &= -c\Delta^2 v \leq 0, \end{aligned} \tag{5.9}$$

which means the system energy progressively decreases until the system energy reaches a minimum energy state. The derivative of equation (5.7) with respect to time shows that the spring damping energy system will converge to a state where $\Delta v(t)$ equals 0, and $\Delta l_A(t)$ equals constant. [Done]

Based on the above definition, we take such a basic spring-damping energy system unit and form it into a more complex energy system by connecting it in series and parallel. We consider using a particular spring-damping energy model (shown as Fig. 5.3) to simulate a vehicle platoon system with no external energy input. A_1, A_2, A_3 represent the agents corresponding to the vehicle in the vehicle platoon system. In this model, K is a specially designed nonlinear spring that also acts as an energy storage element. c represents a damper, which is an energy-consuming element whose rate of energy consumption depends on the velocity difference between agents. The storage element K is assigned specific storage limits $E_{max} + e_1$, where E_{max} denotes the initial energy of the entire system, including the kinetic energy of agents and the potential energy already stored in K, and e_1 is a constant to ensure that the actual energy storage of the spring does not exceed the maximum value. According to (9), the MVS

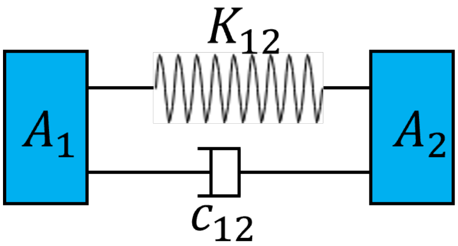

Figure 5.2. A single spring damping energy system.

constitutes an energy consuming system. In the absence of external energy input, the system energy always decreases or maintains a steady state during the task. Therefore, when the total energy of the system is transferred to one spring unit, the energy stored in the spring will not exceed the spring's storage limit. The energy stored in K is a specific function of the distance between the agents. When there is a velocity difference between agents, the energy consuming element c will keep consuming energy. According to the most fundamental law of thermodynamics, in the absence of external energy input, the system's total energy will not increase and may decrease due to the presence of energy-consuming elements. The rest of the energy in the system consists of the energy stored in the spring and the kinetic energy of the agent, which are dynamically converted to each other.

According to the conditions mentioned above, since the system's total energy is always less than or equal to the initial energy of the system, the actual energy stored by the spring can never reach its limit. This property means that the stretch and compression of the spring will not exceed the limited length. In addition, the steady state of the system is achieved when the energy storage of the spring is zero, and the energy consumption of the energy-consuming element is also zero. The above conclusion corresponds to the vehicle platoon system, the distance between vehicles will not be less than the minimum allowable distance, nor will the communication connection be disconnected. The vehicle platoon converges to a state where the velocities of the vehicles are consistent, and the distance between the vehicles satisfies expectations.

5.3.2 Distributed control protocol

This section aims to develop distributed cooperative control algorithm for connected vehicle platoons to achieve the following control objectives:

- Given a leading vehicle with a constant velocity, the velocities of all followers should

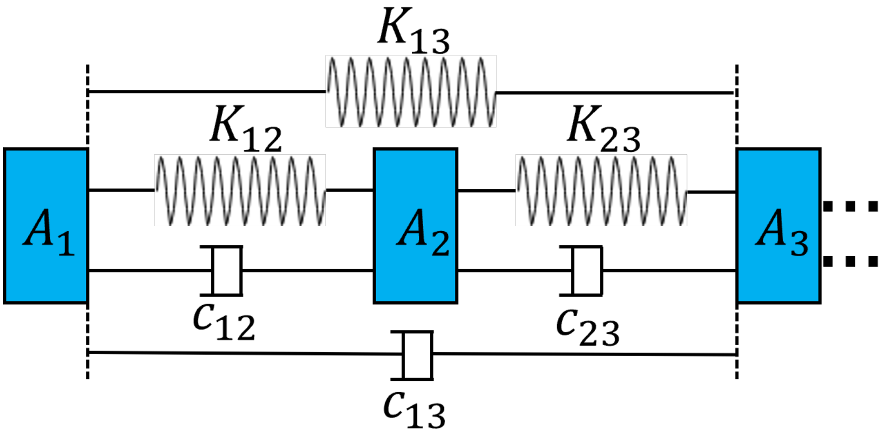

Figure 5.3. A complex spring damping energy model to describe a vehicle platoon system

converge to the leader's velocity.

- In the vehicle platoon, the following distance between all vehicles should be stable and converge to the expected value.
- When V2V communication is lost, the vehicle platoon should still achieve the desired queue.
- The string stability of the platoon must be ensured when there is a sudden change in the velocity of the leader.
- The connectivity of topology should be guaranteed.

The control protocol we designed is given as follows

$$\begin{aligned} u_i = &- \sum_{j\in\mathcal{N}_i} \nabla x_i V_{ij} \left| \sum_{j\in\mathcal{N}_i} a_{ij}(v_i - v_j) \right| - \beta \sum_{j\in\mathcal{N}_i} a_{ij}(v_i - v_j) \\ &- \frac{1}{2}\Big(\sum_{j\in\mathcal{N}_i\cup\{l\}} \nabla_{x_i} V_{ij}\Big) - h_i(v_i - v_0), \end{aligned} \tag{5.10}$$

where $h_i(t) = \begin{cases} 1 & i \in \mathcal{N}_l(t) \\ 0 & \text{others} \end{cases}$, β is the control gain, $\mathcal{N}_l$ denotes the set of neighbours of the leading vehicle. $\mathcal{N}_i$ represents the set of neighbours of the vehicle i, and the communication connection between vehicle i and vehicle j is directional. $\beta(v_i - v_j)$, and $v_i - v_0$ correspond to the damping energy dissipation function in the energy model. $-\sum_{j\in\mathcal{N}_i} \nabla x_i V_{ij} \left|\sum_{j\in\mathcal{N}_i} a_{ij}(v_i - v_j)\right|$ is the product of gradient and velocity difference, which can accelerate the convergence of the vehicle platoon system. V_{ij} is the interaction potential function between vehicles, corresponding to the spring energy function in the energy model. The gradient of V_{ij} is used to achieve obstacle avoidance and distance convergence of the vehicle platoon system. In this case, the interaction field function has to generate repulsive force over the interval $\left[l_j, \hat{S}_{ij}\right)$ and attractive force over the interval $\left[\hat{S}_{ij}, \rho\right)$. Hence, the specific form of the interaction potential function in this control protocol is designed as follows:

$$V_{ij}(\|x_{ij}\|) = \frac{(\|x_{ij}-l_j\| - \hat{S}_{ij} + l_j)^2(\rho - \|x_{ij}\|)}{\|x_{ij}-l_j\| + \frac{(\hat{S}_{ij}-l_j)^2(\rho-\|x_{ij}\|)}{c_1+\Psi_{max}}} + \frac{\|x_{ij}-l_j\|(\|x_{ij}\| - \hat{S}_{ij})^2}{(\rho - \|x_{ij}\|) + \frac{\|x_{ij}-l_j\|(\rho-\hat{S}_{ij})^2}{c_2+\Psi_{max}}}, \tag{5.11}$$

where $\hat{S}_{ij}$ is given by equation (5.2), l_j is the length of vehicle j. Different from the commonly used interactive functions, in addition to meeting the obstacle avoidance function, the potential field function can also achieve the boundedness of the control input and maintain the connectivity of the topology. Equation (5.11) is a smooth and bounded concave function. This function minimizes at $\|x_{ij}\| = \hat{S}_{ij}$, and is monotonically decreasing over the interval $\left[l_j, \hat{S}_{ij}\right)$ and monotonically increasing over the interval $\left[\hat{S}_{ij}, \rho\right)$. Ψ_{max} is the maximum of the system energy function, which is defined as follows

$$\Psi_{max} = \frac{2mN - m^2 + m}{2} V_{max} + \frac{1}{2}\sum_{i=1}^{N}\left(v_i(0) - v_0(0)\right)^2, 1 \leq m \leq N \tag{5.12}$$

where $V_{max} = \max\left\{V(l_j+\xi_1), V(\rho-\xi_2)\right\}$. ξ_1 and ξ_2 are delay constants, used to ensure the stability of the topology connection. V_{max} is the value of the function V_{ij} at $x_{ij} = l_j + \xi_1$ or $x_{ij} = \rho - \xi_2$. It can be seen that V_{max} is not the endpoint value of the function V_{ij}. That is to say, V_{max} is always less than the endpoint value of the function V_{ij}. m is the maximum number of vehicles that can communicate with vehicle i.

According to the definition of SDEM, the maximum energy of the initial platoon system needs to be estimated. Here, we define system energy as consisting of the potential energy of the interaction field between vehicles and the squared deviation of the velocity. Then when the system is in the lowest energy state, the potential energy is zero, and the square of the velocity deviation is also zero. Hence, Ψ_{max} consists of all the interaction potential energy and velocity deviation energy in the system.

To facilitate the proof of the following theorems, we define:

$$f = \sum_{k=1}^{m} max(\|\nabla x_i V_{ik}\|). \tag{5.13}$$

As can be seen from the definition, *f* means the maximum interaction force of the vehicle due to the potential field. In addition, we define a diagonal matrix as follows:

$$H = \text{diag}\left\{h_1(t_0), h_2(t_0), \dots, h_N(t_0)\right\}. \tag{5.14}$$

Theorem 1. *Suppose that the initial connection topology of the vehicle platoon $\mathcal{G}(t_0)$ is connected and the initial system energy $\Psi(t_0)$ is bounded. The connectivity of the time-varying network topology can be guaranteed if the following condition*

$$\lambda_2((\beta Q + 2PH)(t_0)) > 4mf \tag{5.15}$$

is satisfied, where Q and P are defined in Lemma 5.4.

Proof: Let the follower's position and speed deviation from the leading vehicle be $\tilde{x}_i = x_i - x_0$ and $\tilde{v}_i = v_i - v_0$. Therefore, we have

$$\begin{aligned} \dot{\tilde{x}}_i &= \tilde{v}_i \\ \dot{\tilde{v}}_i &= -\sum_{j\in\mathcal{N}_i} \nabla\tilde{x}_i\tilde{V}_{ij}\left|\sum_{j\in\mathcal{N}_l} a_{ij}(\tilde{v}_i-\tilde{v}_j)\right| - \beta\sum_{j\in\mathcal{N}_l} a_{ij}(\tilde{v}_i-\tilde{v}_j) \\ &\quad -\frac{1}{2}(\sum_{j\in\mathcal{N}_l\cup\{l\}} \nabla_{\tilde{x}_i}\tilde{V}_{ij}) - h_i\tilde{v}_i. \end{aligned} \tag{5.16}$$

Define the following non-negative energy function:

$$\Psi = \sum_{i=1}^{N} p_i \sum_{j\in\mathcal{N}_i\cup l} \tilde{V}_{ij}(\|\tilde{x}_{ij}\|) + \tilde{v}^{\mathrm{T}} P\tilde{v}, \tag{5.17}$$

where $\tilde{v} = [\tilde{v}_1, \dots, \tilde{v}_N]^{\mathrm{T}}$.

Suppose $\mathcal{G}(t)$ will change its connection topology at t_e, $e = 1, 2, \dots$, and the system connection topology $\mathcal{G}(t_e)$ will not change during $[t_e, t_{e+1})$. It's easy to verify that $\tilde{V}_{ij}$ is finite according to equation (5.11). Hence, $\Psi(t_0)$ (the initial value of the system energy function) is bounded. Take the derivative of the function in the interval $[t_0, t_1)$:

$$\begin{aligned}\dot{\Psi} &= \sum_{i=1}^{N} \tilde{v}_i^{\mathrm{T}} p_i \sum_{j \in \mathcal{N}_l \cup \{l\}} \nabla \tilde{x}_i \tilde{V}_{ij} \\ &\quad + 2\tilde{v}^{\mathrm{T}} P \Big(-\beta L \tilde{v} - \mathrm{diag}\left\{ \nabla \tilde{x}_i \tilde{V}_i \right\} |L\tilde{v}| - \frac{1}{2} \nabla \tilde{V} - H\tilde{v} \Big),\end{aligned} \tag{5.18}$$

where

$$\begin{cases} \tilde{V}_i = \sum_{j \in \mathcal{N}_i} \tilde{V}_{ij} \\ \nabla \tilde{V} = \sum_{j \in \mathcal{N}_l \cup \{l\}} \nabla_{\tilde{x}_i} \tilde{V}_{ij}. \end{cases}$$

Equation (5.18) can then be simplified as

$$\dot{\Psi} = 2\tilde{v}^{\mathrm{T}} P \Big(-\beta L \tilde{v} - \mathrm{diag}\left\{ \nabla \tilde{x}_i \tilde{V}_i \right\} |L\tilde{v}| - H\tilde{v} \Big). \tag{5.19}$$

According to the definition of f in equation (5.13), we can obtain the following inequality

$$\left| \nabla \tilde{x}_i \tilde{V}_i \right| = \left| \nabla \tilde{x}_i \sum_{j \in \mathcal{N}_i} \tilde{V}_{ij} \right| \leq f. \tag{5.20}$$

Hence, substituting equation (5.20) to equation (5.19), we have

$$\begin{aligned}\dot{\Psi} &\leq -2\tilde{v}^{\mathrm{T}} P (\beta L + H)\, \tilde{v} + 2f \|\tilde{v}\| \|P\| \|L\tilde{v}\| \\ &\leq -\tilde{v}^{\mathrm{T}} \left(\beta Q + 2PH \right) (t_0) \tilde{v} + 2f \|\tilde{v}\| \|P\| \|L\| \|\tilde{v}\|.\end{aligned} \tag{5.21}$$

According to the definition of the Laplace matrix, we can get

$$L(\mathcal{G}) = \mathrm{diag}\{d_i\} - A,$$

where A and diag $\{d_i\}$ are, respectively, the adjacency matrix and in-degree matrix of graph $\mathcal{G}$. According to the communication rules defined in Section II.B, we can determine that the adjacency matrix of the topology of vehicle platoon connection is a strict lower triangular matrix,

$$A = \begin{bmatrix} 0 & \cdots & \cdots & 0 \\ 1 & \ddots & & \vdots \\ \vdots & 1 & \ddots & \vdots \\ * & \cdots & 1 & 0 \end{bmatrix}, \tag{5.22}$$

where $*$ indicates that the value is uncertain and determined by the connection topology at a specific time, which is either 0 or 1. The matrix A indicates that the communication topology of the platoon is directional. Since Max $\{d_i\} = m$, we have $\|L\| \leq 2m$. Then equation (5.21) can be further rewritten as:

$$\begin{aligned} \dot{\Psi} &\leq -\tilde{v}^{\mathrm{T}} \left(\beta Q + 2PH\right)(t_0)\tilde{v} + 4mf \left\|\tilde{v}\right\|^2 \\ &\leq -\left(\lambda_2 \left(\beta Q + 2PH\right)(t_0) - 4mf\right) \left\|\tilde{v}\right\|^2 . \end{aligned} \tag{5.23}$$

Substituting the initial condition $\lambda_2((\beta Q + 2PH)(t_0)) > 4mf$, it gives

$$\dot{\Psi}(t) \leq 0, \forall t \in [t_0, t_1), \tag{5.24}$$

which means that the $\Psi(t)$ is monotonically decreasing function in $[t_0, t_1)$. Take the derivative of equation (5.11), and we get that V_{ij} is monotonically decreasing over the interval $\left[l_j, \hat{S}_{ij}\right)$ and monotonically increasing over the interval $\left[\hat{S}_{ij}, \rho\right)$. Hence, the following relationship can be obtained,

$$\begin{aligned} &V_{ij}(\rho) \geq \Psi_{max} > \Psi(t_0), \forall (i,j) \in \mathcal{V} \\ &V_{ij}(l_j) \geq \Psi_{max} > \Psi(t_0), \forall (i,j) \in \mathcal{V}. \end{aligned} \tag{5.25}$$

This indicates that the distance between the front bumper of vehicle i and vehicle j will not be l_j, which means the vehicle i will not contact the back bumper of vehicle j. On the other hand, the distance between vehicle i and vehicle j will not be equal to or bigger than the communication range ρ. This conclusion ensures that the topological connection of the vehicle platoon will not be interrupted in the process of system transformation over the interval $[t_0, t_1)$. Therefore, the platoon system can only establish new communication connections at time t_1. As a result, the connectivity of the system will be guaranteed. The proof of Theorem

1 is done. [Done]

String stability is an important indicator of the vehicle platoon system. In this chapter, we use asymptotically time-domain string stability (ATSS) to analyze the string stability of the platoon system. According to the definition of ATSS in [55], the origin $e_i = 0$, $i \in \mathbb{N}$ of an interconnected system is ATSS if a given $\delta > 0$ is bounded. Hence we have

$$\sup_i |e_i(0)| < \delta \Longrightarrow \sup_i \|e_i(t)\|_\infty \to 0, \tag{5.26}$$

where $e_i = \tilde{x}_{ij} - \hat{S}_{ij}$. Based on the results obtained from Theorem 1, we can then have the following theorem.

Theorem 2. *Consider a vehicle platoon system with time-varying topology defined in Theorem 1. Suppose that the initial connection topology of the vehicle platoon $\mathcal{G}(t_0)$ is connected and the initial system energy $\Psi(t_0)$ is bounded. If the condition equation* (5.15) *is satisfied, all vehicles' speeds will converge to the lead vehicle's speed. And the following distance between vehicles will converge to the desired value. Meanwhile, the platoon system is ATSS.*

Proof: We expand on the above proof using mathematical induction. Suppose that there are N_1 new connections being added to the platoon system at t_1. N_1 is limited, $\Psi(t_1) < \Psi(t_0) + N_1 V_{max}$, thus $\Psi(t_1)$ is also bounded. Lemma 5.4 indicates that $Q(t_1)$ is the Laplace matrix of graph $\bar{\mathcal{G}(t_1)}$, the weighted mirror graph of a strongly connected directed graph $\mathcal{G}(t_1)$. According to the Lemma 5.2, $\lambda_2(\beta Q(t_0) + 2PH)(t_0) \leq \lambda_2(\beta Q(t_1) + 2PH)(t_1)$ can be obtained. Applying this result to all $t_k (k \geq 2)$ moments, we get the following description

$$\begin{aligned} \lambda_2(\beta Q + 2PH)(t_k) &\geq \lambda_2(\beta Q + 2PH)(t_{k-1}) \\ &\geq \lambda_2(\beta Q + 2PH)(t_0). \end{aligned} \tag{5.27}$$

Therefore, the derivative of $H(t)$ in the interval $[t_{k-1}, t_k)$ can be obtained

$$\begin{aligned} \dot{\Psi}(t) &\leq -\left(\lambda_2\left(\beta Q + 2PH\right)(t_{k-1}) - 4mf\right) \|\tilde{v}\|^2 \\ &\leq -\left(\lambda_2\left(\beta Q + 2PH\right)(t_0) - 4mf\right) \|\tilde{v}\|^2 \\ &\leq 0, \forall t \in [t_{k-1}, t_k). \end{aligned} \tag{5.28}$$

Hence, there exists $\Psi(t_k) \leq \Psi(t_{k-1}) \leq \Psi_{max}), \forall t \in [t_{k-1}, t_k)$. This result also indicates that existing topology connections in the system will not be disconnected in the interval $[t_{k-1}, t_k)$, but a limited number (N_k) of new communication connections will be added at time t_k. The newly established communication connection will satisfy the following equation:

$$\begin{aligned} N_k &\leq \frac{2mN - m^2 + m}{2} - N \\ N_0 + \cdots + N_k &\leq \frac{2mN - m^2 + m}{2} \end{aligned} \tag{5.29}$$

Obviously, $\Psi(t_k) \leq \Psi(t_0) + (N_1 + N_2 + \cdots + N_k)\, V_{max} \leq \Psi_{max}$ can be guaranteed. For a limited number of vehicles in a platoon, the number of topology connections is limited. Therefore, the number of topology switches is also limited. Assume that the vehicle platoon system establishes a stable connection topology at time t_k. Then the string stability of the vehicle platoon will be analyzed over interval $[t_k, \infty)$. Based on the above analysis, we know that the length of the communication connection satisfies the following constraints

$$\begin{cases} \tilde{x}_{ij} \geq \min\left\{\tilde{V}_{ij}^{-1}(\Psi_{max})\right\} \\ \tilde{x}_{ij} \leq \max\left\{\tilde{V}_{ij}^{-1}(\Psi_{max})\right\}. \end{cases} \tag{5.30}$$

Define the following set:

$$\mathrm{S} = \left\{\tilde{x} \in D_1, \tilde{v} \in \mathbb{R}^{N \times N} | \Psi(\tilde{x}, \tilde{v}) \leq \Psi_{max} \right\} \tag{5.31}$$

where $D_1 = \left\{\begin{array}{l} \tilde{x} = \mathbb{R}^{N \times N} | \tilde{x}_{ij} \in \left[\min\left\{\tilde{V}_{ij}^{-1}(\Psi_{max})\right\}, \max\left\{\tilde{V}_{ij}^{-1}(\Psi_{max})\right\} \right], \\ \forall (i,j) \in \mathcal{G}(t_n) \end{array}\right\}$

According to LaSalle's invariance principle, the state trajectory of this vehicle platoon system will converge to the following set:

$$\mathrm{S}_{\text{end}} = \left\{\tilde{x} \in D_1, \tilde{v} \in \mathbb{R}^{N \times N} | \dot{\Psi}(\tilde{x}, \tilde{v}) = 0 \right\}. \tag{5.32}$$

Substituting $\dot{\Psi}(\tilde{x}, \tilde{v}) = 0$ to equation (5.28) , $\tilde{v} = 0$ is obtained, i.e.,

$$v_1 = \cdots = v_N = v_0. \tag{5.33}$$

Hence, $\frac{\mathrm{d}\|x_{ij}\|_2^2}{\mathrm{d}t} = 2x_{ij}^{\mathrm{T}}(v_i - v_j) = 0$, which means the distance between vehicle i and vehicle j will achieve asymptotically stable.

According to the initial condition, v_0 is constant speed, and combined with equation (5.33), we have

$$a = -\begin{bmatrix} \sum_{j\in\mathcal{N}_l\cup\{l\}} \nabla_{\tilde{x}_1}\tilde{V}_{1j} \\ \vdots \\ \sum_{j\in\mathcal{N}_l\cup\{l\}} \nabla_{\tilde{x}_N}\tilde{V}_{Nj} \end{bmatrix} = 0. \tag{5.34}$$

Equation (5.34) shows that the vehicle platoon converges gradually to the geometric configuration corresponding to the extreme point of the global field function. However, only the equilibrium points corresponding to the local minimum points are stable equilibrium points, so the final geometry of the vehicle platoon minimizes the global potential function corresponding to each vehicle. Because the potential field function is non-negative over the interval (l_j, ρ), according to the equation (5.34), $\tilde{V}_{ij} = 0$ is obtained, which means $\tilde{x}_{ij} = \hat{S}_{ij}$, and $e_i = 0$. Hence, equation (5.26) is satisfied, which means the platoon system is ATSS, and the distance between vehicle i and vehicle j will converge to the desired value. [Done]

Algorithm 3 enables the implementation of the distributed control protocol proposed in this section. For each follower vehicle in the vehicle platoon system, this algorithm will be used to achieve cooperative platooning.

Algorithm 3 Distributed controller of each vehicle i

Input: Position and velocity of neighbouring vehicles, x_j, and v_j
Output: Control input u_i for vehicle i.

```
Initial Ψ_max according to (5.12).
Receive the x_j, v_j, x_0, and v_0 within the communication range of vehicle i.
for each vehicle j within the communication range.
    Calculate Ŝ_ij according to (5.2).
    Calculate the gradient ∇x_i V_ij of (5.11).
End for
Calculate the control input u_i according to (5.10)
Return Control input u_i
```

Some methods based on spring-mass-damper have been applied to connected vehicle platoon control [254]–[257]. For example, [257] uses a novel control scheme including the inter-distance reference model. It transforms the longitudinal control problem into a tracking problem of the inter-distance reference signal. But this method does not consider the degradation problem of CACC. In the traditional spring-mass-damper methods, the controller parameters are designed from a mechanical perspective. Stabilisation and platooning of the vehicle platoon system can be achieved by setting the appropriate spring constant and the damping coefficient. However, due to the linear superposition characteristics of the spring-mass-damping, these controllers may cause very large control inputs to the vehicle, which should be avoided in real-world applications. In addition, these approaches cannot ensure the preservation of topology connectivity in the vehicle platoon system. On the contrary, our proposed SDEM considers the car row system from the perspective of energy and dissipative system. We design a nonlinear bounded interaction function to ensure the boundedness of the vehicle control input. Besides, it is demonstrated that the topological connectivity of the vehicle platoon system is maintained and enhanced under our control algorithm.

5.3.3 Robustness to V2V communication loss

Under the framework of the traditional CACC algorithm, the stability of the platoon highly relies on V2V communication. Once V2V communication is lost due to hardware faults, CACC will degenerate into ACC, thus increasing the risk of vehicle collision [123]. As we know, when vehicle i in CACC status degenerates into ACC status, the vehicle i lacks the state information of vehicle $i-2$ out of the radar field of view. Once vehicle $i-2$ has a rapid and unexpected deceleration, vehicle $i-1$ may have enough time to respond to braking or deceleration. However, vehicle i may not be able to complete braking or deceleration in a short time because it cannot recognize the unexpected behaviour until the completion of vehicle $i-1$ response. However, V2V communication loss is widespread in practical applications. The causing reasons could be hacking, malfunctioning communications equipment, or jammers[233]. This section will analyze how the distributed control algorithm based on the SDEM can resist V2V communication loss.

Suppose that the V2V communication connection between vehicle i and vehicle $i+2$ is lost, which means that spring $K_{i,i+2}$ and the damping element $c_{i,i+2}$ breaks off in the corresponding SDEM (shown in Fig. 5.3). When $K_{i,i+2}$ breaks, the energy stored in $K_{i,i+2}$ disappears, which means that the total current energy of the system decreases. Since the total system energy is decreasing, the energy stored in the other springs can never exceed the upper limit of the spring's energy storage. This proves that the distance between the two agents is still no less than the compression limit of the spring and no more than the tensile limit. Therefore, for the platoon system, when the communication between vehicle $i+2$ and vehicle i is lost, vehicle $i+2$ can still maintain the topological connection with vehicle $i+1$ through the front radar, and at the same time ensure that the vehicle will not collide with vehicle i, which is not achieved by the existing CACC algorithm.

We reiterate two of the critical preconditions of Theorem 1 and Theorem 2. The initial connection topology of the vehicle platoon $\mathcal{G}(t_0)$ is connected and the initial system energy $\Psi(t_0)$ is bounded. Assume that V2V communication is lost in some vehicles of the vehicle platoon system. Then the CACC state will degrade to the ACC state. The vehicle can only obtain the status information of the vehicle in front through the onboard sensors, thus establishing the simplest directional topology connection. The connection topology still satisfies the precondition that the initial topology is connected. When CACC degrades, the number of topology connections in the platoon system will decrease. According to the definition of equation (5.12), the total energy of the system will decrease when the topological connections are reduced. Hence, the total energy of the platoon system still satisfies the condition that the energy is bounded. Therefore, Theorem 1 and Theorem 1 and Theorem 2 still hold despite the loss of communication, which means that the stability of the vehicle platoon, the connectivity between vehicles, and collision avoidance can always be guaranteed under the proposed protocol equation (5.10).

5.4 Experimental verification

In this section, we focus on verifying the effectiveness of the proposed theoretical results through simulation experiments. We use MATLAB and Unreal Engine for the simulation experiments. In Unreal Engine, the evolution of the vehicle platoon system can be observed visually. We consider how the algorithm performs with different communication topologies and how it works in the case of V2V communication loss. The parameters used in the simulation experiments are given as follows:

- The vehicle platoon consists of five followers and one leader. The initial connection topology of the vehicle platoon is connected.
- The communication range of a vehicle ρ is 17 m and a communication link can be established between vehicles once the distance is less than 17 m.

- The desired distance between the front bumper of each vehicle and the back bumper of its adjacent vehicle ahead is 4 m, and the vehicle body length is 4 m.
- The leader's speed is 6 m/s and the initial speed of each following vehicle is obtained randomly in interval $[2, 6]$ m/s. The maximum velocity of each vehicle v_{max} is 30 m/s.
- The sampling time is 0.025 s, control gain $\beta = 10$, $\xi_1 = \xi_2 = 2$, $c_1 = c_2 = 2$. Furthermore, we determine the $\Psi_{max} = 10$ according to (5.12).

In addition, in this section, we introduce the time-to-collision (TTC) [258] notion to evaluate the safety of the vehicle platoon system. TTC is defined as:

$$TTC_i(t_k) \begin{cases} \frac{x_{i-1}(t_k)-x_i(t_k)-l_{i-1}}{v_i(t_k)-v_{i-1}(t_k)} & \text{if } v_i(t_k) > v_{i-1}(t_k) \\ \infty & \text{if } v_i(t_k) \leq v_{i-1}(t_k) \end{cases} . \tag{5.35}$$

TTC indicates the time for the collision of two consecutive vehicles in the same lane to occur if they maintain their current velocity when the vehicle $i-1$ in front of them is moving slower than i. A smaller TTC value characterizes a more dangerous traffic condition.

5.4.1 Case 1: dynamic topology

In this case, the effectiveness of the algorithm under dynamic network topology is verified. All the vehicles will disconnect or establish new communication connections in real-time, depending on the status of the surrounding vehicles. Note that the number of topological connections characterizes the system's stability to a certain extent, so in the case of dynamic topology, the increase of the system communication connections is beneficial for the stability of the vehicle platoon system.

Fig. 5.4 depicts the evolution of the entire vehicle platoon system. It is intuitive to see that with the application of the CACC algorithm proposed in this chapter, the vehicle successfully forms a stable vehicle platoon system with a safe following distance. Fig. 5.5 indicates the velocity changes of vehicle platoon for dynamic network topology. The result shows that the velocity of every follower can converge to the velocity of the leader. There is an apparent phenomenon of a sudden change in the speed of the vehicle as it converges. According to our analysis of the experimental results, the abrupt change in speed is mainly caused by the

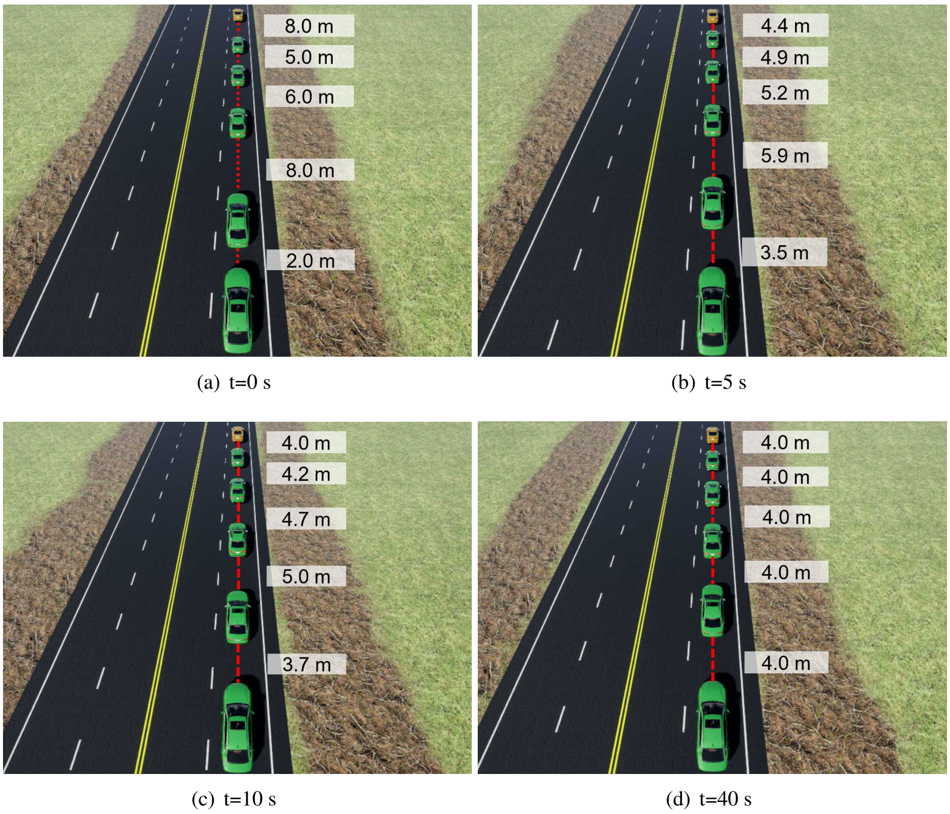

Figure 5.4. Process of the vehicle platooning task under dynamic network topology. The yellow car denotes the leader, and the green cars represent the followers.

new communication connections. It is clear from the control protocol (5.10) that when a new communication connection is added at the moment t_k, the vehicle's control input at the moment t_k will suddenly increase or decrease. From Fig. 5.6, the following distance will also converge to the desired value which is defined as 4 m. Meanwhile, we can note that the following distance is always greater than 2 m, which means the vehicle will never be in a collision with its neighbours. In addition, the communication connection topology of the vehicle platoon changes dynamically as the following distance changes. As can be seen in Fig. 5.7, the initial number of connections in the platoon is 5, and after $t = 17.15$ s, the number of connections in the platoon rises to 9 connections. This also means that the convergence speed and stability of the whole platoon system are improved. We can also observe the process of generating new connections for the vehicle platoon in Fig. 5.8. From all these figures, it is now concluded that the desired vehicle platooning is achieved under the influence of the dynamic network topology.

Moreover, the effectiveness of the proposed algorithm in high-speed scenarios is also verified. The leader's speed is 28 m/s and the initial speed of each following vehicle is obtained randomly in the interval $[20, 30]$ m/s. The maximum velocity of each vehicle v_{max} is 30 m/s.

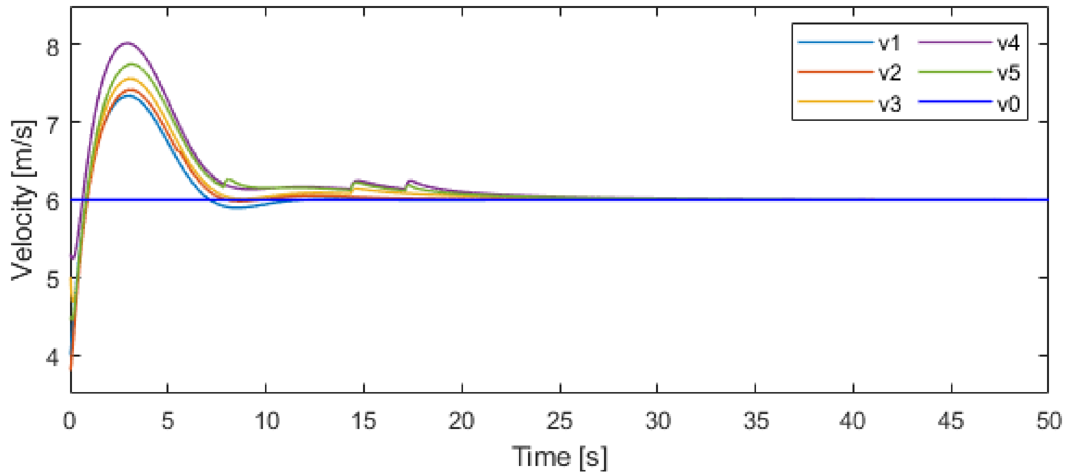

Figure 5.5. Time-variation of the velocities of the vehicles, where v_0 represents the velocity of the leader and v_1-v_5 represent the velocities of 5 followers.

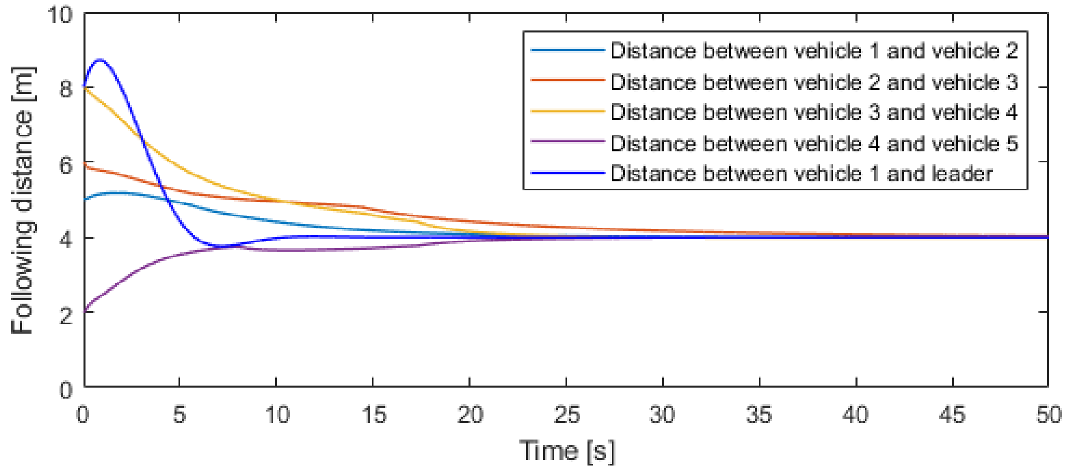

Figure 5.6. Time-variation of the vehicle following distances, where the length of the vehicle is defined as 4 m and the desired distance between the vehicle head and the rear of the vehicle in front of it is set as 4 m.

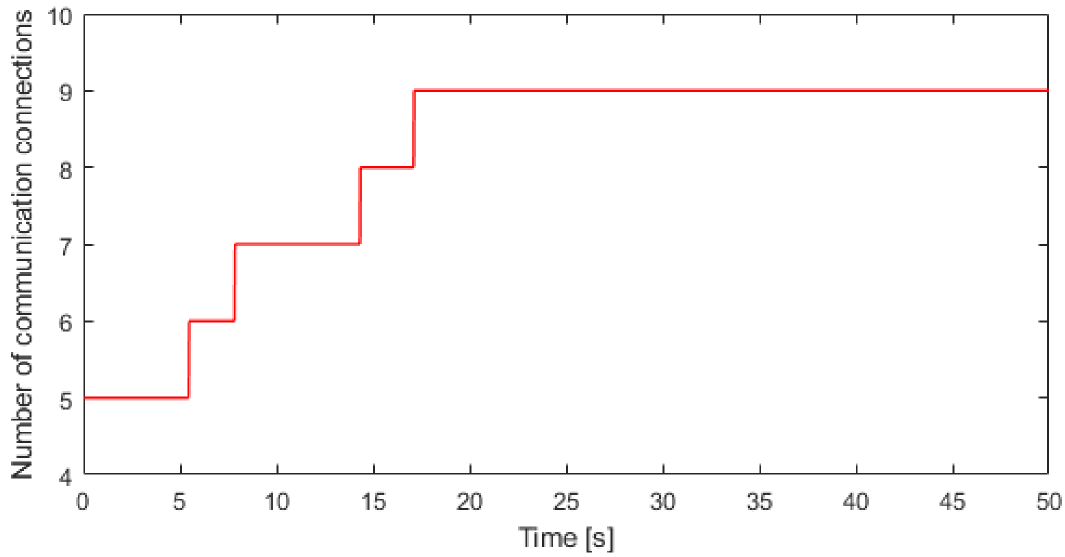

Figure 5.7. Time-variation of the number of communication connections.

Fig. 5.9 and 5.10 show that the velocities and following distances of the vehicle platoon system successfully converge to the desired value in the high-speed scenario. Therefore, the proposed algorithm is applicable in both low-speed and high-speed scenarios.

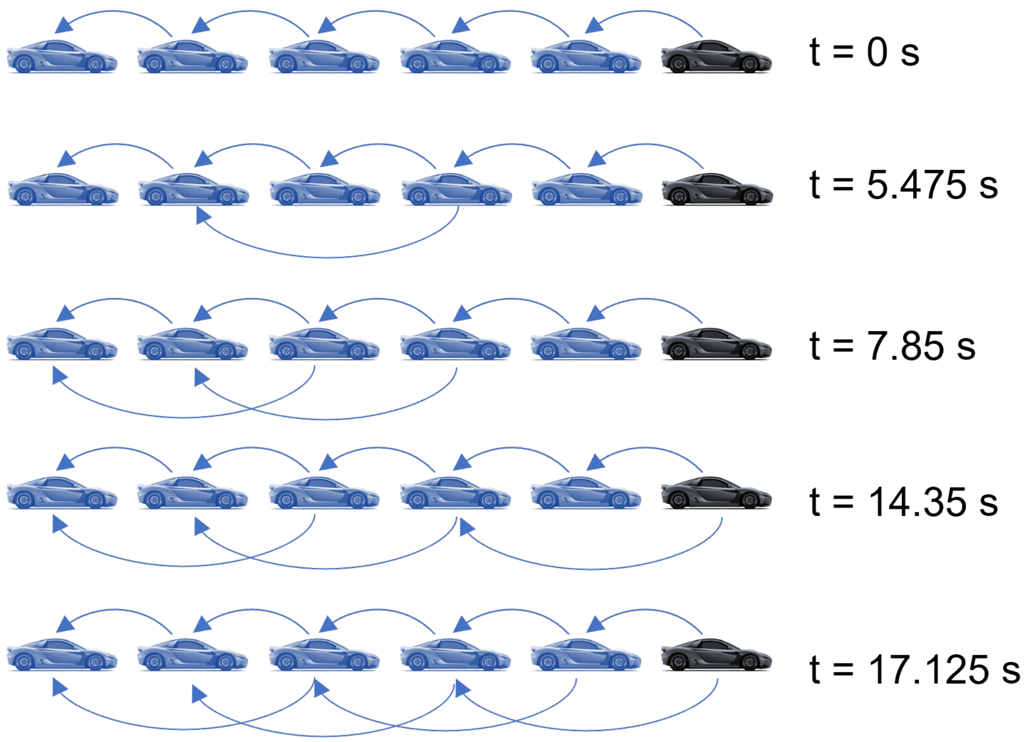

Figure 5.8. The dynamic vehicle communication network topology at a certain time instant.

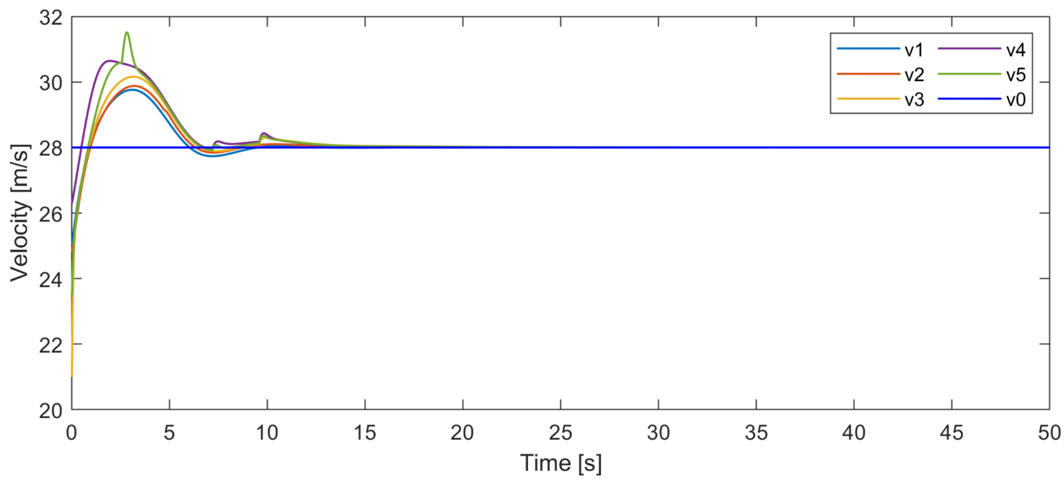

Figure 5.9. Time-variation of velocities of vehicle platoon system with dynamic communication topology in motorway mainline scenario.

5.4.2 Case 2: fixed topology with V2V communication loss

In this subsection, we verify the effectiveness of the algorithm for fixed network topology. Here, a worst-case fixed topology is considered, e.g., V2V communication is completely disabled, and the topological connection between vehicles is only achieved by the onboard radar, i.e. the vehicle can only acquire the position and speed information of the closest vehicle ahead. The connection topology is as shown in Fig. 5.8 at moment $t = 0$ s. With this fixed communication topology, the results in Fig. 5.11 and Fig. 5.12 show that the speed and following distance of the vehicle platoon still converge to the desired values although

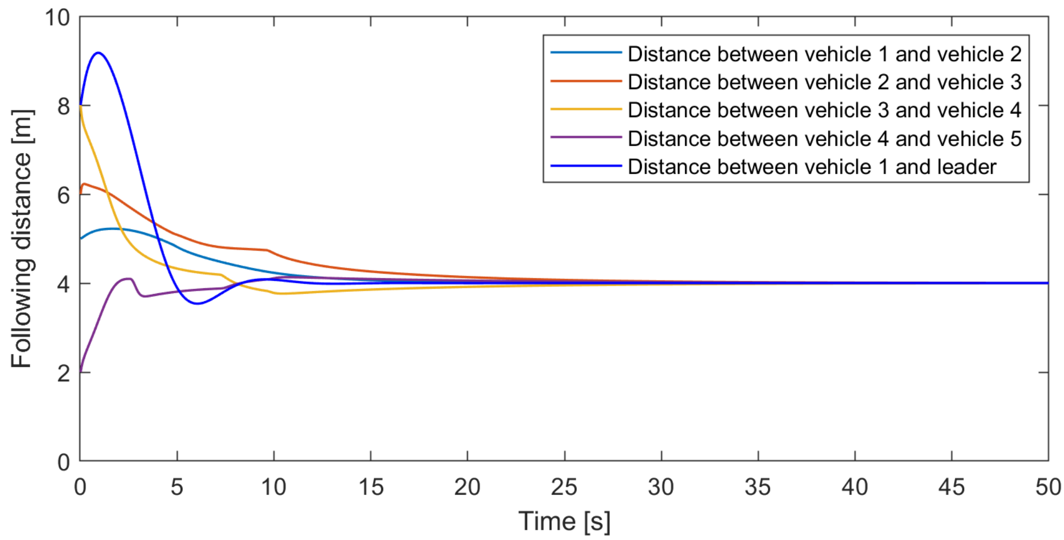

Figure 5.10. Time-variation of the following distance of vehicle platoon system with dynamic communication topology in motorway mainline scenario.

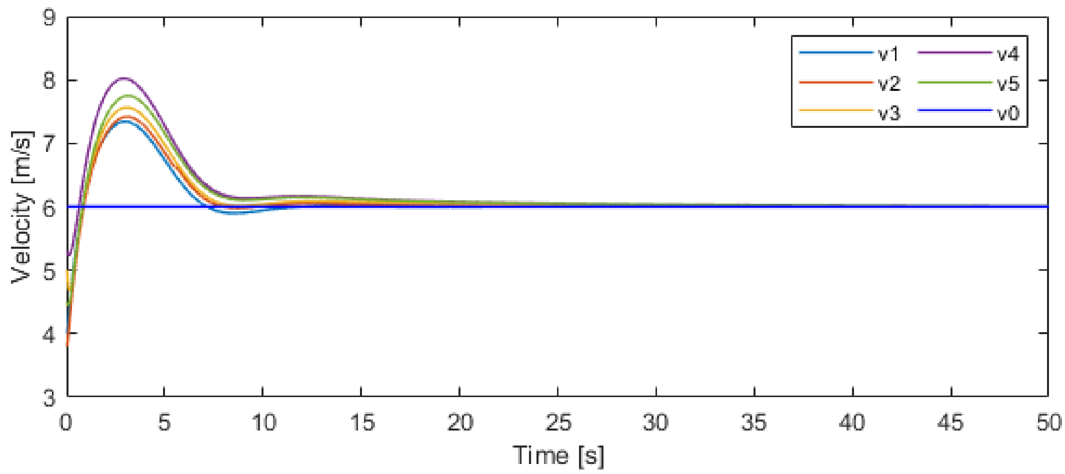

Figure 5.11. Time-variation of the velocities of the vehicle platoon without V2V communication.

the CACC completely degrades to an ACC. Unlike dynamic topologies, the fixed topology does not experience sudden speed changes under this control protocol (5.10). This scenario is of great practical importance. When the vehicle platoon is subject to network attacks or communication blocking, the energy model and distributed control protocol proposed can ensure that the vehicle platoon continues to converge safely to a steady state. However, the negative impact of communication loss is also obvious, i.e., it reduces the system convergence speed. A careful comparison of Fig. 5.6 and Fig. 5.12 shows that the following distance of the vehicle platoon system converges to the desired value more quickly in the CACC state.

5.4.3 Case 3: vehicle platoon merging

Vehicle merging is a common driving scenario. The merging of two different vehicle platoon systems can cause a shock to the original system. Therefore, the CACC algorithm must ensure

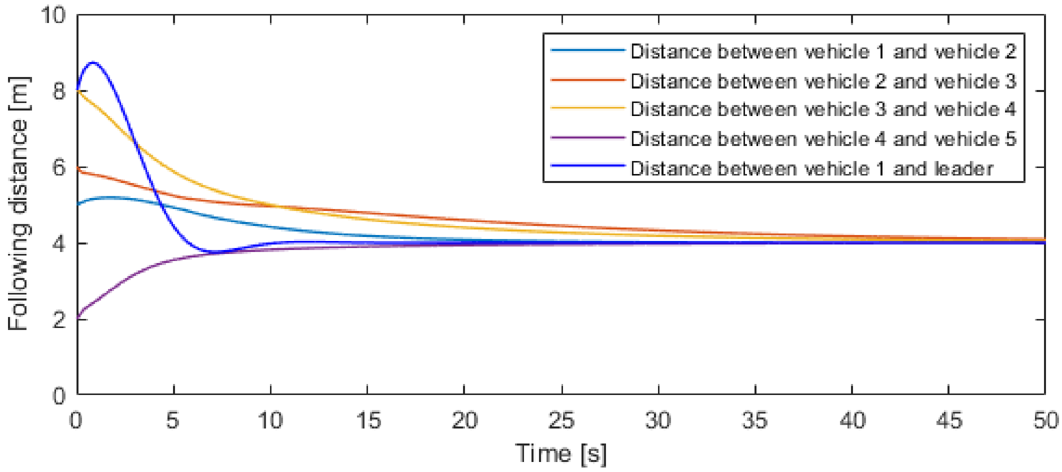

Figure 5.12. Time-variation of the vehicle following distances without V2V communication.

that multi-vehicle platoon systems are safe and reliable during the merging process. As shown in Fig. 5.13, for this scenario, we selected two initial vehicle platoon systems that did not enter the steady state. Both platoon systems have their leaders, and when the left platoon system merges with the right platoon, the leader of the left platoon system automatically becomes the follower of the new platoon system. The new platoon system gradually converges to the same velocity as the leader and maintains the desired following distance. Figures 5.14, 5.15, 5.16, and 5.17 show the process of changing vehicle acceleration, velocity, following distance and communication topology connections, respectively. The experimental results fully demonstrate that the CACC algorithm we introduced can achieve a safe and effective merging of two vehicle platoon systems. Note that high peaks can be found in Fig. 5.15, which are mainly caused by switching communication topology. As can be seen in Fig. 5.17, two topological connections are established at about t = 45 s, which causes a sudden change in the velocity of the vehicle. At that moment, the acceleration of v4 and v5 is approximately 4.5 m/s^2. The lower and upper bounds of acceleration are -8 m/s^2 and 8 m/s^2, respectively.

5.4.4 Case 4: vehicle platoon separating

Another common scenario exists during vehicle platooning, where a vehicle in a CACC state disengages from the current vehicle platoon system. A vehicle platoon system in a steady state is bound to leave the original steady state after losing some of its communication nodes. The CACC algorithm must ensure that the platoon system can form a new steady state in a limited time. As shown in Fig. 5.18, we consider a scenario where there are two follower vehicles in a steady-state platoon system ready to leave the original platoon, move into the

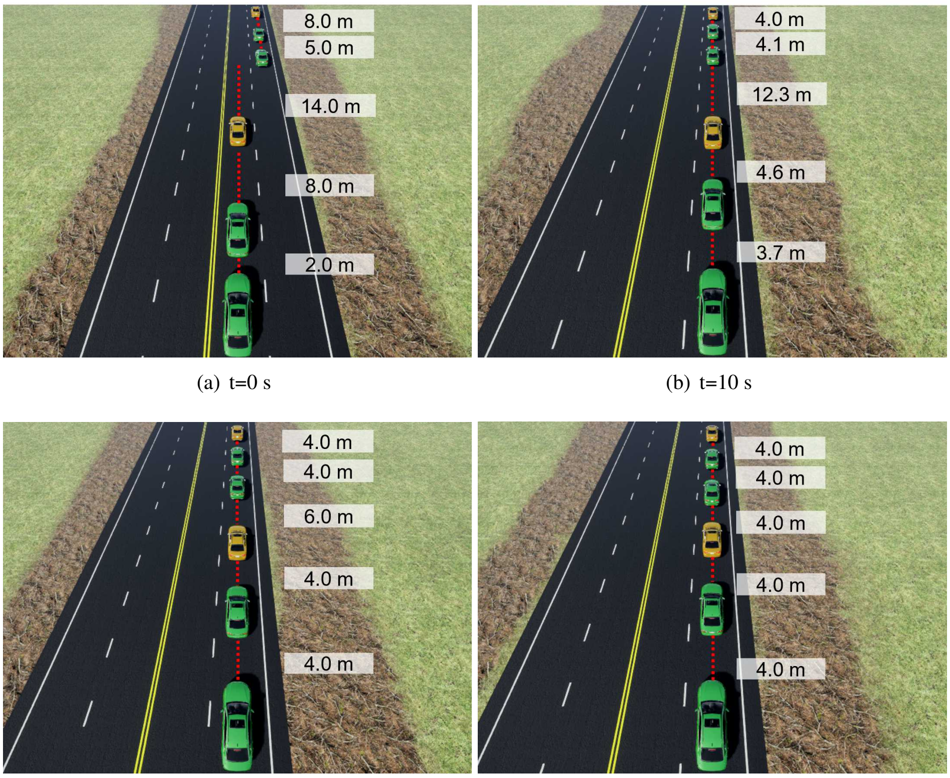

(a) t=0 s

(b) t=10 s

(c) t=40 s

(d) t=70 s

Figure 5.13. Two vehicle platoons merge and form a new platoon system. The yellow car denotes the leaders of two initial vehicle platoons, and the green cars represent the followers.

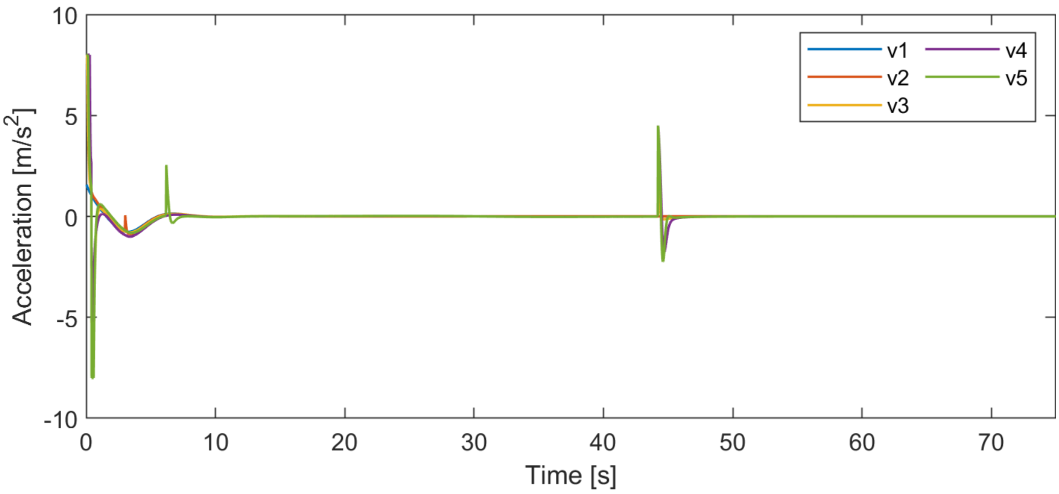

Figure 5.14. Time-variation of acceleration of the two vehicle platoons merging process.

adjacent lane and form a new platoon system. Fig. 5.18 illustrates the separation of the entire platoon system into two platoon systems and the formation of a new steady state. Fig. 5.19 and Fig. 5.20 also show that after the separation of the platoon system, the two newly formed platoon systems also converge to the desired velocity and following distance in a finite time.

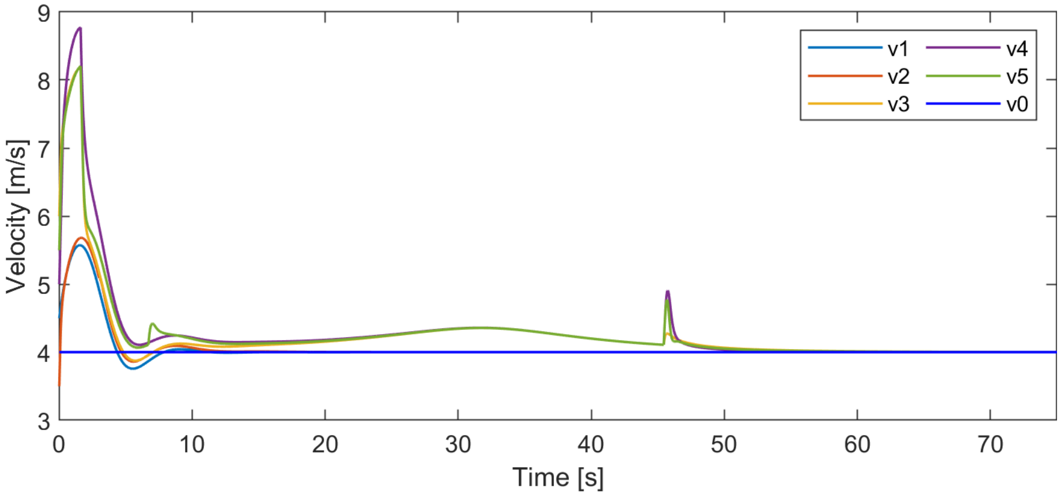

Figure 5.15. Time-variation of the velocities of the two vehicle platoons merging process.

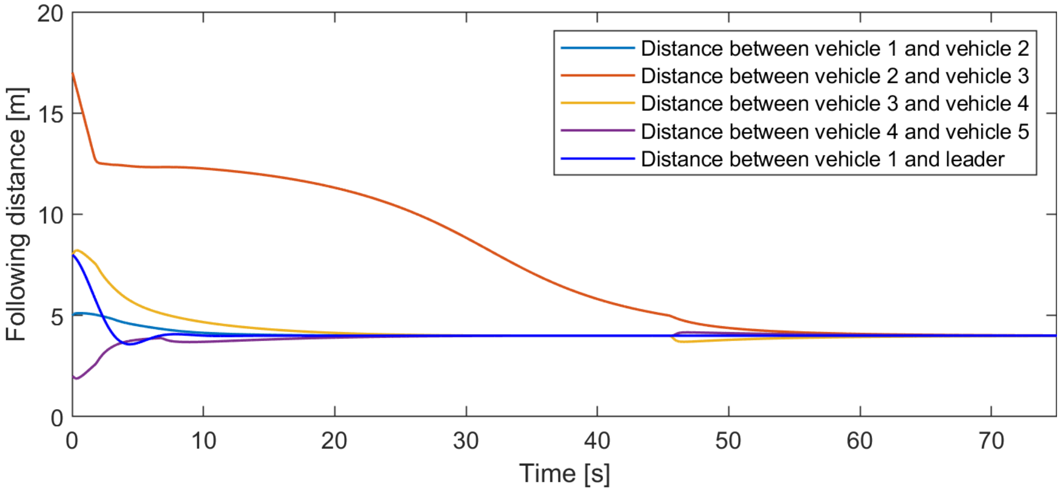

Figure 5.16. Time-variation of the following distance of the two vehicle platoons merging process.

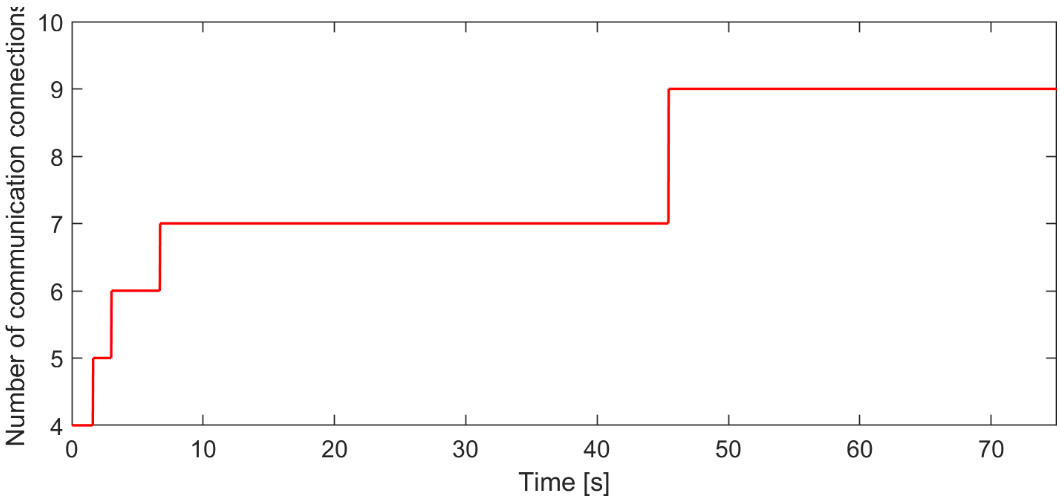

Figure 5.17. Time-variation of the number of communication connections of the two vehicle platoons merging process.

5.4.5 Case 5: sudden velocity change of the leader

In this subsection, we explore how the steady-state platoon system responds to the leader's temporary unpredicted acceleration or deceleration. The impact of sudden changes in the

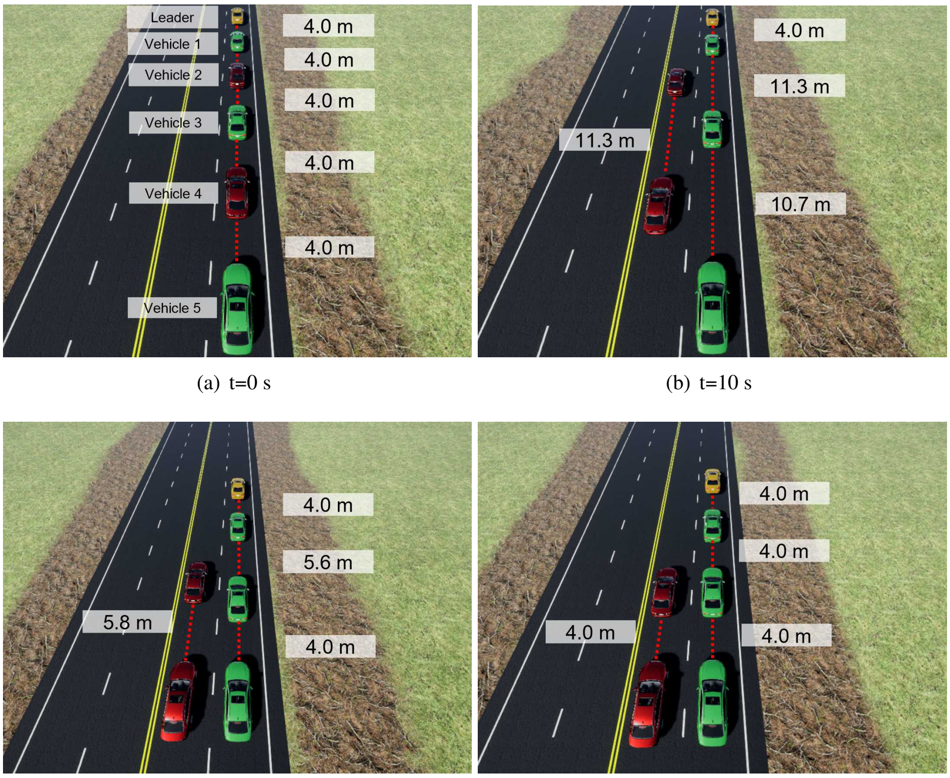

(a) t=0 s (b) t=10 s

(c) t=30 s (d) t=60 s

Figure 5.18. Some of the followers break away from the platoon system and form a new platoon. The red cars represent the followers which are out of the platoon.

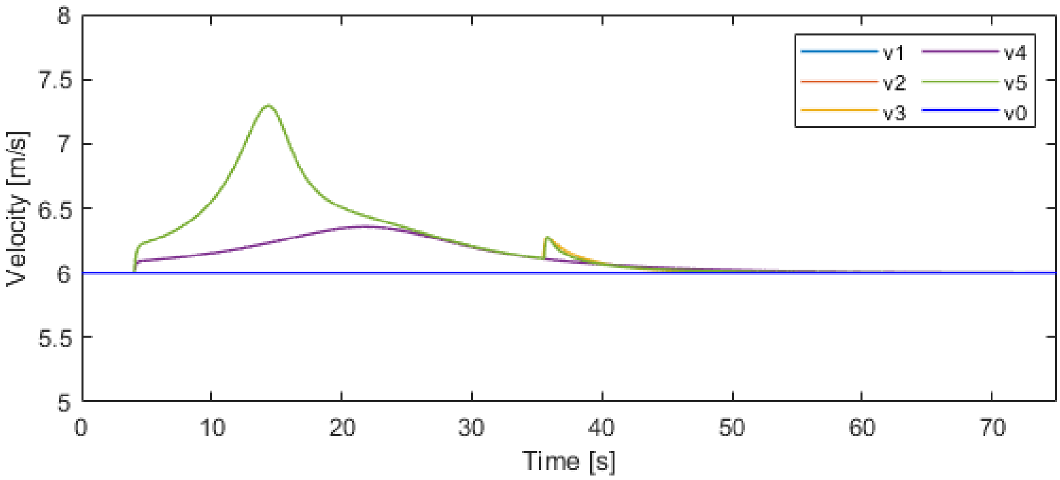

Figure 5.19. Time-variation of the velocities of vehicle platoons separating process.

leader's speed on the entire platoon system is obvious, which places a high requirement on the string stability of the platoon system. In [259], a distributed predictive control approach was used to implement the string stability of the vehicle platoon. The results demonstrate the effectiveness of the distributed predictive control approach for speed convergence, with the fleet speed responding quickly to changes in reference vehicle speed and converging back to a steady state. However, one obvious drawback is that the vehicles travel a different distance when they converge to a new steady state, which means that the vehicle spacing in the platoon does not recover to the desired steady state value. It can be further observed that the spacing

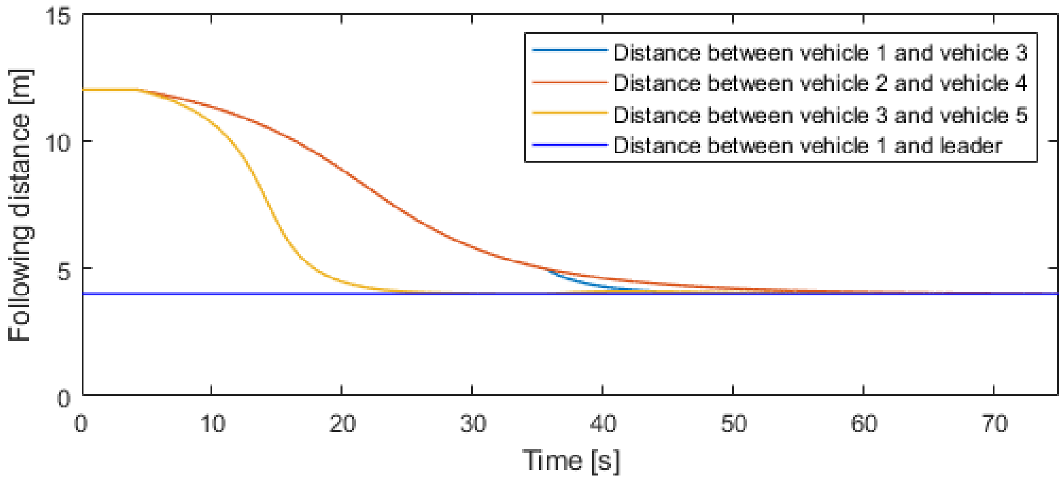

Figure 5.20. Time-variation of the following distance of vehicle platoons separating process.

between vehicles is increased. The increased following distance of the same platoon of vehicles in two different steady states means that the capacity of the road decreases. However, such a drawback can be overcome by the method proposed in this chapter. Fig. 5.21 (a) and (b) depict the string stability performance of the vehicle platoon under the control protocol proposed in this chapter. After a sudden acceleration or deceleration of the leader, the vehicle platoon system is able to converge back to a steady state in a limited time. In addition, the velocity variation shows that the speed of the follower vehicle remains almost synchronized throughout the variation.

5.4.6 Comparisons and discussions

We compare the performance of the proposed method in this chapter with the traditional CACC algorithm [10] in scenarios where the leader experienced unintended acceleration or deceleration. The results in Fig. 5.21 (a) and (c) show that the algorithm proposed in this chapter has a faster convergence rate and also a better consistency in the velocity of the followers in the vehicle platoon system. Additionally, Fig. 5.21 (b) and (d) also indicate that the vehicle platoon system with our algorithm has more stable following distances when the leader experiences unintended acceleration or deceleration. More importantly, according to the (5.35), the minimum value of TCC is calculated and shown in Fig. 5.21 (a) and (c). The results show that our algorithm has a higher TCC value than the traditional CACC algorithm, which means our algorithm is safer.

There are existing control methods that switch between ACC and CACC to address topology changes while still maintaining stability. [121] uses state estimation to deal with the degradation of CACC. This method uses a discrete-time Kalman filter to estimate the object vehicle acceleration and replaces the desired acceleration with the estimated value. Moreover, [13] addresses the degradation of CACC from a communication perspective. This approach requires an extra message-sending function for the vehicle to optimise the information flow topology, thus ensuring fleet stability when CACC degrades. In this chapter, we tackle the degradation problem of CACC from the control perspective and propose a control algorithm that can be applied to both CACC and ACC, thus reducing the development cost of the vehicle. The simulation results also show that the algorithm ensures the vehicle platoon system in both CACC and ACC states with good convergence and stability.

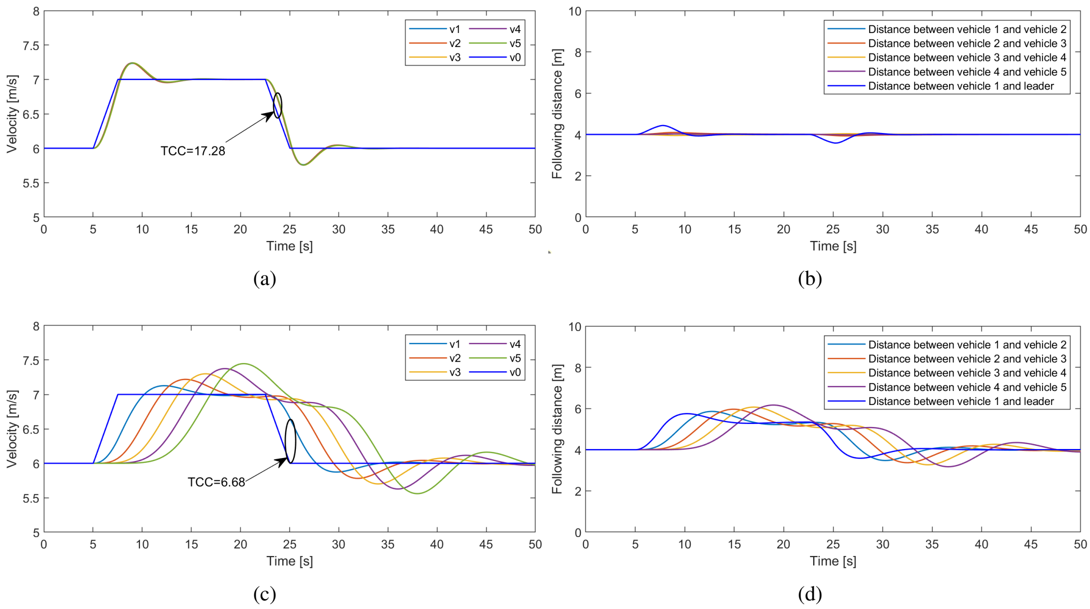

Figure 5.21. Simulation results show the performance achieved by the proposed distributed CACC algorithm based SEDM and the traditional CACC algorithm [10] to a platoon of six vehicles of which one acts as the leader while the rest five are followers. (a) Time-variation of the velocities with proposed distributed CACC algorithm based on SEDM, (b) Time-variation of the following distance with proposed distributed CACC algorithm based on SEDM, (c) Time-variation of the velocities with traditional CACC algorithm, and (d) Time-variation of the following distance with traditional CACC algorithm. In (a) and (c), the minimum value of TCC is calculated and shown.

5.5 Summary

In this chapter, we proposed a distributed CACC control protocol based on SDEM. Under this control protocol, the vehicle-to-vehicle relationship was defined by a special nonlinear spring and linear damping. Through rigorous mathematical proofs, the stability of the connected vehicle platoon was guaranteed, and vehicle platoon connectivity was maintained and enhanced during the evolution of the vehicle platoon system. This control protocol enables distance, and speed stabilisation of the connected platoon, i.e. the whole platoon will converge to the leader's speed and maintain the desired following distance. The control protocol also enables stable control and maintains the stability of the platoon system in the event of loss of platoon communication. In addition, we simulated a large number of usage scenarios using numerical simulations. The results show that the SDEM and control protocol are suitable for vehicles in the CACC state and also work well for vehicles in the ACC state. Meanwhile, the proposed algorithm ensures the safety and stability of the platoon system for both platoon merging and separation scenarios. For sudden speed shifting of the leader, the vehicle platoon has good string stability. One limitation of this work is that vehicle platoon with time-varying topology may experience abrupt changes in control inputs, which may reduce the comfort of the vehicle. However, we will address and optimise this limitation in our future work. Additionally, in this work, we only consider the constant spacing policy in the control design. In future research, we would like to explore the CACC control algorithm under the dynamic spacing policy.

Chapter 6

Conclusions and future works

This chapter summarises the main contributions of this thesis and explores possible directions for future research. This thesis aimed to generate advanced cooperative control algorithms for the MVCC system and to find possible practical applications using the proposed multi-vehicle cooperative algorithms. To this end, a multi-vehicle CACC algorithm for CAVs using SDEM was designed. Furthermore, a distributed motion planning algorithm was developed for the overtaking scenario of the CAVs platoon system.

6.1 Conclusions

This thesis began with a review of three basic and important aspects of MVCC systems including i) system architecture and functional strategies, ii) control methods, and iii) application scenarios. The review indicated that there are still many challenges in many aspects of MVCC systems. These challenges include the increased control difficulty of the MVCC system in mixed traffic flows, the system degradation of the MVCC system in the event of loss of communication, and the inability of existing MVCC algorithms to be used in more complex driving scenarios, such as merging, overtaking, etc.

A solution to the distributed motion control problem for CAVs in a complex multi-lane platoon was presented, which may consist of both CAVs and human-operated vehicles. The proposed algorithm includes a mechanism for safe overtaking, that employs Velocity Difference Potential Field (VDPF) and Acceleration Difference Potential Field (ADPF) techniques as an improvement over the conventional Artificial Potential Field (APF) method. The overtaking problem was treated as a formation tracking problem where human-operated vehicles are set as targets. The proposed technique effectively dealt with sudden changes in acceleration of the leader vehicle due to obstacles or neighbouring vehicles and ensures speed synchronisation of follower unmanned vehicles with the leader's variable acceleration. Moreover, the follower vehicles avoid obstacles while complying with the desired formation tracking objectives. The simulation results, obtained using Matlab and Unreal Engine software platforms, demonstrated the feasibility and usefulness of the proposed algorithm. The simulation showed that a group of autonomous vehicles could operate safely in a complex, heterogeneous multi-lane platoon, performing overtaking, lane-changing, obstacle avoidance, and dynamic target tracking scenarios.

A distributed CACC algorithm for the CAV platoon was developed based on SDEM, which defines the vehicle-to-vehicle relationship using a special nonlinear spring and linear damping. Mathematical proofs were used to demonstrate the stability of the connected vehicle platoon under this control protocol, which enables distance and speed stabilisation of platoon members. The platoon could converge to the leader's speed and maintain the desired following distance while ensuring stable control and maintaining system stability even if platoon communication is shortly lost. Numerical simulations were conducted to simulate a wide range of application scenarios, demonstrating that the SDEM and control protocol are suitable for vehicles in both CACC and ACC states. The proposed algorithm ensured the safety and stability of the platoon system in scenarios involving platoon merging and separation, as well as sudden speed shifting of the leader, with sufficient string stability. However, it is worth noting that when the information flow topology changes dynamically, a small abrupt change in the vehicle speed occurred, which was a limitation coming out of the distributed control protocol presented in Chapter 5. Such small speed abrupt changes can reduce the comfort performance of the vehicle.

6.2 Future works

Some potential research directions are listed below:

- In this thesis, all algorithm verification is done based on numerical simulations. To better explore the feasibility of the proposed algorithms in practical applications, it is necessary to use real-world mobile robots or intelligent vehicles to complete the testing of the algorithms.

- The CACC algorithm designed in Chapter 5 may cause sudden speed changes at the moment of information flow topology switching, and in the future, the motion planning generated by the CACC algorithm needs to be optimised in real-time by trajectory optimisation methods.
- The proof of string stability for all vehicle platoons in this thesis is based on the premise that all vehicles in the platoon are CAVs. However, in realistic scenarios, non-connected vehicles are objectively present in large numbers. It is worthwhile to investigate the impact of non-connected vehicles on the stability of connected vehicles platoon. At the same time, the cooperative control method of a mixed heterogeneous MVS is also worthy of deeper investigation.
- In this thesis, the research work focused on motion planning and control for the MVCC system. It does not address the other focus of the multi-vehicle collaboration task, decision-making. Studies about decision-making for the MVCC system are mainly based on rule systems. Still, as the complexity of the scenario rises, the rule systems are continuously populated, thus reducing the interpretability of the system. Using multi-agent reinforcement learning for MVCC system decision-making tasks is a worthwhile research direction.

References

[1] S. E. Shladover, "Path at 20—history and major milestones," *IEEE Transactions on Intelligent Transportation Systems*, vol. 8, no. 4, pp. 584–592, 2007.

[2] K.-S. Chang, W. Li, P. Devlin, A. Shaikhbahai, P. Varaiya, J. Hedrick, D. McMahon, V. Narendran, D. Swaroop, and J. Olds, "Experimentation with a vehicle platoon control system," in *Vehicle Navigation and Information Systems Conference, 1991*, IEEE, vol. 2, 1991, pp. 1117–1124.

[3] V. Milanés, S. E. Shladover, J. Spring, C. Nowakowski, H. Kawazoe, and M. Nakamura, "Cooperative adaptive cruise control in real traffic situations," *IEEE Transactions on Intelligent Transportation Systems*, vol. 15, no. 1, pp. 296–305, 2013.

[4] H. Liu, L. Xiao, X. D. Kan, S. E. Shladover, X.-Y. Lu, M. Wang, W. Schakel, and B. van Arem, "Using cooperative adaptive cruise control (cacc) to form high-performance vehicle streams. final report," 2018.

[5] S. E. Shladover, X. Yun, L. Yang, H. Ramezani, J. Spring, C. V. Nowakowski, D. Nelson, D. Thompson, A. Kailas, *et al.*, "Cooperative adaptive cruise control (cacc) for partially automated truck platooning," California. Dept. of Transportation. Division of Research and Innovation, Tech. Rep., 2018.

[6] M. Schulze, "Chauffeur-the european way towards an automated highway system," in *Mobility for Everyone. 4th World Congress on Intelligent Transport Systems, 21-24 October 1997, Berlin.(Paper No. 2311)*, 1997.

[7] S. Maiti, S. Winter, and L. Kulik, "A conceptualization of vehicle platoons and platoon operations," *Transportation Research Part C: Emerging Technologies*, vol. 80, pp. 1–19, 2017.

[8] M. Larburu, A. Urquiza, and J. Sanchez, "Safe road trains for the environment (sartre): Validation of sartre platoon service and the sartre hmi," in *19th ITS World CongressERTICO-ITS EuropeEuropean CommissionITS AmericaITS Asia-Pacific*, 2012.

[9] C. Bergenhem, Q. Huang, A. Benmimoun, and T. Robinson, "Challenges of platooning on public motorways," in *17th World Congress on Intelligent Transport Systems*, 2010, pp. 1–12.

[10] V. Milanés and S. E. Shladover, "Modeling cooperative and autonomous adaptive cruise control dynamic responses using experimental data," *Transportation Research Part C: Emerging Technologies*, vol. 48, pp. 285–300, 2014.

[11] L. Xiao, M. Wang, and B. Van Arem, "Realistic car-following models for microscopic simulation of adaptive and cooperative adaptive cruise control vehicles," *Transportation Research Record*, vol. 2623, no. 1, pp. 1–9, 2017.

[12] L. Xiao, M. Wang, W. Schakel, and B. van Arem, "Unravelling effects of cooperative adaptive cruise control deactivation on traffic flow characteristics at merging bottlenecks," *Transportation Research Part C: Emerging Technologies*, vol. 96, pp. 380–397, 2018.

[13] C. Wang, S. Gong, A. Zhou, T. Li, and S. Peeta, "Cooperative adaptive cruise control for connected autonomous vehicles by factoring communication-related constraints," *Transportation Research Part C: Emerging Technologies*, vol. 113, pp. 124–145, 2020.

[14] S. Gong, A. Zhou, and S. Peeta, "Cooperative adaptive cruise control for a platoon of connected and autonomous vehicles considering dynamic information flow topology," *Transportation Research Record*, vol. 2673, no. 10, pp. 185–198, 2019.

[15] H. Yang, H. Rakha, and M. V. Ala, "Eco-cooperative adaptive cruise control at signalized intersections considering queue effects," *IEEE Transactions on Intelligent Transportation Systems*, vol. 18, no. 6, pp. 1575–1585, 2016.

[16] T. Stanger and L. del Re, "A model predictive cooperative adaptive cruise control approach," in *2013 American Control Conference*, IEEE, 2013, pp. 1374–1379.

[17] M. Di Bernardo, A. Salvi, and S. Santini, "Distributed consensus strategy for platooning of vehicles in the presence of time-varying heterogeneous communication delays," *IEEE Transactions on Intelligent Transportation Systems*, vol. 16, no. 1, pp. 102–112, 2014.

[18] J. Wang and X. Hu, "Distributed consensus in multi-vehicle cooperative control: Theory and applications (ren, w. and beard, rw; 2008)[book shelf]," *IEEE Control Systems Magazine*, vol. 30, no. 3, pp. 85–86, 2010.

[19] T. Tapli and M. Akar, "Cooperative adaptive cruise control algorithms for vehicular platoons based on distributed model predictive control," in *2020 IEEE 16th International Workshop on Advanced Motion Control (AMC)*, IEEE, 2020, pp. 305–310.

[20] G. Nie, B. Xie, Z. Hao, H. Hu, and Y. Tian, "A distributed model predictive control approach to cooperative adaptive cruise control of the heterogeneous platoon," *Proceedings of the Institution of Mechanical Engineers, Part D: Journal of Automobile Engineering*, vol. 236, no. 14, pp. 3153–3167, 2022.

[21] Y. Li, Y. Wu, and S. He, “Distributed consensus control for a group of autonomous marine vehicles with nonlinearity and external disturbances,” *Neurocomputing*, vol. 443, pp. 380–387, 2021.

[22] A. Farag, O. M. AbdelAziz, A. Hussein, and O. M. Shehata, “Reinforcement learning based approach for multi-vehicle platooning problem with nonlinear dynamic behavior,” 2020.

[23] S. Lu, Y. Cai, L. Chen, H. Wang, X. Sun, and Y. Jia, “A sharing deep reinforcement learning method for efficient vehicle platooning control,” *IET Intelligent Transport Systems*, vol. 16, no. 12, pp. 1697–1709, 2022.

[24] G. J. Naus, R. P. Vugts, J. Ploeg, M. J. van De Molengraft, and M. Steinbuch, “String-stable cacc design and experimental validation: A frequency-domain approach,” *IEEE Transactions on Vehicular Technology*, vol. 59, no. 9, pp. 4268–4279, 2010.

[25] H. Xing, J. Ploeg, and H. Nijmeijer, “Robust cacc in the presence of uncertain delays,” *IEEE Transactions on Vehicular Technology*, vol. 71, no. 4, pp. 3507–3518, 2022.

[26] F. Gao, S. E. Li, Y. Zheng, and D. Kum, “Robust control of heterogeneous vehicular platoon with uncertain dynamics and communication delay,” *IET Intelligent Transport Systems*, vol. 10, no. 7, pp. 503–513, 2016.

[27] X. Chang, H. Li, J. Rong, X. Zhao, *et al.*, “Analysis on traffic stability and capacity for mixed traffic flow with platoons of intelligent connected vehicles,” *Physica A: Statistical Mechanics and Its Applications*, vol. 557, p. 124 829, 2020.

[28] J. N. Yasin, S. A. S. Mohamed, M.-H. Haghbayan, J. Heikkonen, H. Tenhunen, M. M. Yasin, and J. Plosila, “Energy-efficient formation morphing for collision avoidance in a swarm of drones,” *IEEE Access*, vol. 8, pp. 170 681–170 695, 2020.

[29] P. Zhang, G. Chen, Y. Li, and W. Dong, “Agile formation control of drone flocking enhanced with active vision-based relative localization,” *IEEE Robotics and Automation Letters*, vol. 7, no. 3, pp. 6359–6366, 2022.

[30] M. Rouholamini, C. Wang, H. Nehrir, X. Hu, Z. Hu, H. Aki, B. Zhao, Z. Miao, and K. Strunz, “A review of modeling, management, and applications of grid-connected li-ion battery storage systems,” *IEEE Transactions on Smart Grid*, vol. 13, no. 6, pp. 4505–4524, 2022.

[31] H. Min, Y. Yang, Y. Fang, P. Sun, and X. Zhao, “Constrained optimization and distributed model predictive control-based merging strategies for adjacent connected autonomous vehicle platoons,” *IEEE Access*, vol. 7, pp. 163 085–163 096, 2019.

[32] D. Kandris, C. Nakas, D. Vomvas, and G. Koulouras, “Applications of wireless sensor networks: An up-to-date survey,” *Applied System Innovation*, vol. 3, no. 1, p. 14, 2020.

[33] D. Yue, H. Zhang, and S. Weng, *Distributed Cooperative Control and Communication for Multi-agent Systems*. Springer, 2021.

[34] C. W. Reynolds, "Flocks, herds and schools: A distributed behavioral model," in *Proceedings of the 14th annual Conference on Computer Graphics and Interactive Techniques*, 1987, pp. 25–34.

[35] I. D. Couzin, J. Krause, N. R. Franks, and S. A. Levin, "Effective leadership and decision-making in animal groups on the move," *Nature*, vol. 433, no. 7025, pp. 513–516, 2005.

[36] V. Gazi and K. M. Passino, "Stability analysis of swarms," *IEEE Transactions on Automatic Control*, vol. 48, no. 4, pp. 692–697, 2003.

[37] J. H. Reif and H. Wang, "Social potential fields: A distributed behavioral control for autonomous robots," *Robotics and Autonomous Systems*, vol. 27, no. 3, pp. 171–194, 1999.

[38] T. Vicsek, A. Czirók, E. Ben-Jacob, I. Cohen, and O. Shochet, "Novel type of phase transition in a system of self-driven particles," *Physical Review Letters*, vol. 75, no. 6, p. 1226, 1995.

[39] S. H. Strogatz, "From kuramoto to crawford: Exploring the onset of synchronization in populations of coupled oscillators," *Physica D: Nonlinear Phenomena*, vol. 143, no. 1-4, pp. 1–20, 2000.

[40] L. Moreau, "Stability of multiagent systems with time-dependent communication links," *IEEE Transactions on Automatic Control*, vol. 50, no. 2, pp. 169–182, 2005.

[41] Y. Guo and Z. Qu, "Control of frictional dynamics of a one-dimensional particle array," *Automatica*, vol. 44, no. 10, pp. 2560–2569, 2008.

[42] L. Ding, Q.-L. Han, X. Ge, and X.-M. Zhang, "An overview of recent advances in event-triggered consensus of multiagent systems," *IEEE Transactions on Cybernetics*, vol. 48, no. 4, pp. 1110–1123, 2017.

[43] Y. Cao, W. Yu, W. Ren, and G. Chen, "An overview of recent progress in the study of distributed multi-agent coordination," *IEEE Transactions on Industrial Informatics*, vol. 9, no. 1, pp. 427–438, 2012.

[44] D. Wang, Z. Wang, M. Chen, and W. Wang, "Distributed optimization for multi-agent systems with constraints set and communication time-delay over a directed graph," *Information Sciences*, vol. 438, pp. 1–14, 2018.

[45] T. Ding, S. Zhu, J. He, C. Chen, and X. Guan, "Consensus-based distributed optimization in multi-agent systems: Convergence and differential privacy," in *2018 IEEE Conference on Decision and Control (CDC)*, IEEE, 2018, pp. 3409–3414.

[46] A. Nedić and J. Liu, "Distributed optimization for control," *Annual Review of Control, Robotics, and Autonomous Systems*, vol. 1, pp. 77–103, 2018.

[47] M. Benosman, "Model-based vs data-driven adaptive control: An overview," *International Journal of Adaptive Control and Signal Processing*, vol. 32, no. 5, pp. 753–776, 2018.

[48] Y. Liu, Y. Fan, and Y. Jia, "Iterative learning formation control for continuous-time multi-agent systems with randomly varying trial lengths," *Journal of the Franklin Institute*, vol. 357, no. 14, pp. 9268–9287, 2020.

[49] X. Bu, J. Liang, Z. Hou, and R. Chi, "Data-driven terminal iterative learning consensus for nonlinear multiagent systems with output saturation," *IEEE Transactions on Neural Networks and Learning Systems*, vol. 32, no. 5, pp. 1963–1973, 2020.

[50] C. Hua, Y. Qiu, and X. Guan, "Event-triggered iterative learning containment control of model-free multiagent systems," *IEEE Transactions on Systems, Man, and Cybernetics: Systems*, vol. 51, no. 12, pp. 7719–7726, 2020.

[51] W. Zhao and H. Zhang, "Distributed optimal coordination control for nonlinear multi-agent systems using event-triggered adaptive dynamic programming method," *ISA Transactions*, vol. 91, pp. 184–195, 2019.

[52] H. Modares, S. P. Nageshrao, G. A. D. Lopes, R. Babuška, and F. L. Lewis, "Optimal model-free output synchronization of heterogeneous systems using off-policy reinforcement learning," *Automatica*, vol. 71, pp. 334–341, 2016.

[53] Q. Jiao, H. Modares, S. Xu, F. L. Lewis, and K. G. Vamvoudakis, "Multi-agent zero-sum differential graphical games for disturbance rejection in distributed control," *Automatica*, vol. 69, pp. 24–34, 2016.

[54] M. E. Khatir and E. J. Davidson, "Bounded stability and eventual string stability of a large platoon of vehicles using non-identical controllers," in *2004 43rd IEEE Conference on Decision and Control (CDC)(IEEE Cat. No. 04CH37601)*, IEEE, vol. 1, 2004, pp. 1111–1116.

[55] S. Feng, Y. Zhang, S. E. Li, Z. Cao, H. X. Liu, and L. Li, "String stability for vehicular platoon control: Definitions and analysis methods," *Annual Reviews in Control*, vol. 47, pp. 81–97, 2019.

[56] I. G. Jin and G. Orosz, "Optimal control of connected vehicle systems with communication delay and driver reaction time," *IEEE Transactions on Intelligent Transportation Systems*, vol. 18, no. 8, pp. 2056–2070, 2016.

[57] D. Swaroop and J. K. Hedrick, "String stability of interconnected systems," *IEEE Transactions on Automatic Control*, vol. 41, no. 3, pp. 349–357, 1996.

[58] C. N. Mokogwu and K. Hashtrudi-Zaad, “Energy-based analysis of string stability in vehicle platoons,” *IEEE Transactions on Vehicular Technology*, vol. 71, no. 6, pp. 5915–5929, 2022.

[59] S. Zeadally, J. Guerrero, and J. Contreras, “A tutorial survey on vehicle-to-vehicle communications,” *Telecommunication Systems*, vol. 73, pp. 469–489, 2020.

[60] A. Demba and D. P. Möller, “Vehicle-to-vehicle communication technology,” in *2018 IEEE international Conference on Electro/Information Technology (EIT)*, IEEE, 2018, pp. 0459–0464.

[61] S. Ucar, T. Higuchi, and O. Altintas, “Signal phase and timing by a vehicular cloud,” in *GLOBECOM 2020-2020 IEEE Global Communications Conference*, IEEE, 2020, pp. 1–6.

[62] M. Muhammad and G. A. Safdar, “5g-based v2v broadcast communications: A security perspective,” *Array*, vol. 11, p. 100 084, 2021.

[63] I. Soto, M. Calderon, O. Amador, and M. Urueña, “A survey on road safety and traffic efficiency vehicular applications based on c-v2x technologies,” *Vehicular Communications*, vol. 33, p. 100 428, 2022.

[64] J. Lioris, R. Pedarsani, F. Y. Tascikaraoglu, and P. Varaiya, “Platoons of connected vehicles can double throughput in urban roads,” *Transportation Research Part C: Emerging Technologies*, vol. 77, pp. 292–305, 2017.

[65] J. Lee, H. Huang, J. Wang, and M. Quddus, *Road safety under the environment of intelligent connected vehicles*, 2022.

[66] P. Kopelias, E. Demiridi, K. Vogiatzis, A. Skabardonis, and V. Zafiropoulou, “Connected & autonomous vehicles–environmental impacts–a review,” *Science of the Total Environment*, vol. 712, p. 135 237, 2020.

[67] D.-y. Qu, Z.-x. Zhao, H. Song, T. Wang, and Y.-f. Jia, “Design of vehicle–road cooperative assistant decision system for active safety at intersections,” *Journal of Transportation Engineering, Part A: Systems*, vol. 148, no. 5, p. 04 022 022, 2022.

[68] S. E. Shladover, “Truck automation operational concept alternatives,” in *2010 IEEE Intelligent Vehicles Symposium*, IEEE, 2010, pp. 1072–1077.

[69] D. Wang, M. Hu, Y. Wang, J. Wang, H. Qin, and Y. Bian, “Model predictive control–based cooperative lane change strategy for improving traffic flow,” *Advances in Mechanical Engineering*, vol. 8, no. 2, p. 1 687 814 016 632 992, 2016.

[70] Y. Shi, L. Lv, Y. Qi, and R. Xie, "A cooperative control algorithm for real-time on-ramp merging of connected and automated vehicles," in *2022 IEEE 25th International Conference on Computer Supported Cooperative Work in Design (CSCWD)*, IEEE, 2022, pp. 659–664.

[71] M. Kneissl, A. K. Madhusudhanan, A. Molin, H. Esen, and S. Hirche, "A multi-vehicle control framework with application to automated valet parking," *IEEE Transactions on Intelligent Transportation Systems*, vol. 22, no. 9, pp. 5697–5707, 2021.

[72] S. I. Guler, M. Menendez, and L. Meier, "Using connected vehicle technology to improve the efficiency of intersections," *Transportation Research Part C: Emerging Technologies*, vol. 46, pp. 121–131, 2014.

[73] J. Wang, F. Ma, Y. Yu, S. Zhu, S. Y. Gelbal, B. Aksun-Guvenc, and L. Guvenc, "Optimization design of the decentralized multi-vehicle cooperative controller for freeway ramp entrance," *International Journal of Automotive Technology*, vol. 22, no. 3, pp. 799–810, 2021.

[74] J. Ploeg, B. T. Scheepers, E. Van Nunen, N. Van de Wouw, and H. Nijmeijer, "Design and experimental evaluation of cooperative adaptive cruise control," in *2011 14th International IEEE Conference on Intelligent Transportation Systems (ITSC)*, IEEE, 2011, pp. 260–265.

[75] G. J. Naus, R. P. Vugts, J. Ploeg, M. J. van De Molengraft, and M. Steinbuch, "String-stable cacc design and experimental validation: A frequency-domain approach," *IEEE Transactions on Vehicular Technology*, vol. 59, no. 9, pp. 4268–4279, 2010.

[76] S. Knorn, A. Donaire, J. C. Agüero, and R. H. Middleton, "Passivity-based control for multi-vehicle systems subject to string constraints," *Automatica*, vol. 50, no. 12, pp. 3224–3230, 2014.

[77] Z. Wang, G. Wu, and M. J. Barth, "A review on cooperative adaptive cruise control (cacc) systems: Architectures, controls, and applications," in *2018 21st International Conference on Intelligent Transportation Systems (ITSC)*, IEEE, 2018, pp. 2884–2891.

[78] Y. Zheng, S. E. Li, J. Wang, D. Cao, and K. Li, "Stability and scalability of homogeneous vehicular platoon: Study on the influence of information flow topologies," *IEEE Transactions on Intelligent Transportation Systems*, vol. 17, no. 1, pp. 14–26, 2015.

[79] S. E. Li, Y. Zheng, K. Li, and J. Wang, "An overview of vehicular platoon control under the four-component framework," in *2015 IEEE Intelligent Vehicles Symposium (IV)*, IEEE, 2015, pp. 286–291.

[80] Y. He, B. Ciuffo, Q. Zhou, M. Makridis, K. Mattas, J. Li, Z. Li, F. Yan, and H. Xu, "Adaptive cruise control strategies implemented on experimental vehicles: A review," *IFAC-PapersOnLine*, vol. 52, no. 5, pp. 21–27, 2019.

[81] R. Rajamani, *Vehicle dynamics and control*. Springer Science & Business Media, 2011.

[82] L. Xiao and F. Gao, "A comprehensive review of the development of adaptive cruise control systems," *Vehicle system dynamics*, vol. 48, no. 10, pp. 1167–1192, 2010.

[83] W. Pananurak, S. Thanok, and M. Parnichkun, "Adaptive cruise control for an intelligent vehicle," in *2008 IEEE International Conference on Robotics and Biomimetics*, IEEE, 2009, pp. 1794–1799.

[84] J. Chen, Y. Zhou, and H. Liang, "Effects of acc and cacc vehicles on traffic flow based on an improved variable time headway spacing strategy," *IET Intelligent Transport Systems*, vol. 13, no. 9, pp. 1365–1373, 2019.

[85] D. Swaroop, J. K. Hedrick, C. Chien, and P. Ioannou, "A comparision of spacing and headway control laws for automatically controlled vehicles1," *Vehicle System Dynamics*, vol. 23, no. 1, pp. 597–625, 1994.

[86] J. Zhou and H. Peng, "Range policy of adaptive cruise control vehicles for improved flow stability and string stability," *IEEE Transactions on Intelligent Transportation Systems*, vol. 6, no. 2, pp. 229–237, 2005.

[87] M. Weinberger, H. Winner, and H. Bubb, "Adaptive cruise control field operational test—the learning phase," *JSAE Review*, vol. 22, no. 4, pp. 487–494, 2001.

[88] W. Prestl, T. Sauer, J. Steinle, and O. Tschernoster, "The bmw active cruise control acc," SAE Technical Paper, Tech. Rep., 2000.

[89] R. Kumar and R. Pathak, "Adaptive cruise control-towards a safer driving experience," *International Journal of Scientific and Engineering Research*, vol. 3, no. 8, pp. 3–7, 2012.

[90] A. Kesting, M. Treiber, M. Schönhof, F. Kranke, and D. Helbing, "Jam-avoiding adaptive cruise control (acc) and its impact on traffic dynamics," in *Traffic and Granular Flow'05*, Springer, 2007, pp. 633–643.

[91] P. Venhovens, K. Naab, and B. Adiprasito, "Stop and go cruise control," *International Journal of Automotive Technology*, vol. 1, no. 2, pp. 61–69, 2000.

[92] Y. Zhang, Q. Lin, J. Wang, S. Verwer, and J. M. Dolan, "Lane-change intention estimation for car-following control in autonomous driving," *IEEE Transactions on Intelligent Vehicles*, vol. 3, no. 3, pp. 276–286, 2018.

[93] S. Miyata, T. Nakagami, S. Kobayashi, T. Izumi, H. Naito, A. Yanou, H. Nakamura, and S. Takehara, "Improvement of adaptive cruise control performance," *EURASIP Journal on Advances in Signal Processing*, vol. 2010, pp. 1–8, 2010.

[94] L. Wischhof, A. Ebner, and H. Rohling, "Information dissemination in self-organizing intervehicle networks," *IEEE Transactions on Intelligent Transportation Systems*, vol. 6, no. 1, pp. 90–101, 2005.

[95] E. Uhlemann, "Connected-vehicles applications are emerging [connected vehicles]," *IEEE Vehicular Technology Magazine*, vol. 11, no. 1, pp. 25–96, 2016.

[96] K. N. Porfyri, E. Mintsis, and E. Mitsakis, "Assessment of acc and cacc systems using sumo," *EPiC Series in Engineering*, vol. 2, pp. 82–93, 2018.

[97] L. Gong, L. Luo, H. Wang, and H. Liu, "Adaptive cruise control design based on fuzzy-pid," in *2010 International Conference on E-Product E-Service and E-Entertainment*, IEEE, 2010, pp. 1–4.

[98] J. Yang, X. Liu, S. Liu, D. Chu, L. Lu, and C. Wu, "Longitudinal tracking control of vehicle platooning using ddpg-based pid," in *2020 4th CAA International Conference on Vehicular Control and Intelligence (CVCI)*, IEEE, 2020, pp. 656–661.

[99] L. Y. Wang, A. Syed, G. G. Yin, A. Pandya, and H. Zhang, "Control of vehicle platoons for highway safety and efficient utility: Consensus with communications and vehicle dynamics," *Journal of Systems Science and Complexity*, vol. 27, pp. 605–631, 2014.

[100] Y. Li, C. Tang, K. Li, X. He, S. Peeta, and Y. Wang, "Consensus-based cooperative control for multi-platoon under the connected vehicles environment," *IEEE Transactions on Intelligent Transportation Systems*, vol. 20, no. 6, pp. 2220–2229, 2018.

[101] J. Hu, P. Bhowmick, F. Arvin, A. Lanzon, and B. Lennox, "Cooperative control of heterogeneous connected vehicle platoons: An adaptive leader-following approach," *IEEE Robotics and Automation Letters*, vol. 5, no. 2, pp. 977–984, 2020.

[102] Y. Li, C. Tang, S. Peeta, and Y. Wang, "Nonlinear consensus-based connected vehicle platoon control incorporating car-following interactions and heterogeneous time delays," *IEEE Transactions on Intelligent Transportation Systems*, vol. 20, no. 6, pp. 2209–2219, 2018.

[103] W. Wang, C. Wang, Z. Wang, B. Han, C. He, J. Cheng, X. Luo, M. Yuan, and J. Kurths, "Nonlinear consensus-based autonomous vehicle platoon control under event-triggered strategy in the presence of time delays," *Applied Mathematics and Computation*, vol. 404, p. 126 246, 2021.

[104] P. Yang, Y. Tang, M. Yan, and X. Zhu, “Consensus based control algorithm for nonlinear vehicle platoons in the presence of time delay,” *International Journal of Control, Automation and Systems*, vol. 17, no. 3, pp. 752–764, 2019.

[105] Z. Wang, G. Wu, P. Hao, K. Boriboonsomsin, and M. Barth, “Developing a platoon-wide eco-cooperative adaptive cruise control (cacc) system,” in *2017 IEEE Intelligent Vehicles Symposium (IV)*, IEEE, 2017, pp. 1256–1261.

[106] Y. Li, C. Tang, K. Li, S. Peeta, X. He, and Y. Wang, “Nonlinear finite-time consensus-based connected vehicle platoon control under fixed and switching communication topologies,” *Transportation Research Part C: Emerging Technologies*, vol. 93, pp. 525–543, 2018.

[107] G. Yu, P. K. Wong, W. Huang, J. Zhao, X.-B. Wang, and Z.-X. Yang, “Distributed adaptive consensus protocol for connected vehicle platoon with heterogeneous time-varying delays and switching topologies,” *IEEE Transactions on Intelligent Transportation Systems*, vol. 23, no. 10, pp. 17 620–17 631, 2022.

[108] V. Turri, B. Besselink, and K. H. Johansson, “Cooperative look-ahead control for fuel-efficient and safe heavy-duty vehicle platooning,” *IEEE Transactions on Control Systems Technology*, vol. 25, no. 1, pp. 12–28, 2016.

[109] S. Van De Hoef, K. H. Johansson, and D. V. Dimarogonas, “Fuel-efficient en route formation of truck platoons,” *IEEE Transactions on Intelligent Transportation Systems*, vol. 19, no. 1, pp. 102–112, 2017.

[110] I. H. Zohdy and H. Rakha, “Game theory algorithm for intersection-based cooperative adaptive cruise control (cacc) systems,” in *2012 15th International IEEE Conference on Intelligent Transportation Systems*, IEEE, 2012, pp. 1097–1102.

[111] R. Kianfar, P. Falcone, and J. Fredriksson, “A receding horizon approach to string stable cooperative adaptive cruise control,” in *2011 14th International IEEE Conference on Intelligent Transportation Systems (ITSC)*, IEEE, 2011, pp. 734–739.

[112] F. Bu, H.-S. Tan, and J. Huang, “Design and field testing of a cooperative adaptive cruise control system,” in *Proceedings of the 2010 American Control Conference*, IEEE, 2010, pp. 4616–4621.

[113] A. Peake, J. McCalmon, B. Raiford, T. Liu, and S. Alqahtani, “Multi-agent reinforcement learning for cooperative adaptive cruise control,” in *2020 IEEE 32nd International Conference on Tools with Artificial Intelligence (ICTAI)*, IEEE, 2020, pp. 15–22.

[114] H. Shi, Y. Zhou, K. Wu, X. Wang, Y. Lin, and B. Ran, "Connected automated vehicle cooperative control with a deep reinforcement learning approach in a mixed traffic environment," *Transportation Research Part C: Emerging Technologies*, vol. 133, p. 103 421, 2021.

[115] S. E. Shladover, C. Nowakowski, X.-Y. Lu, and R. Ferlis, "Cooperative adaptive cruise control: Definitions and operating concepts," *Transportation Research Record*, vol. 2489, no. 1, pp. 145–152, 2015.

[116] H. Xing, J. Ploeg, and H. Nijmeijer, "Compensation of communication delays in a cooperative acc system," *IEEE Transactions on Vehicular Technology*, vol. 69, no. 2, pp. 1177–1189, 2019.

[117] Y. Zhang, Y. Bai, M. Wang, and J. Hu, "Cooperative adaptive cruise control with robustness against communication delay: An approach in the space domain," *IEEE Transactions on Intelligent Transportation Systems*, vol. 22, no. 9, pp. 5496–5507, 2020.

[118] A. Maxim, O. Pauca, C. F. Caruntu, and C. Lazar, "Distributed model predictive control algorithm with time-varying communication delays for a cacc vehicle platoon," in *2020 24th International Conference on System Theory, Control and Computing (ICSTCC)*, IEEE, 2020, pp. 775–780.

[119] J. Ploeg, N. van de Wouw, and H. Nijmeijer, "Fault tolerance of cooperative vehicle platoons subject to communication delay," *IFAC-PapersOnLine*, vol. 48, no. 12, pp. 352–357, 2015.

[120] B. Tian, X. Deng, Z. Xu, Y. Zhang, and X. Zhao, "Modeling and numerical analysis on communication delay boundary for cacc string stability," *IEEE Access*, vol. 7, pp. 168 870–168 884, 2019.

[121] J. Ploeg, E. Semsar-Kazerooni, G. Lijster, N. van de Wouw, and H. Nijmeijer, "Graceful degradation of cacc performance subject to unreliable wireless communication," in *16th International IEEE Conference on Intelligent Transportation Systems (ITSC 2013)*, IEEE, 2013, pp. 1210–1216.

[122] F. Acciani, P. Frasca, G. Heijenk, and A. A. Stoorvogel, "Stochastic string stability of vehicle platoons via cooperative adaptive cruise control with lossy communication," *IEEE Transactions on Intelligent Transportation Systems*, 2021.

[123] C. Wu, Y. Lin, and A. Eskandarian, "Cooperative adaptive cruise control with adaptive kalman filter subject to temporary communication loss," *IEEE Access*, vol. 7, pp. 93 558–93 568, 2019.

[124] Y. Tu, W. Wang, Y. Li, C. Xu, T. Xu, and X. Li, "Longitudinal safety impacts of cooperative adaptive cruise control vehicle's degradation," *Journal of Safety Research*, vol. 69, pp. 177–192, 2019.

[125] C. Lei, E. Van Eenennaam, W. K. Wolterink, G. Karagiannis, G. Heijenk, and J. Ploeg, "Impact of packet loss on cacc string stability performance," in *2011 11th International Conference on ITS Telecommunications*, IEEE, 2011, pp. 381–386.

[126] M. Razzaghpour, S. Shahram, R. Valiente, and Y. P. Fallah, "Impact of communication loss on mpc based cooperative adaptive cruise control and platooning," in *2021 IEEE 94th Vehicular Technology Conference (VTC2021-Fall)*, IEEE, 2021, pp. 01–07.

[127] R. Kunze, R. Ramakers, K. Henning, and S. Jeschke, "Organization and operation of electronically coupled truck platoons on german motorways," in *Automation, Communication and Cybernetics in Science and Engineering 2009/2010*, Springer, 2011, pp. 427–439.

[128] S. Tsugawa, "Results and issues of an automated truck platoon within the energy its project," in *2014 IEEE Intelligent Vehicles Symposium Proceedings*, IEEE, 2014, pp. 642–647.

[129] J. Yoshida, T. Sugimachi, T. Fukao, Y. Suzuki, and K. Aoki, "Autonomous driving of a truck based on path following control," in *Proc. 10th Int. Symposium on Advanced Vehicle Control (CD-ROM)*, 2010.

[130] T. Sugimachi, T. Fukao, Y. Suzuki, and H. Kawashima, "Development of autonomous platooning system for heavy-duty trucks," *IFAC Proceedings Volumes*, vol. 46, no. 21, pp. 52–57, 2013.

[131] S. Ellwanger and E. Wohlfarth, "Truck platooning application," in *2017 IEEE Intelligent Vehicles Symposium (IV)*, IEEE, 2017, pp. 966–971.

[132] C. Nowakowski, S. E. Shladover, X.-Y. Lu, D. Thompson, and A. Kailas, "Cooperative adaptive cruise control (cacc) for truck platooning: Operational concept alternatives," 2015.

[133] C. Foreman, M. Keen, M. Petrella, S. Plotnick, *et al.*, "Fhwa research and technology evaluation techbrief: Truck platooning," United States. Federal Highway Administration. Research and Technology, Tech. Rep., 2021.

[134] M. Shawky, "Factors affecting lane change crashes," *IATSS Research*, vol. 44, no. 2, pp. 155–161, 2020.

[135] M. Sun, Z. Chen, H. Li, and B. Fu, "Cooperative lane-changing strategy for intelligent vehicles," in *2021 40th Chinese Control Conference (CCC)*, IEEE, 2021, pp. 6022–6027.

[136] J. Ni, J. Han, and F. Dong, “Multivehicle cooperative lane change control strategy for intelligent connected vehicle,” *Journal of Advanced Transportation*, vol. 2020, 2020.

[137] H. Kim and F. Borrelli, “Facilitating cooperative and distributed multi-vehicle lane change maneuvers,” *arXiv preprint arXiv:2301.04316*, 2023.

[138] T. Li, J. Wu, C.-Y. Chan, M. Liu, C. Zhu, W. Lu, and K. Hu, “A cooperative lane change model for connected and automated vehicles,” *IEEE Access*, vol. 8, pp. 54 940–54 951, 2020.

[139] Y. Luo, G. Yang, M. Xu, Z. Qin, and K. Li, “Cooperative lane-change maneuver for multiple automated vehicles on a highway,” *Automotive Innovation*, vol. 2, no. 3, pp. 157–168, 2019.

[140] S. Zhang, G. Deng, E. Yang, and J. Ou, “Optimal vehicle lane change trajectory planning in multi-vehicle traffic environments,” *Applied Sciences*, vol. 12, no. 19, p. 9662, 2022.

[141] Z. Hu, J. Huang, Z. Yang, and Z. Zhong, “Embedding robust constraint-following control in cooperative on-ramp merging,” *IEEE Transactions on Vehicular Technology*, vol. 70, no. 1, pp. 133–145, 2021.

[142] Y. Chen, E. Weniuan, X. Wang, and C. Wang, “Multi-vehicle cooperative confluence strategy in freeway merging area under new mixed traffic environment,” in *2022 5th International Conference on Intelligent Autonomous Systems (ICoIAS)*, IEEE, 2022, pp. 358–363.

[143] M. Goli and A. Eskandarian, “Mpc-based lateral controller with look-ahead design for autonomous multi-vehicle merging into platoon,” in *2019 American Control Conference (ACC)*, IEEE, 2019, pp. 5284–5291.

[144] P. Hang, C. Lv, C. Huang, Y. Xing, and Z. Hu, “Cooperative decision making of connected automated vehicles at multi-lane merging zone: A coalitional game approach,” *IEEE Transactions on Intelligent Transportation Systems*, vol. 23, no. 4, pp. 3829–3841, 2021.

[145] L. Zhang, Y. Wang, and H. Zhu, “Theory and experiment of cooperative control at multi-intersections in intelligent connected vehicle environment: Review and perspectives,” *Sustainability*, vol. 14, no. 3, p. 1542, 2022.

[146] Z. Deng, Y. Shi, Q. Han, L. Lv, and W. Shen, “A conflict duration graph-based coordination method for connected and automated vehicles at signal-free intersections,” *Applied Sciences*, vol. 10, no. 18, p. 6223, 2020.

[147] J. Yu, F. Jiang, Y. Luo, and W. Kong, "Networked predictive control method of multi-vehicle cooperative control at communication-constrained unsignalized multi-intersection," *IET Intelligent Transport Systems*, 2022.

[148] N. Li, Y. Yao, I. Kolmanovsky, E. Atkins, and A. R. Girard, "Game-theoretic modeling of multi-vehicle interactions at uncontrolled intersections," *IEEE Transactions on Intelligent Transportation Systems*, vol. 23, no. 2, pp. 1428–1442, 2020.

[149] M. Cai, Q. Xu, C. Chen, J. Wang, K. Li, J. Wang, and X. Wu, "Multi-lane unsignalized intersection cooperation with flexible lane direction based on multi-vehicle formation control," *IEEE Transactions on Vehicular Technology*, vol. 71, no. 6, pp. 5787–5798, 2022.

[150] Y. Cheng, Y. Zhao, R. Zhang, and L. Gao, "Conflict resolution model of automated vehicles based on multi-vehicle cooperative optimization at intersections," *Sustainability*, vol. 14, no. 7, p. 3838, 2022.

[151] Q. Ge, G. Sartoretti, J. Duan, S. E. Li, Y. Yin, and S. Zheng, "Distributed model predictive control of connected multi-vehicle systems at unsignalized intersections," in *2022 IEEE International Conference on Unmanned Systems (ICUS)*, IEEE, 2022, pp. 1466–1472.

[152] W. Wang, Y. Song, J. Zhang, and H. Deng, "Automatic parking of vehicles: A review of literatures," *International Journal of Automotive Technology*, vol. 15, no. 6, pp. 967–978, 2014.

[153] A. Yamazaki, Y. Izumi, K. Yamane, T. Nomura, and Y. Seike, *Development of control technology for controlling automated valet parking*, 2020.

[154] T. Kessler and A. Knoll, "Multi vehicle trajectory coordination for automated parking," in *2017 IEEE Intelligent Vehicles Symposium (IV)*, IEEE, 2017, pp. 661–666.

[155] B. Wu, L. Qian, M. Lu, D. Qiu, and H. Liang, "Optimal control problem of multi-vehicle cooperative autonomous parking trajectory planning in a connected vehicle environment," *IET Intelligent Transport Systems*, vol. 13, no. 11, pp. 1677–1685, 2019.

[156] B. Li, Y. Zhang, Z. Shao, and N. Jia, "Simultaneous versus joint computing: A case study of multi-vehicle parking motion planning," *Journal of Computational Science*, vol. 20, pp. 30–40, 2017.

[157] P. Mrazovic, E. Eser, H. Ferhatosmanoglu, J. L. Larriba-Pey, and M. Matskin, "Multi-vehicle route planning for efficient urban freight transport," in *2018 International Conference on Intelligent Systems (IS)*, IEEE, 2018, pp. 744–753.

[158] M. Kneissl, S. vom Dorff, A. Molin, M. Denniel, T. D. Son, N. O. Lleras, H. Esen, and S. Hirche, "Mixed-reality testing of multi-vehicle coordination in an automated valet parking environment," *IFAC-PapersOnLine*, vol. 53, no. 2, pp. 17 564–17 571, 2020.

[159] A. Alipour-Fanid, M. Dabaghchian, and K. Zeng, "Impact of jamming attacks on vehicular cooperative adaptive cruise control systems," *IEEE Transactions on Vehicular Technology*, vol. 69, no. 11, pp. 12 679–12 693, 2020.

[160] L. Du, L. Chen, X. Hou, and Y. Chen, "Cooperative vehicle localization base on extended kalman filter in intelligent transportation system," in *2019 28th Wireless and Optical Communications Conference (WOCC)*, IEEE, 2019, pp. 1–5.

[161] S. Zhang, C. Lu, S. Jiang, L. Shan, and N. N. Xiong, "An unmanned intelligent transportation scheduling system for open-pit mine vehicles based on 5g and big data," *IEEE Access*, vol. 8, pp. 135 524–135 539, 2020.

[162] M. Yang, S. Wei, R. Jiang, F. Ali, and B. Yang, "Single-message-based cooperative authentication scheme for intelligent transportation systems," *Computers & Electrical Engineering*, vol. 96, p. 107 390, 2021.

[163] S. Wu, H. Wang, W. Yu, K. Yang, D. Cao, and F. Wang, "A new sotif scenario hierarchy and its critical test case generation based on potential risk assessment," in *2021 IEEE 1st International Conference on Digital Twins and Parallel Intelligence (DTPI)*, IEEE, 2021, pp. 399–409.

[164] R. Zhou, Y. Liu, K. Zhang, and O. Yang, "Genetic algorithm-based challenging scenarios generation for autonomous vehicle testing," *IEEE Journal of Radio Frequency Identification*, vol. 6, pp. 928–933, 2022.

[165] W. H. Organization *et al.*, "Global status report on road safety 2018: Summary," World Health Organization, Tech. Rep., 2018.

[166] U. Montanaro, S. Dixit, S. Fallah, M. Dianati, A. Stevens, D. Oxtoby, and A. Mouzakitis, "Towards connected autonomous driving: Review of use-cases," *Vehicle System Dynamics*, vol. 57, no. 6, pp. 779–814, 2019.

[167] A. Eskandarian, *Handbook of intelligent vehicles*. Springer, 2012, vol. 2.

[168] S. Singh, "Critical reasons for crashes investigated in the national motor vehicle crash causation survey," Tech. Rep., 2015.

[169] W. Payre, J. Cestac, and P. Delhomme, "Intention to use a fully automated car: Attitudes and a priori acceptability," *Transportation Research Part F: Traffic Psychology and Behaviour*, vol. 27, pp. 252–263, 2014.

[170] D. Rojas-Rueda, M. J. Nieuwenhuijsen, H. Khreis, and H. Frumkin, “Autonomous vehicles and public health,” *Annual Review of Public Health*, vol. 41, pp. 329–345, 2020.

[171] D. A. Roozemond, “Using intelligent agents for pro-active, real-time urban intersection control,” *European Journal of Operational Research*, vol. 131, no. 2, pp. 293–301, 2001, issn: 0377-2217.

[172] D. González, J. Pérez, V. Milanés, and F. Nashashibi, “A review of motion planning techniques for automated vehicles,” *IEEE Transactions on Intelligent Transportation Systems*, vol. 17, no. 4, pp. 1135–1145, 2015.

[173] A. Haydari and Y. Yılmaz, “Deep reinforcement learning for intelligent transportation systems: A survey,” *IEEE Transactions on Intelligent Transportation Systems*, vol. 23, no. 1, pp. 11–32, 2022.

[174] J. Hu, A. E. Turgut, B. Lennox, and F. Arvin, “Robust formation coordination of robot swarms with nonlinear dynamics and unknown disturbances: Design and experiments,” *IEEE Transactions on Circuits and Systems II: Express Briefs*, vol. 69, no. 1, pp. 114–118, 2022.

[175] J. Jiang and A. Astolfi, “Lateral control of an autonomous vehicle,” *IEEE Transactions on Intelligent Vehicles*, vol. 3, no. 2, pp. 228–237, 2018.

[176] H. Zhu, K.-V. Yuen, L. Mihaylova, and H. Leung, “Overview of environment perception for intelligent vehicles,” *IEEE Transactions on Intelligent Transportation Systems*, vol. 18, no. 10, pp. 2584–2601, 2017.

[177] J. Hu, B. Lennox, and F. Arvin, “Robust formation control for networked robotic systems using negative imaginary dynamics,” *Automatica*, vol. 140, p. 110 235, 2022.

[178] S. Xie, J. Hu, Z. Ding, and F. Arvin, “Collaborative overtaking of multi-vehicle systems in dynamic environments: A distributed artificial potential field approach,” in *2021 20th International Conference on Advanced Robotics (ICAR)*, 2021, pp. 873–878.

[179] J. Hu, P. Bhowmick, I. Jang, F. Arvin, and A. Lanzon, “A decentralized cluster formation containment framework for multirobot systems,” *IEEE Transactions on Robotics*, vol. 37, no. 6, pp. 1936–1955, 2021.

[180] Y. Liu and R. Bucknall, “A survey of formation control and motion planning of multiple unmanned vehicles,” *Robotica*, vol. 36, no. 7, pp. 1019–1047, 2018.

[181] K. Wu, J. Hu, Z. Ding, and F. Arvin, “Mixed controller design for multi-vehicle formation based on edge and bearing measurements,” in *2022 20th European Control Conference (ECC)*, 2022.

[182] B. Wang, H. Ashrafiuon, and S. Nersesov, “Leader–follower formation stabilization and tracking control for heterogeneous planar underactuated vehicle networks,” *Systems & Control Letters*, vol. 156, p. 105 008, 2021.

[183] J. Hu, H. Niu, J. Carrasco, B. Lennox, and F. Arvin, “Fault-tolerant cooperative navigation of networked uav swarms for forest fire monitoring,” *Aerospace Science and Technology*, vol. 123, p. 107 494, 2022.

[184] M. Goli and A. Eskandarian, “A nonlinear model predictive control design for autonomous multivehicle merging into platoons,” *SAE International Journal of Transportation Safety*, vol. 10, no. 09-10-01-0004, 2021.

[185] ——, “Merging strategies, trajectory planning and controls for platoon of connected, and autonomous vehicles,” *International Journal of Intelligent Transportation Systems Research*, vol. 18, no. 1, pp. 153–173, 2020.

[186] S. Dixit, U. Montanaro, M. Dianati, D. Oxtoby, T. Mizutani, A. Mouzakitis, and S. Fallah, “Trajectory planning for autonomous high-speed overtaking in structured environments using robust mpc,” *IEEE Transactions on Intelligent Transportation Systems*, vol. 21, no. 6, pp. 2310–2323, 2019.

[187] S. Dixit, S. Fallah, U. Montanaro, M. Dianati, A. Stevens, F. Mccullough, and A. Mouzakitis, “Trajectory planning and tracking for autonomous overtaking: State-of-the-art and future prospects,” *Annual Reviews in Control*, vol. 45, pp. 76–86, 2018.

[188] B. Németh, P. Gáspár, and T. Hegedűs, “Optimal control of overtaking maneuver for intelligent vehicles,” *Journal of Advanced Transportation*, vol. 2018, 2018.

[189] J. Karlsson, N. Murgovski, and J. Sjöberg, “Computationally efficient autonomous overtaking on highways,” *IEEE Transactions on Intelligent Transportation Systems*, vol. 21, no. 8, pp. 3169–3183, 2019.

[190] R. Deng, B. Di, and L. Song, “Cooperative collision avoidance for overtaking maneuvers in cellular v2x-based autonomous driving,” *IEEE Transactions on Vehicular Technology*, vol. 68, no. 5, pp. 4434–4446, 2019.

[191] R. Chai, A. Tsourdos, A. Savvaris, S. Chai, Y. Xia, and C. L. Philip Chen, “Multiobjective overtaking maneuver planning for autonomous ground vehicles,” *IEEE Transactions on Cybernetics*, vol. 51, no. 8, pp. 4035–4049, 2021.

[192] U. S. Ghumman, F. Kunwar, B. Benhabib, *et al.*, *Guidance-based on-line motion planning for autonomous highway overtaking*. University of Toronto, 2008, [Ph.D. thesis].

[193] J. Li, M. Ran, and L. Xie, “Design and experimental evaluation of a hierarchical controller for an autonomous ground vehicle with large uncertainties,” *IEEE Transactions on Control Systems Technology*, pp. 1–13, 2021.

[194] R. Lattarulo, D. He, and J. Pérez, "A linear model predictive planning approach for overtaking manoeuvres under possible collision circumstances," in *2018 IEEE Intelligent Vehicles Symposium (IV)*, 2018, pp. 1340–1345.

[195] C. Burger and M. Lauer, "Cooperative multiple vehicle trajectory planning using miqp," in *2018 21st International Conference on Intelligent Transportation Systems (ITSC)*, 2018, pp. 602–607.

[196] J. Li, M. Ran, and L. Xie, "Efficient trajectory planning for multiple non-holonomic mobile robots via prioritized trajectory optimization," *IEEE Robotics and Automation Letters*, vol. 6, no. 2, pp. 405–412, 2020.

[197] Y. Kuwata, J. Teo, G. Fiore, S. Karaman, E. Frazzoli, and J. P. How, "Real-time motion planning with applications to autonomous urban driving," *IEEE Transactions on Control Systems Technology*, vol. 17, no. 5, pp. 1105–1118, 2009.

[198] L. Labakhua, U. Nunes, R. Rodrigues, and F. S. Leite, "Smooth trajectory planning for fully automated passengers vehicles: Spline and clothoid based methods and its simulation," in *Informatics in Control Automation and Robotics*, 2008, pp. 169–182.

[199] M. Kaushik, N. Singhania, and K. M. Krishna, "Parameter sharing reinforcement learning architecture for multi agent driving," in *Proceedings of the Advances in Robotics*, 2019, pp. 1–7.

[200] M. Kaushik, V. Prasad, K. M. Krishna, and B. Ravindran, "Overtaking maneuvers in simulated highway driving using deep reinforcement learning," in *2018 IEEE Intelligent Vehicles Symposium (IV)*, 2018, pp. 1885–1890.

[201] X. Li, X. Qiu, J. Wang, and Y. Shen, "A deep reinforcement learning based approach for autonomous overtaking," in *IEEE International Conference on Communications Workshops (ICC Workshops)*, 2020, pp. 1–5.

[202] L. Yu, X. Shao, and X. Yan, "Autonomous overtaking decision making of driverless bus based on deep q-learning method," in *IEEE International Conference on Robotics and Biomimetics (ROBIO)*, 2017, pp. 2267–2272.

[203] S. Na, H. Niu, B. Lennox, and F. Arvin, "Bio-inspired collision avoidance in swarm systems via deep reinforcement learning," *IEEE Transactions on Vehicular Technology*, vol. 71, no. 3, pp. 2511–2526, 2022.

[204] T. Hegedűs, B. Németh, and P. Gáspár, "Graph-based multi-vehicle overtaking strategy for autonomous vehicles," *IFAC-PapersOnLine*, vol. 52, no. 5, pp. 372–377, 2019.

[205] B. Németh, T. Hegedűs, and P. Gáspár, "Model predictive control design for overtaking maneuvers for multi-vehicle scenarios," in *18th European Control Conference (ECC)*, 2019, pp. 744–749.

[206] I. B. Viana, H. Kanchwala, K. Ahiska, and N. Aouf, “A comparison of trajectory planning and control frameworks for cooperative autonomous driving,” *Journal of Dynamic Systems, Measurement, and Control*, vol. 143, no. 7, p. 071 002, 2021.

[207] Í. B. Viana and N. Aouf, “Distributed cooperative path-planning for autonomous vehicles integrating human driver trajectories,” in *International Conference on Intelligent Systems (IS)*, 2018, pp. 655–661.

[208] J. Karlsson, C.-I. Vasile, J. Tumova, S. Karaman, and D. Rus, “Multi-vehicle motion planning for social optimal mobility-on-demand,” in *IEEE International Conference on Robotics and Automation (ICRA)*, 2018, pp. 7298–7305.

[209] J. Harding, G. Powell, R. Yoon, J. Fikentscher, C. Doyle, D. Sade, M. Lukuc, J. Simons, J. Wang, *et al.*, “Vehicle-to-vehicle communications: Readiness of V2V technology for application.,” United States. National Highway Traffic Safety Administration, Tech. Rep., 2014.

[210] F. Bounini, D. Gingras, H. Pollart, and D. Gruyer, “Modified artificial potential field method for online path planning applications,” in *IEEE Intelligent Vehicles Symposium (IV)*, 2017, pp. 180–185.

[211] Y. Wang, Q. Shao, J. Zhou, H. Zheng, and H. Chen, “Longitudinal and lateral control of autonomous vehicles in multi-vehicle driving environments,” *IET Intelligent Transport Systems*, vol. 14, no. 8, pp. 924–935, 2020.

[212] I. Bae, J. Moon, H. Park, J. H. Kim, and S. Kim, “Path generation and tracking based on a bezier curve for a steering rate controller of autonomous vehicles,” in *16th International IEEE Conference on Intelligent Transportation Systems (ITSC)*, 2013, pp. 436–441.

[213] F. Chen, Y. Cao, and W. Ren, “Distributed average tracking of multiple time-varying reference signals with bounded derivatives,” *IEEE Transactions on Automatic Control*, vol. 57, no. 12, pp. 3169–3174, 2012.

[214] C. Jie, *Collaborative clustering motion control for multi-agent systems*. Science Press, 2017.

[215] H. Haes Alhelou, M. E. H. Golshan, and N. D. Hatziargyriou, “A decentralized functional observer based optimal lfc considering unknown inputs, uncertainties, and cyber-attacks,” *IEEE Transactions on Power Systems*, vol. 34, no. 6, pp. 4408–4417, 2019.

[216] H. X. Pham, H. M. La, D. Feil-Seifer, and M. C. Deans, “A distributed control framework of multiple unmanned aerial vehicles for dynamic wildfire tracking,” *IEEE Transactions on Systems, Man, and Cybernetics: Systems*, vol. 50, no. 4, pp. 1537–1548, 2018.

[217] K. C. Dey, L. Yan, X. Wang, Y. Wang, H. Shen, M. Chowdhury, L. Yu, C. Qiu, and V. Soundararaj, "A review of communication, driver characteristics, and controls aspects of cooperative adaptive cruise control (CACC)," *IEEE Transactions on Intelligent Transportation Systems*, vol. 17, no. 2, pp. 491–509, 2015.

[218] Y. Kim, J. Guanetti, and F. Borrelli, "Compact cooperative adaptive cruise control for energy saving: Air drag modelling and simulation," *IEEE Transactions on Vehicular Technology*, vol. 70, no. 10, pp. 9838–9848, 2021.

[219] Y. Qin, H. Wang, and B. Ran, "Impacts of cooperative adaptive cruise control platoons on emissions under traffic oscillation," *Journal of Intelligent Transportation Systems*, pp. 1–8, 2019.

[220] X. Wu, G. Qin, H. Yu, S. Gao, L. Liu, and Y. Xue, "Using improved chaotic ant swarm to tune pid controller on cooperative adaptive cruise control," *Optik*, vol. 127, no. 6, pp. 3445–3450, 2016.

[221] Y. Wei, C. Avcı, J. Liu, B. Belezamo, N. Aydın, P. T. Li, and X. Zhou, "Dynamic programming-based multi-vehicle longitudinal trajectory optimization with simplified car following models," *Transportation Research Part B: Methodological*, vol. 106, pp. 102–129, 2017.

[222] R. Schmied, H. Waschl, R. Quirynen, M. Diehl, and L. del Re, "Nonlinear mpc for emission efficient cooperative adaptive cruise control," *IFAC-Papersonline*, vol. 48, no. 23, pp. 160–165, 2015.

[223] H. Kazemi, H. N. Mahjoub, A. Tahmasbi-Sarvestani, and Y. P. Fallah, "A learning-based stochastic mpc design for cooperative adaptive cruise control to handle interfering vehicles," *IEEE Transactions on Intelligent Vehicles*, vol. 3, no. 3, pp. 266–275, 2018.

[224] S. Gong and L. Du, "Cooperative platoon control for a mixed traffic flow including human drive vehicles and connected and autonomous vehicles," *Transportation Research Part B: Methodological*, vol. 116, pp. 25–61, 2018.

[225] Y. Zheng, S. E. Li, K. Li, F. Borrelli, and J. K. Hedrick, "Distributed model predictive control for heterogeneous vehicle platoons under unidirectional topologies," *IEEE Transactions on Control Systems Technology*, vol. 25, no. 3, pp. 899–910, 2016.

[226] C. Zhai, X. Chen, C. Yan, Y. Liu, and H. Li, "Ecological cooperative adaptive cruise control for a heterogeneous platoon of heavy-duty vehicles with time delays," *IEEE Access*, vol. 8, pp. 146 208–146 219, 2020.

[227] S. E. Li, Y. Zheng, K. Li, Y. Wu, J. K. Hedrick, F. Gao, and H. Zhang, "Dynamical modeling and distributed control of connected and automated vehicles: Challenges and opportunities," *IEEE Intelligent Transportation Systems Magazine*, vol. 9, no. 3, pp. 46–58, 2017.

[228] Ş. Sabău, C. Oară, S. Warnick, and A. Jadbabaie, "Optimal distributed control for platooning via sparse coprime factorizations," *IEEE Transactions on Automatic Control*, vol. 62, no. 1, pp. 305–320, 2016.

[229] Y. Zhou, S. Ahn, M. Chitturi, and D. A. Noyce, "Rolling horizon stochastic optimal control strategy for acc and cacc under uncertainty," *Transportation Research Part C: Emerging Technologies*, vol. 83, pp. 61–76, 2017.

[230] Y. Zhu, D. Zhao, and Z. Zhong, "Adaptive optimal control of heterogeneous cacc system with uncertain dynamics," *IEEE Transactions on Control Systems Technology*, vol. 27, no. 4, pp. 1772–1779, 2018.

[231] T. Chu and U. Kalabić, "Model-based deep reinforcement learning for cacc in mixed-autonomy vehicle platoon," in *2019 IEEE 58th Conference on Decision and Control (CDC)*, IEEE, 2019, pp. 4079–4084.

[232] W. Gao, J. Gao, K. Ozbay, and Z.-P. Jiang, "Reinforcement-learning-based cooperative adaptive cruise control of buses in the lincoln tunnel corridor with time-varying topology," *IEEE Transactions on Intelligent Transportation Systems*, vol. 20, no. 10, pp. 3796–3805, 2019.

[233] Y. G. Dantas, V. Nigam, and C. Talcott, "A formal security assessment framework for cooperative adaptive cruise control," in *2020 IEEE Vehicular Networking Conference (VNC)*, IEEE, 2020, pp. 1–8.

[234] R. van der Heijden, T. Lukaseder, and F. Kargl, "Analyzing attacks on cooperative adaptive cruise control (cacc)," in *2017 IEEE Vehicular Networking Conference (VNC)*, IEEE, 2017, pp. 45–52.

[235] Y. He, M. Makridis, G. Fontaras, K. Mattas, H. Xu, and B. Ciuffo, "The energy impact of adaptive cruise control in real-world highway multiple-car-following scenarios," *European Transport Research Review*, vol. 12, no. 1, pp. 1–11, 2020.

[236] B. Ciuffo, K. Mattas, M. Makridis, G. Albano, A. Anesiadou, Y. He, S. Josvai, D. Komnos, M. Pataki, S. Vass, *et al.*, "Requiem on the positive effects of commercial adaptive cruise control on motorway traffic and recommendations for future automated driving systems," *Transportation Research Part C: Emerging Technologies*, vol. 130, p. 103 305, 2021.

[237] Y. He, K. Mattas, R. Dona, G. Albano, and B. Ciuffo, "Introducing the effects of road geometry into microscopic traffic models for automated vehicles," *IEEE Transactions on Intelligent Transportation Systems*, 2021.

[238] F. Alotibi and M. Abdelhakim, "Anomaly detection for cooperative adaptive cruise control in autonomous vehicles using statistical learning and kinematic model," *IEEE Transactions on Intelligent Transportation Systems*, vol. 22, no. 6, pp. 3468–3478, 2020.

[239] M. Iorio, F. Risso, R. Sisto, A. Buttiglieri, and M. Reineri, "Detecting injection attacks on cooperative adaptive cruise control," in *2019 IEEE Vehicular Networking Conference (VNC)*, IEEE, 2019, pp. 1–8.

[240] V.-L. Nguyen, P.-C. Lin, and R.-H. Hwang, "Enhancing misbehavior detection in 5g vehicle-to-vehicle communications," *IEEE Transactions on Vehicular Technology*, vol. 69, no. 9, pp. 9417–9430, 2020.

[241] G. Bella, P. Biondi, G. Costantino, and I. Matteucci, "Cinnamon: A module for autosar secure onboard communication," in *2020 16th European Dependable Computing Conference (EDCC)*, IEEE, 2020, pp. 103–110.

[242] J. Sawant, U. Chaskar, and D. Ginoya, "Robust control of cooperative adaptive cruise control in the absence of information about preceding vehicle acceleration," *IEEE Transactions on Intelligent Transportation Systems*, 2020.

[243] P. E. Paré, E. Hashemi, R. Stern, H. Sandberg, and K. H. Johansson, "Networked model for cooperative adaptive cruise control," *IFAC-PapersOnLine*, vol. 52, no. 20, pp. 151–156, 2019.

[244] W. Schinkel, T. van der Sande, and H. Nijmeijer, "State estimation for cooperative lateral vehicle following using vehicle-to-vehicle communication," *Electronics*, vol. 10, no. 6, p. 651, 2021.

[245] Z. Wang, K. Han, and P. Han, "Motion estimation of connected and automated vehicles under communication delay and packet loss of v2x communications," *arXiv preprint arXiv:2101.07756*, 2021.

[246] S. Wei, Y. Zou, X. Zhang, T. Zhang, and X. Li, "An integrated longitudinal and lateral vehicle following control system with radar and vehicle-to-vehicle communication," *IEEE Transactions on Vehicular Technology*, vol. 68, no. 2, pp. 1116–1127, 2019.

[247] C. Zhai, F. Luo, Y. Liu, and Z. Chen, "Ecological cooperative look-ahead control for automated vehicles travelling on freeways with varying slopes," *IEEE Transactions on Vehicular Technology*, vol. 68, no. 2, pp. 1208–1221, 2019.

[248] H. Chehardoli, “Robust optimal control and identification of adaptive cruise control systems in the presence of time delay and parameter uncertainties,” *Journal of Vibration and Control*, vol. 26, no. 17-18, pp. 1590–1601, 2020.

[249] A. Ghasemi, R. Kazemi, and S. Azadi, “Stable decentralized control of a platoon of vehicles with heterogeneous information feedback,” *IEEE Transactions on Vehicular Technology*, vol. 62, no. 9, pp. 4299–4308, 2013.

[250] C. Wu, Z. Xu, Y. Liu, C. Fu, K. Li, and M. Hu, “Spacing policies for adaptive cruise control: A survey,” *IEEE Access*, vol. 8, pp. 50 149–50 162, 2020.

[251] X. Song, X. Lou, and L. Meng, “Time-delay feedback cooperative adaptive cruise control of connected vehicles by heterogeneous channel transmission,” *Measurement and Control*, vol. 52, no. 5-6, pp. 369–378, 2019.

[252] F. L. Lewis, H. Zhang, K. Hengster-Movric, and A. Das, *Cooperative control of multi-agent systems: optimal and adaptive design approaches*. Springer Science & Business Media, 2013.

[253] Z. Qu, *Cooperative Control of Dynamical Systems: Applications to Autonomous Vehicles*. U.K., London: Springer, 2009.

[254] S. Bang and S. Ahn, “Platooning strategy for connected and autonomous vehicles: Transition from light traffic,” *Transportation Research Record*, vol. 2623, no. 1, pp. 73–81, 2017.

[255] G. C. Calafiore, C. Possieri, and A. V. Proskurnikov, “Collision-avoiding decentralized control for vehicle platoons: A mechanical perspective,” *IFAC-PapersOnLine*, vol. 53, no. 2, pp. 15 235–15 240, 2020.

[256] J. M. Contet, F. Gechter, P. Gruer, and A. Koukam, “Multiagent system model for vehicle platooning with merge and split capabilities,” in *Third International Conference on Autonomous Robots and Agents*, Citeseer, 2006, pp. 41–46.

[257] J.-J. Martinez and C. Canudas-de-Wit, “A safe longitudinal control for adaptive cruise control and stop-and-go scenarios,” *IEEE Transactions on Control Systems Technology*, vol. 15, no. 2, pp. 246–258, 2007.

[258] Y. Li, Z. Li, H. Wang, W. Wang, and L. Xing, “Evaluating the safety impact of adaptive cruise control in traffic oscillations on freeways,” *Accident Analysis & Prevention*, vol. 104, pp. 137–145, 2017.

[259] E. van Nunen, J. Reinders, E. Semsar-Kazerooni, and N. Van De Wouw, “String stable model predictive cooperative adaptive cruise control for heterogeneous platoons,” *IEEE Transactions on Intelligent Vehicles*, vol. 4, no. 2, pp. 186–196, 2019.